https://ntrs.nasa.gov/search.jsp?R=19880005578 2020-03-20T07:42:48+00:00Z

NASA Contractor Report 172137

FINAL REPORT

P-112
IN-02
117203
DATE OVERRIDE

Laminar Flow Control Leading Edge Glove Flight Test Article Development

(NASA-CR-172137) LAMINAR FLOW CONTROL LEADING EDGE GLOVE FLIGHT TEST ARTICLE DEVELOPMENT Final Report (Douglas Aircraft Co.) 112 p CSCL 01A
N88-14960
Unclas
G3/02 0117203

DOUGLAS AIRCRAFT COMPANY
MCDONNELL DOUGLAS CORPORATION
LONG BEACH, CALIFORNIA

CONTRACT NAS1-16220
NOVEMBER 1984

National Aeronautics and Space Administration

Langley Research Center
Hampton, Virginia 23665

marked on any reproduction of this data in whole or in part. Date for general release will be three (3) years from date indicated on the document.

COPY NO. 84

NASA Contractor Report 172137

FINAL REPORT

Laminar Flow Control Leading Edge Glove Flight Test Article Development

DOUGLAS AIRCRAFT COMPANY
MCDONNELL DOUGLAS CORPORATION
LONG BEACH, CALIFORNIA

CONTRACT NAS1-16220
NOVEMBER 1984

NASA
National Aeronautics and
Space Administration

Langley Research Center
Hampton, Virginia 23665

ORIGINAL PAGE IS
OF POOR QUALITY

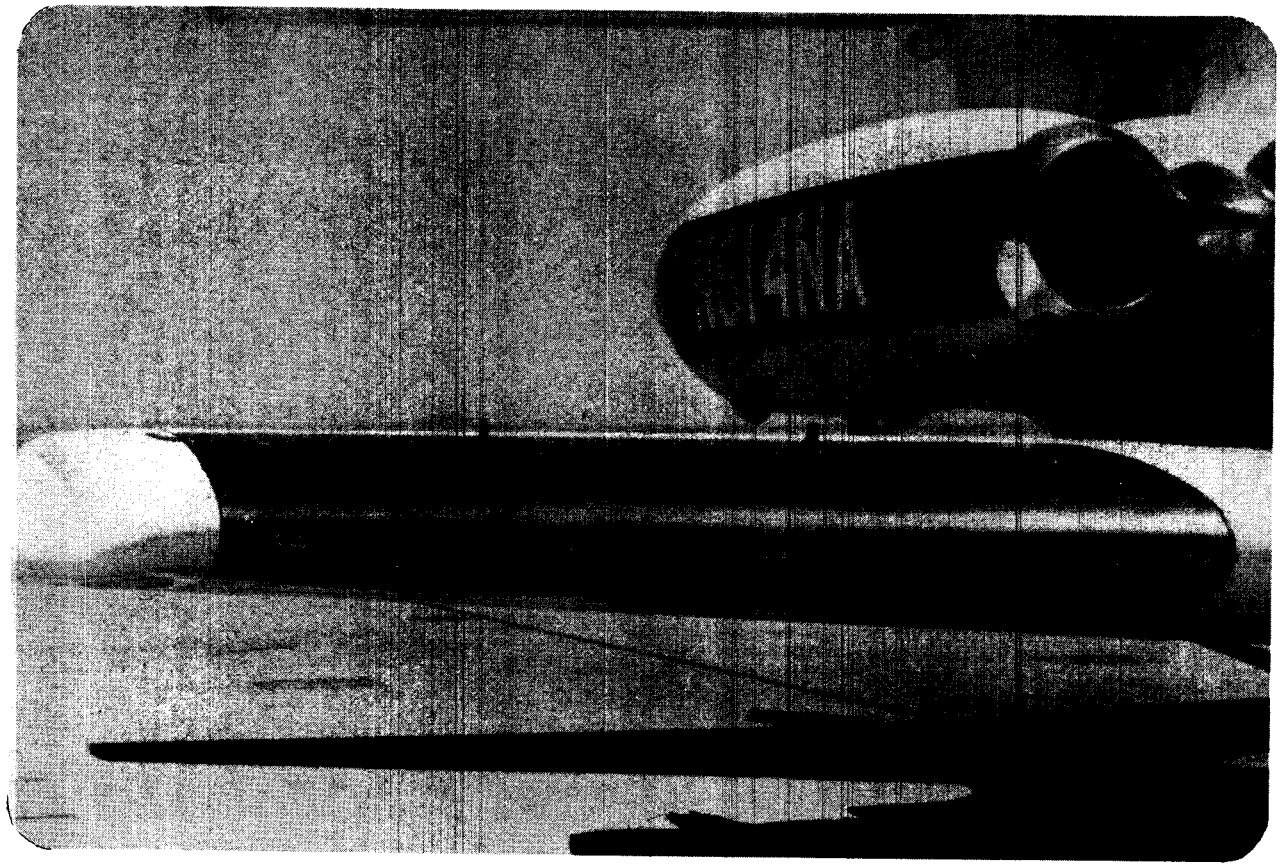

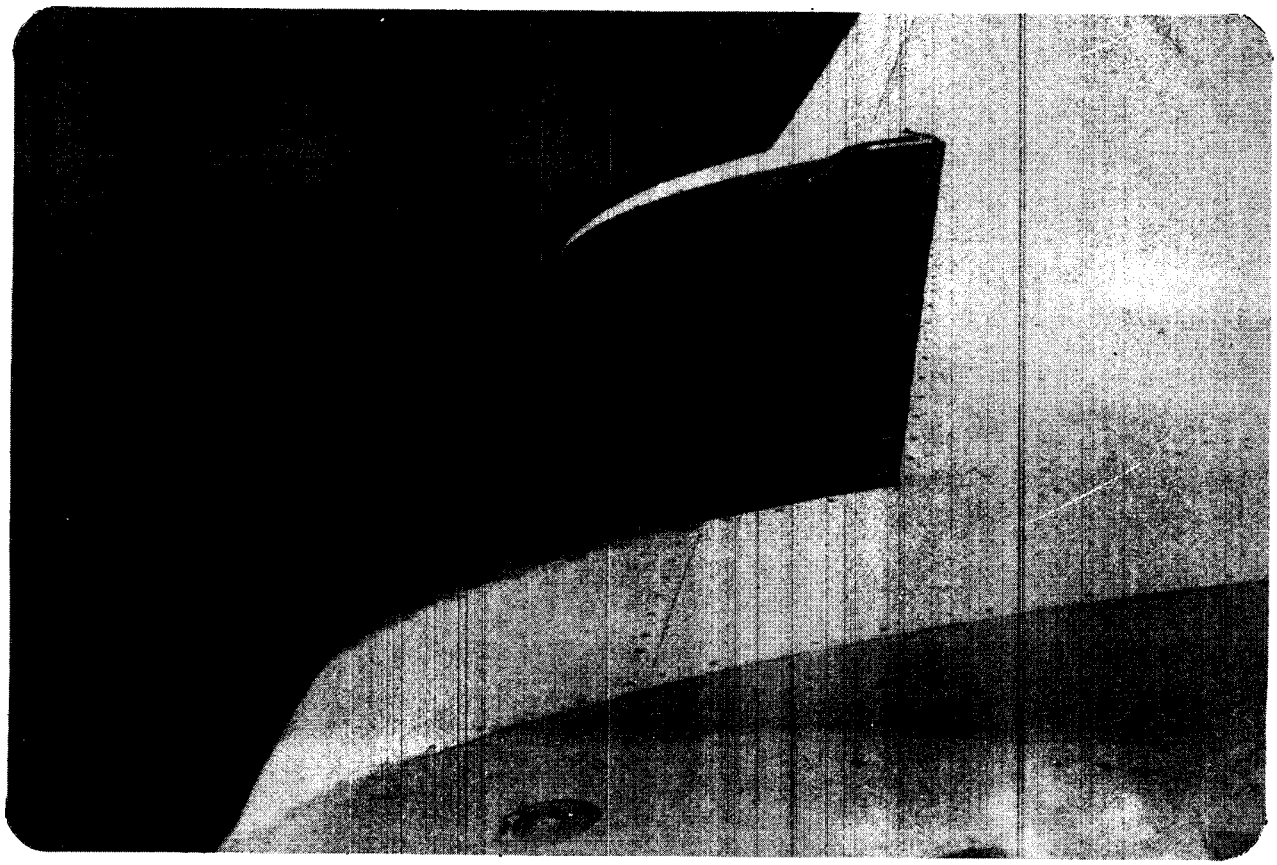

ORIGINAL PAGE IS
OF POOR QUALITY

FOREWORD

This document covers the contract work performed by the Douglas Aircraft Company of the McDonnell Douglas Corporation, on "Laminar Flow Control Leading Edge Glove Flight Test Article Development" (LEFT) - NASA Contract NAS1-16220. The LEFT program is part of the overall Aircraft Energy Efficient (ACEE) program supported by NASA through the Langley Research Center.

Acknowledgement for their support and guidance is given to the NASA Laminar Flow Control (LFC) Project Manager, Mr. R. Wagner, the Project Technical Monitor, Mr. M. Fischer and to Mr. A. Wright.

The Douglas personnel primarily responsible for this work were:

Max Klotzsche	ACEE Program Manager
Wil Pearce	LFC Project Manager
Dave McNay	LEFT Project Manager
Phil Bono	Structures
Ron Smith	Structures
Jack Thelander	Aerodynamics
John Allen	Aerodynamics
Walt Boronow	Environmental
Chantal Joubert	Environmental
Glen Primavera	Suction System
Frank Gallimore	Materials and Processing
Cy Coppage	Tooling

CONTENTS

		Page
1	SUMMARY	1
2	INTRODUCTION	3
3	SYMBOLS & ABBREVIATIONS	5
4	CONCEPT SELECTION	7
	4.1 Design Requirements	7
	4.2 Design & Performance Specifications	7
	4.3 Configuration Concept	9
5	AERODYNAMIC ANALYSIS	15
	5.1 Leading Edge Glove Shape Development	15
	5.2 JetStar Wind Tunnel Model Test	27
	5.3 LFC Leading Edge Glove Defining Airfoils	36
	5.4 LFC Suction Flow Requirements	40
	5.5 LFC Surface Waviness Criteria	53
6	LOW SPEED SWEPT WING MODEL TEST	55
	6.1 Model Description and Installation	55
	6.2 Test Results and Analysis	57
7	DETAIL DESIGN	61
	7.1 LFC Suction Panel	61
	Porous Surface	
	Flute Requirements	
	Panel Configuration	
	7.2 L.E. Support Structure	64
	7.3 High-Lift Shield	64
	7.4 Suction System	65
	7.5 Environmental Protection & Surface Cleaning	66

		Page
8	STRUCTURAL TESTING	69
	8.1 E.B. Perforated Titanium Surface	69
	8.2 Bond Strength	69
	Shear	
	Peel	
	PGME/Temperature Effect	
	Burst Test	
	8.3 Nose Box Test	73
9	STRUCTURAL ANALYSIS	75
	9.1 Requirements	75
	9.2 Design Loads	75
	9.3 Fail Safe Aspects	75
10	TOOLING	77
	10.1 Suction Panel	78
	Molding/Bonding Tool	
	Flute Mandrel Tooling	
	10.2 L.E. Support Structure	81
	10.3 High-Lift Shield and Actuation System	81
	10.4 Assembly Jig and Holding Fixture	82
11	FABRICATION & ASSEMBLY	85
	11.1 Suction Panel	85
	Suction Surface	
	Substructure	
	Bonded Assembly	
	11.2 Sensor Panel	90
	11.3 High-Lift Shield	91
	11.4 Assembly	92
12	LFC TEST ARTICLE INSTRUMENTATION	93
	CONCLUDING REMARKS	99
	REFERENCES	100

LIST OF FIGURES

Figure		Page
1	NASA JetStar Airplane	3
2	LFC Test Article - Principal Components	3
3	Leading Edge Flute and Suction Tube Configuration	11
4	LFC Chamber Valve Preliminary Layout	11
5	Leading Edge Contamination Avoidance Concept	13
6	Leading Edge Ice Protection Concept	13
7	Desired LFC Glove Pressure Distribution	15
8	JetStar LFC Test Article Planform	16
9	Upper Surface Pressure Distribution - JetStar with Desired LFC Glove Pressures	19
10	Upper Surface Isobars - Preliminary Glove Shape	21
11	Upper Surface Isobars - LFC Test Article - Desired Pressure Distribution	22
12	Upper Surface Isobars - LFC Test Article - Modified Flat Roof-Top Pressure Distribution	24
13	Upper Surface Isobars - LFC Test Article - Modified Roof-Top Geometry with Straight Line Elements	25
14	Garabedian Two-Dimensional Solution for Modified Flat Roof-Top Geometry	26
15	Surface Pressure Distribution - LFC Test Article - MOD 7Q Shape on JetStar Wing	28
16	Surface Isobars - LFC Test Article - MOD 7Q Shape on JetStar Wing	29
17	Comparison of Analytical and Experimental Pressures on LFC Glove - 10 Percent Scale JetStar Model Glove Configuration X_{28} and Jameson Analytical Result	30

LIST OF FIGURES (continued)

Figure		Page
18	Comparison of Basic JetStar Wing Sections and MOD 8 LFC Glove Defining Airfoil Shapes	30
19	Representative Example of Nacelle Effect on Wing Pressures - JetStar Model Test	32
20	Summary of Incremental Pressure Coefficient Due to Nacelles - JetStar Model Test	33
21a	Predicted Pressure Distribution, Nacelles on - LFC Test Article MOD 8 Shape (41.54 Percent Semispan)	33
21b	Predicted Pressure Distribution, Nacelles on - LFC Test Article - MOD 8 Shape (45.85 Percent Semispan)	34
21c	Predicted Pressure Distribution, Nacelles on - LFC Test Article - MOD 8 Shape (50.18 Percent Semispan)	34
21d	Predicted Pressure Distribution, Nacelles on - LFC Test Article - MOD 8 Shape (54.52 Percent Semispan)	35
21e	Predicted Pressure Distribution, Nacelles on - LFC Test Article - MOD 8 Shape (58.85 Percent Semispan)	35
22	Comparison of Predicted Pressure Distribution with JetStar Model Test Data and Desired LFC Pressure Distribution	37
23	Predicted Off-Design Pressure Profiles at LFC Test Article Midspan	37
24	Attachment Line Location - MOD 8 LFC Glove - Flight Test Article	41
25	Boundary Layer Stability - MOD 8 LFC Glove - Suction Off	43
26	Boundary Layer Stability - MOD 8 LFC Glove - Effects of Suction Distribution	43
27	Basic Suction Distribution	45
28	Douglas LFC Leading Edge Suction Panel Boundary Layer Stability	46
29	Perforated Strip Arrangement	47
30	Pressure Drop Characteristics of EB Perforated Titanium	50
31	Nominal and 150 percent Flow Distribution	50
32	LFC Flight Test Article Specification Waviness Limits - Multiple-Wave Criteria	53

LIST OF FIGURES (continued)

Figure		Page
33	Swept-Wing Model Leading Edge Panel Cross Section	56
34	Swept-Wing Model in DAC Tunnel	56
35	Attachment Line Band and Flute Number 1	62
36	Constant C_p Lines and Flute Configuration	62
37	Leading Edge Flute Configuration	63
38	Suction Flute Fitting	63
39	Inboard Actuator Rib Linkage Installation	64
40	CA Liquid Spray Nozzles on Shield	67
41	Control for CA Spray and IP Systems	67
42	TKS IP Installation on Shield Leading Edge	68
43	Burst Specimen	72
44	Axial Compression/Torsional Shear Test Specimen	73
45	Waviness Measurements Under Load - 20-Inch Leading Edge Specimen	74
46	JetStar Flutter Envelope - Shield Extended	76
47	Cross Section of Suction Panel	77
48	Steel Forming and Bonding Tool	78
49	Flute Forming Mandrel Assembly	79
50	Intermediate Flute Forming Mandrels	80
51	AF31 Adhesive Attachment to Lands	80
52	NC Machining of Shield	81
53	Shield Assembly Jig	82
54	Main Assembly Jig	83
55	Rib Attach Tee Tooling	83

LIST OF FIGURES (continued)

Figure		Page
56	Five-Point Indexing Frame	84
57	Attach Tee Base Forming Caul Plates	86
58	Attach Tee Base Formed by Caul Plate	86
59	Completed Substructure Assembly	87
60	Adhesive Attachment and Flute Openings	89
61	Flute Forming Mandrels in Place	89
62	Flute Fitting Installation	90
63	High-Lift Shield Assembly	91
64	Douglas LFC Leading Edge Surface Instrumentation	94

LIST OF TABLES

Table		Page
1	Leading Edge Glove Defining Airfoil Coordinates Inboard Station, Y = 134.750	36
2	Leading Edge Glove Defining Airfoil Coordinates Outboard Station, Y = 196.000	37
3	Adjusted Interface Flow Conditions Baseline - Nominal Flow	48
4	Adjusted Interface Flow Conditions Baseline - 150 Percent Nominal Flow	50
5	Summary of EB Perforated Titanium Fatigue Tests	67
6	Mechanical Properties Test Results	68
7	Douglas Leta Instrumentation Locations Static Ports, Outboard Array - A	95
8	Douglas Leta Instrumentation Locations Static Ports, Center Array - B	96
9	Douglas Leta Instrumentation Locations Static Ports, Inboard Array - C	97
10	Douglas Leta Instrumentation Locations Hot Film Sensors	98

SECTION 1
SUMMARY

The Douglas contribution to the NASA LFC Leading Edge Glove Flight Test Development Program was the design and fabrication of a leading edge test article for the NASA JetStar aircraft. This article will achieve laminar flow over the leading edge box by controlled suction through a perforated titanium surface.

The 6-foot-span test article was designed to be located in the space on the right wing leading edge that is opened up by removal of the slipper fuel tank. The active suction panel is on the upper surface only, from just below the leading edge attachment line to the vicinity of the front spar. An unperforated titanium-surfaced sensor panel forms a smooth continuation of the upper surface to a line approximately 6 inches aft of the front spar. The lower surface is composed of access panels and the outer surface of the stowed retractable high-lift shield contoured to the airfoil shape. In the extended position, the shield protects the perforated titanium upper surface from airborne debris during takeoff and landing. The shield also supports an anti-icing system and a fluid spray system that can be used to provide additional protection against contamination and for ice removal from the leading edge region.

SECTION 2
INTRODUCTION

Under the sponsorship of the NASA ACEE Project Office at Langley, Douglas Aircraft Company of McDonnell Douglas Corporation, designed and fabricated a laminar flow control (LFC) wing leading edge flight test component. The test component is incorporated in a glove on the right wing of the NASA JetStar aircraft (See Figure 1) and will be flight-tested under conditions approximating those of future LFC commercial transport aircraft operation.

The 72-inch-long test component is located approximately midway between the fuselage side and the wing tip and extends aft to approximately 12 percent of the chord. LFC is achieved using suction through the porous outer surface to stabilize the laminar boundary layer and avoid transition to turbulent flow. The test region includes attachment line, crossflow, and, to a lesser degree, Tollmein-Schlichting instability conditions.

The Douglas concept for achieving LFC takes advantage of new techniques in material processing that were not available to earlier LFC flight researchers such as Raspet and Pfenninger in the U.S. and Lachman in England (References 1, 2, and 3, respectively). In particular, the outer porous surface is electron-beam-perforated titanium. The electron-beam perforating equipment was developed comparatively recently by Steigerwald in Germany; improvements in technique in the use of this equipment at Pratt and Whitney in the U.S. now enable the attainment of a closely spaced pattern of 0.0020- to 0.0025-inch-diameter holes in 0.025-inch-thick titanium sheet material. Douglas has developed welding, forming, and bonding methods using this material to obtain an LFC surface that has the desired porosity characteristics and meets surface waviness criteria.

The perforated titanium surface is bonded to a fluted substructure that provides integral ducting for collecting the suction airflow through the surface. This system has been demonstrated to be highly effective and tolerant of off-design conditions during extensive wind tunnel testing at Douglas. For test purposes, the suction airflow from each flute is controlled separately.

To achieve laminar flow, it is essential to maintain an uncontaminated surface. The Douglas design incorporates a retractable leading edge shield, which when deployed, provides the primary protection against impingement of insects and other airborne debris. In addition, a contamination avoidance fluid spray system is mounted on the back of the shield to maintain a wet film over the wing leading edge during exposure to airborne contaminants. This is in case some contaminants are not totally deflected by the shield. This fluid spray system also provides the anti-icing function for the perforated leading edge with the shield extended. The shield leading edge is protected from ice accumulation by a standard TKS de-icing system which exudes a glycol-based freezing point depressant through a porous surface. The exploded view in Figure 2 illustrates the relationship of components.

The Douglas LFC leading edge component was delivered to NASA Dryden Flight Research Facility in May 1983. Acceptance ground and flight testing began in November 1983.

PRECEDING PAGE BLANK NOT FILMED

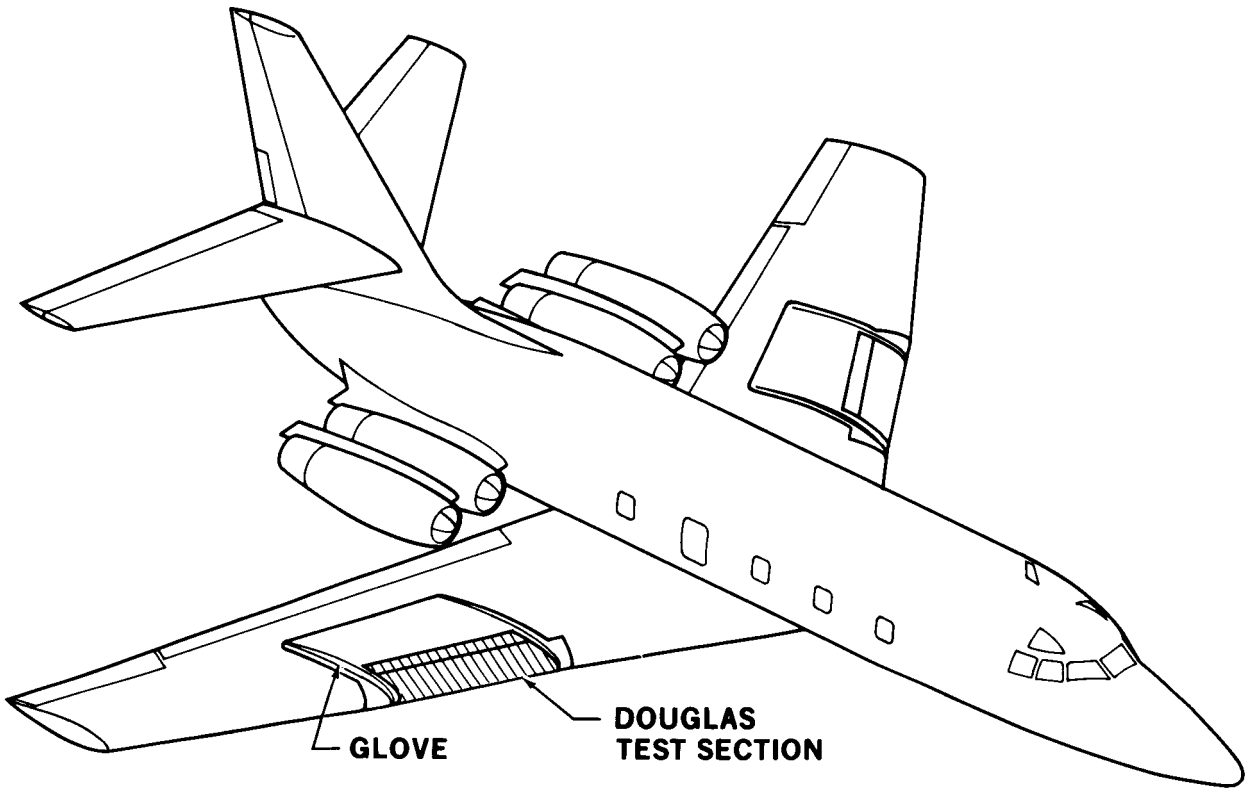

FIGURE 1. NASA JETSTAR AIRPLANE

81-GEN-22604 C

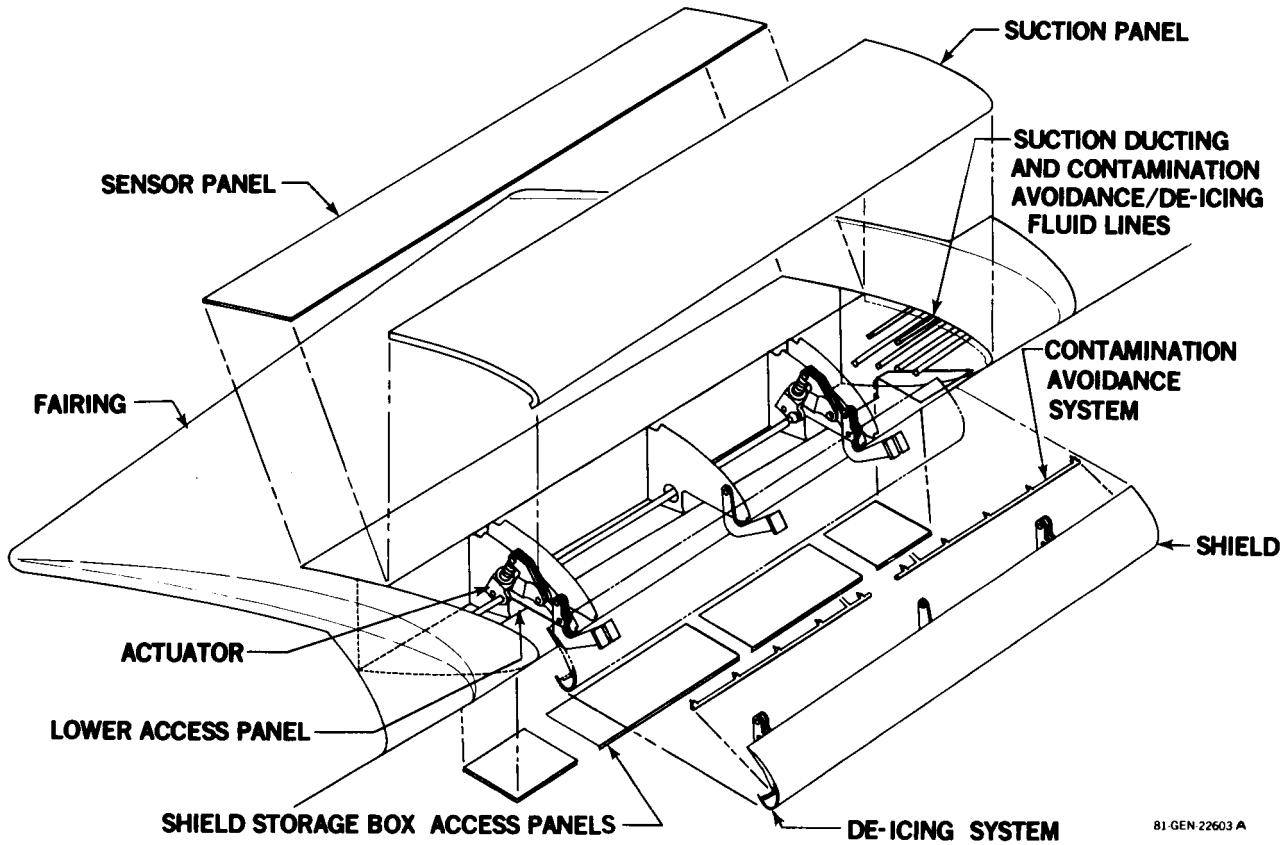

81-GEN-22603 A

FIGURE 2. LFC TEST ARTICLE – PRINCIPAL COMPONENTS

SECTION 3
SYMBOLS & ABBREVIATIONS

ACEE	Aircraft energy efficiency
AF31	Phenolic adhesive
BLC	Boundary layer control
CA	Contamination avoidance
CALSPAN	Cornell Aeronautical Laboratory
C_L	Lift coefficient
$C_{L_{AC}}$	Aircraft lift coefficient
C_P	Pressure coefficient
$\Delta C_{Pnacelles}$	Pressure coefficient increment due to Nacelles
C_Q	Surface mass flow coefficient (suction negative)
DAC	Douglas Aircraft Company
EB	Electron beam
EGME	Ethylene glycol methyl ether
FAR	Federal Air Regulations
FL022	Three-Dimensional Transonic Potential Flow Analysis Computer Code
FM73	Epoxy adhesive
GELAC	Lockheed-Georgia Company
h	Surface deviation from mean contour (waviness condition)
h_P	Pressure altitude
IP	Ice protection
KEAS	Knots equivalent airpseed
L.E.S.	Leading edge station

LETA	Leading edge test article
LFC	Laminar flow control
M_N	Normal Mach number
MARIA	Boundary layer stability analysis code
N-Factor	Boundary layer instability amplification factor
PGME	Propylene glycol methyl ether
psf	Pounds per square foot
psi	Pounds per square inch
R_θ	Attachment line Reynolds number
S_A	Surface distance measured streamwise from leading edge
SALLY	Boundary layer stability analysis code
SCFM	Standard cubic feet per minute
TIG	Tungsten inert gas (welding process)
TKS	TKS Ltd. (aircraft deicing)
V_D	Limit dive speed
W.S.	Wing station - inches from aircraft plane of symmetry
x/c	Nondimensional chordwise coordinate
x	Wing (Airfoil) chordwise coordinate
y/c	Nondimensional spanwise coordinate
Y	Wing spanwise coordinate
z/c	Nondimensional normal coordinate
z	Wing (airfoil) normal coordinate
Λ	Surface wavelength

SECTION 4
CONCEPT SELECTION

4.1 DESIGN REQUIREMENTS

In the early phase of the Leading Edge Glove Flight Test Article Development program, data exchange between NASA, the integration contractor, Lockheed-Georgia Company, and McDonnell Douglas Corporation established design criteria and interface requirements. This series of exchanges and consultations with NASA provided a basis for structural loads analysis and mechanical joining requirements for the leading edge test article (LETA) and the deployable leading edge shield/slat.

The LETA developed by Douglas is attached to the right wing spar of the JetStar at about mid-semispan for a distance of about 72 inches. As specified by Lockheed, the LETA cannot impose any significant load on the upper or lower spar caps. Also, the deployable leading edge device cannot adversely influence the stability and control of the JetStar during deployment and retraction.

4.2 DESIGN AND PERFORMANCE SPECIFICATIONS

To adequately define the interface parameters of each of the LETA systems, specifications were drawn up to describe the requirements of each system and its necessary relationship to the other systems for the successful achievement of LFC. Five specifications were generated to guide the design, fabrication, and performance testing of the Douglas test article:

(a) The Aerodynamic Surface Specification details the aerodynamic requirements for achieving LFC using a porous external skin and fluted substructure to provide the plenums and ducting for the application of suction through the surface. Individual metering and control of the suction flow are to be provided for each suction flute. The leading edge shape is defined by two sets of chordwise coordinates with straight line elements maintained between them. Waviness criteria are defined as no deviation from chordwise loft line greater than 0.010 inch and no resulting waviness greater than the crest-to-trough depth divided by the crest-to-crest length greater than 0.001. Steps and gaps in the surface at necessary joints are to be as near imperceptible as possible but not to exceed the following:

Forward facing step	0.011 inch
Aft facing step	0.005 inch
Gap across flow	0.090 inch
Gap along flow	0.013 inch

Leakage throughout the system from one suction flute to another must be effectively nil in order to insure positive flow control.

(b) The Suction System Specification details the suction pressure and flow requirements that the system must provide, monitor and control in order to assure LFC. To control each individual flute from zero to maximum suction flow, a series of control valves is specified along with a means of monitoring and adjusting them from a control console. The control valves operate in a common chamber that is continuously being evacuated by the suction pump. Each valve allows flow to dump into the chamber and maintains the required flow by holding at a precalibrated position which can also be adjusted as required from the console.

(c) The Clearing System Specification defines how the suction system controls, valves and ducting are used to direct a high-pressure airflow in the reverse direction out through the porous surface to clear any liquids from the pores. These pores can be blocked by rain, contamination avoidance fluid or ice protection fluid, all of which must be purged or cleared from the openings in the surface prior to applying suction. The source of pressurized air is either the aircraft air conditioning/pressurization system or the emergency pressurization system (above 12,000 feet). The same chamber valve assembly, needle valves and flute ducting are used to channel and control the clearing air to the underside of the porous surface. By maintaining pressure in the flutes and providing sufficient flow as fluid is cleared from the pores, the porosity is restored to the original or dry condition. Approximately 1 psi is sufficient pressure to accomplish clearing of perforated titanium. Heating of the clearing air allows clearing to be completed in reduced time.

(d) The Contamination Avoidance (CA) Spray System Specification details the requirements of an auxiliary means of coating the perforated leading edge surface with a liquid that will prevent contaminants from sticking to the surface. A series of spray nozzles attached to the underside of the extended shield/slat primary protection system provides for a freezing point depressant solution to be sprayed directly onto the leading edge.

When extended in front of the leading edge, the shield deflects oncoming airborne debris, principally insects, and prevents it from contacting the perforated leading edge surface. To supplement the shield protection against any debris that may possibly escape the shield and impact the LFC surface and stick to it, the liquid spray provides a means of maintaining a wet coating of liquid so that debris will not adhere to the surface. The control specified for the spray systems permits pulsing the flow as required to maintain a wet coating without excess flow.

The liquid specified for the CA spray system is a solution of 60% propylene glycol methyl ether (PGME) and 40% water. PGME is a freezing-point depressant which allows the CA liquid's use at below freezing temperatures to supplement the ice protection system. However, to avoid liquid remaining in the lines and nozzles exposed to very low temperature at cruising altitudes, a high-pressure nitrogen gas purging capability is incorporated in the system. Interlocks prevent operation of the CA spray system other than when the Shield is in the fully extended position.

(e) The Shield Ice Protection Specification details a means of preventing ice from forming on the shield by secretion of a fluid through a porous leading edge surface. The porous leading edge is a TKS Ltd. unit built to Douglas specification and fitted to form the leading edge of the shield. With the shield extended during icing conditions, the TKS ice protection unit keeps the shield free of ice and the shield in turn keeps ice from accumulating on the porous leading edge. The CA spray system can be operated after any icing encounter to clear the perforated leading edge surface of any residue left by the TKS operation and to provide supplemental ice protection.

4.3 CONFIGURATION CONCEPT

The concept for laminar flow control that evolved from previous studies and wind tunnel research at Douglas is based on a porous surface through which some of the boundary layer can be drawn by distributed suction. The suction air can be controlled in pressure and volume along spanwise strips of variable width and orientation. The suction pressure applied individually to the spanwise subsurface ducts or flutes (as they are referred to in this report) creates a more negative pressure beneath the porous surface than exists above on the airfoil surface. This differential pressure causes the flow through the surface. This is the mechanism by which the laminar boundary layer is stabilized, delaying transition from laminar to turbulent flow.

Although other research in boundary layer control (BLC) has achieved significant modification of the boundary layer to produce high lift or reduction in drag, the attainment of true laminar flow control (LFC) was difficult because of the lack of suitable porous surface material. Flight researchers such as Drs. Raspet and Pfenninger in the United States and Lachman in England used very fine punched or drilled holes to create pseudo-porous surfaces or finely sawed slots to create a means of systematically removing a portion of the boundary layer either uniformally or at specified intervals in the case of slots. Sintered material as well as woven wire had also been tried with varying success as a means of achieving a uniform porous surface (References 1, 2, and 3, respectively).

Since the difficulties of manufacturing and maintaining finely sawed slots in a very accurate aerodynamic surface are well documented by the work on the Northrop X21 program, the Douglas approach has been to re-examine the possibility of using porous materials for achieving LFC.

Two promising materials were evaluated under a NASA-sponsored study (Reference 4). Both a smooth finely woven stainless steel mesh, Dynapore, and an electron beam (EB) perforated titanium sheet material were evaluated extensively. The EB perforated titanium, made using a process developed by Steigerwald in Germany, was selected as the most practical surface material because of its better structural and damage-resistant properties. The Steigerwald equipment with improvements by Pratt and Whitney produces a small hole of 0.0020- to 0.0025-inch diameter uniformly in 0.025-inch-thick titanium sheet, with a spacing between holes as required to achieve the surface porosity desired. This computer-controlled process allows sheets of perforated material to be produced which very closely approximate a uniformly porous surface material that can be welded, formed, attached, and otherwise handled like any other structural material used in aircraft fabrication.

Using the EB perforated titanium as a basis for the porous surface, a preliminary design for the LETA evolved as follows:

The surface of 0.025-inch-thick titanium is supported and stabilized by a corrugated carbon and fiberglass substructure approximately 1 inch thick and formed in such a way as to provide the spanwise suction flutes which in turn divide the surface into chordwise bands or strips. The alternate flutes between the suction flutes form lands that provide contoured surfaces to which the titanium is bonded to both hold the shape and separate the flutes into individually controllable units. A preliminary cross section concept of the Suction Panel is shown in Figure 3. Individual flute fittings carry the suction air from each flute to a tube which goes to a control valve that regulates the rate of suction airflow. An early concept of the valves required to control the flow in each tube consisted of individually adjustable valves manifolded to a common suction source. However, based on the LFC wind tunnel work at Langley where a special chamber valve assembly was under development, it was decided to develop a similar chamber valve to be fitted in the cabin of the JetStar. An early concept of the chamber valve configured with 15 needle valves is shown in Figure 4.

Besides the above basic system for achieving laminar flow by suction through a perforated surface, the DAC concept incorporates a protective shield/slat with provisions for extending and retracting it as required by the pilot. The primary purpose of the shield is to protect the airfoil surface from oncoming airborne debris that would otherwise strike the wing leading edge. Since during low-altitude operation the wing leading edge is most vulnerable to airborne contaminants such as insects, the shield is positioned ahead of the leading edge to intercept these contaminants during takeoff and landing operations. The shape of such a device that can be incorporated into a leading edge shape also makes it adaptable for use as a lift augmentation device, very much like a slat. Two other auxiliary systems attach to the shield and are operable only when the shield is in the fully extended position.

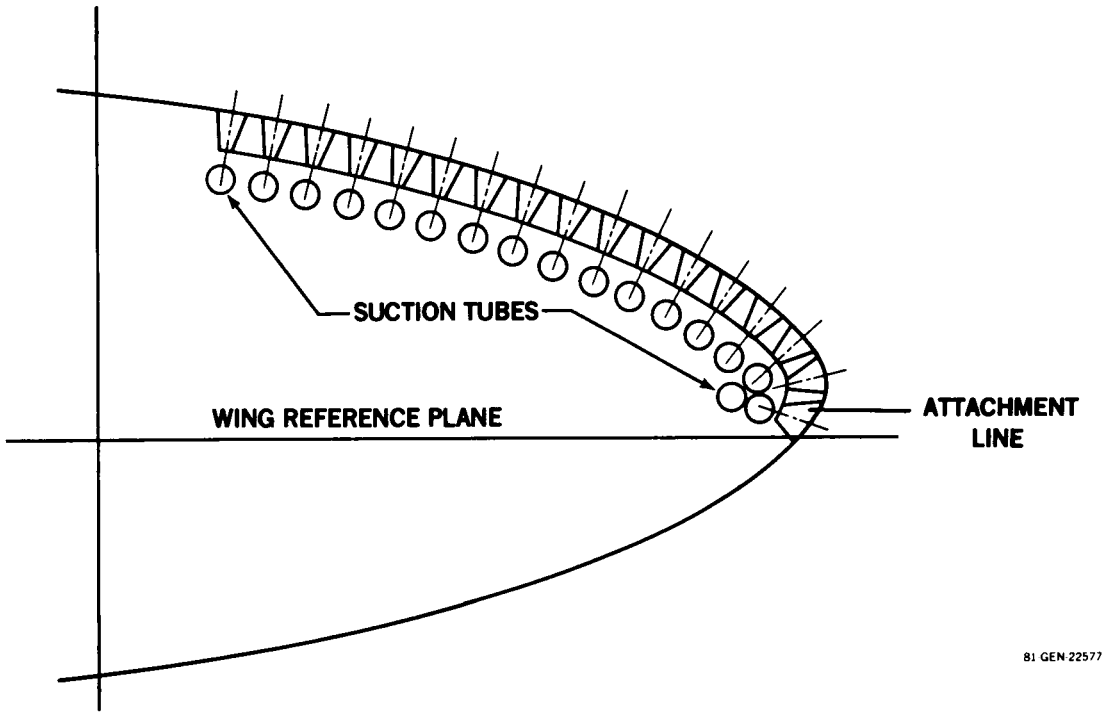

FIGURE 3. LEADING EDGE FLUTE AND SUCTION TUBE CONFIGURATION

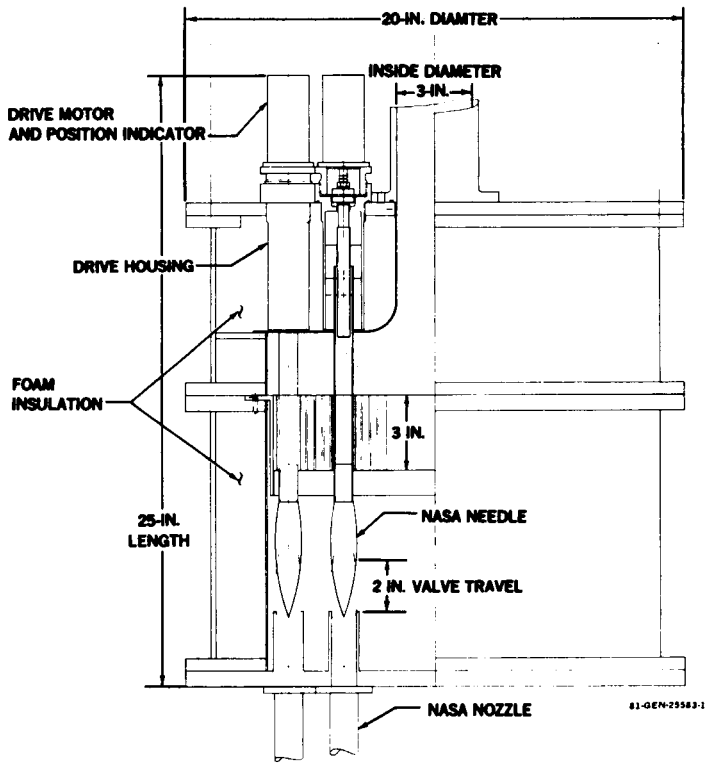

FIGURE 4. LFC CHAMBER VALVE PRELIMINARY LAYOUT

To supplement the protection from debris afforded by the shield, a contamination avoidance (CA) spray system is attached to the underside of the shield, Figure 5. This system consists of a series of fine spray nozzles directed at the leading edge so that a freezing point depressant liquid may be sprayed on the leading edge, coating the surface sufficiently to prevent any contaminant that eludes the shield from sticking to the leading edge. To prevent the liquid from passing through the perforated surface and flooding the suction passages, a small positive pressure is maintained in each flute relative to the surface pressure. The same valving system that regulates suction pressure can be utilized to control this positive pressure. Since the positive pressure required is quite small, any convenient source, such as engine bleed or cabin air pressurization, can supply this air for clearing the flutes and porous surface skin of any liquid, including rain and deicing fluids. Since most liquids become more viscous with lowering surface temperatures, the clearing air should be as warm as permissible in order to clear the surface as quickly as possible.

The second system is a deicing or ice protection (IP) system supplied by TKS of England. This consists of a thin reservoir shaped to form the leading edge of the shield, Figure 6. The outer surface of the reservoir is porous such that a glycol fluid pumped into the reservoir under pressure will ooze uniformly to wet the surface of the shield and prevent leading edge ice accumulation. Since the glycol fluid will migrate back onto the suction surface, the CA spray system may be needed for cleaning after the encounter. The CA spray is itself effective as a deicing agent for the leading edge suction surface. Since the PGME fluid in the CA spray is a freezing point depressant, it can be used to supplement the shield IP system.

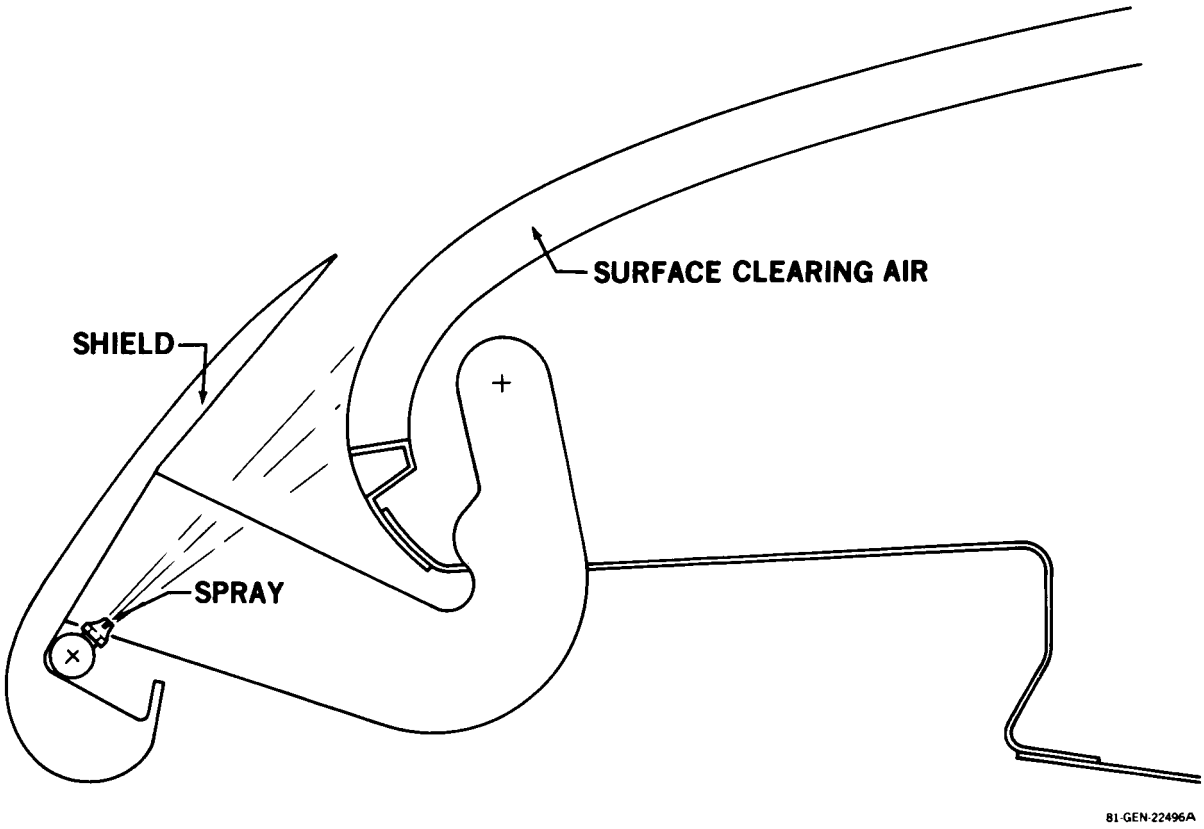

FIGURE 5. LEADING EDGE CONTAMINATION AVOIDANCE CONCEPT

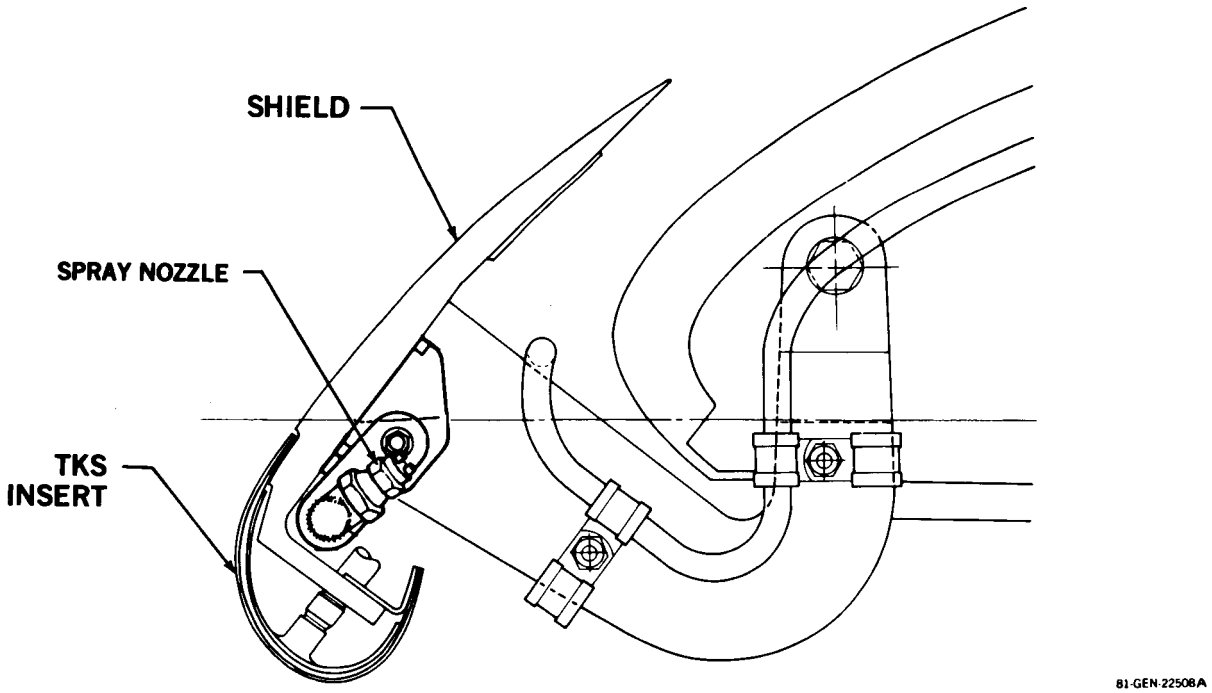

FIGURE 6. LEADING EDGE ICE PROTECTION CONCEPT

SECTION 5
AERODYNAMIC ANALYSIS

5.1 LEADING EDGE GLOVE SHAPE DEVELOPMENT

Desired LFC Glove Pressure Distribution and Design Criteria

Development of the aerodynamic shape for the LFC leading edge glove on the JetStar test vehicle began with the establishment of the desired pressure distribution for the test region and the desired flight test conditions. These items, along with the planform of the flight test article and fairings, were agreed to by NASA, GELAC, and DAC. The desired pressure distribution is shown in Figure 7, followed by the planform sketched in Figure 8.

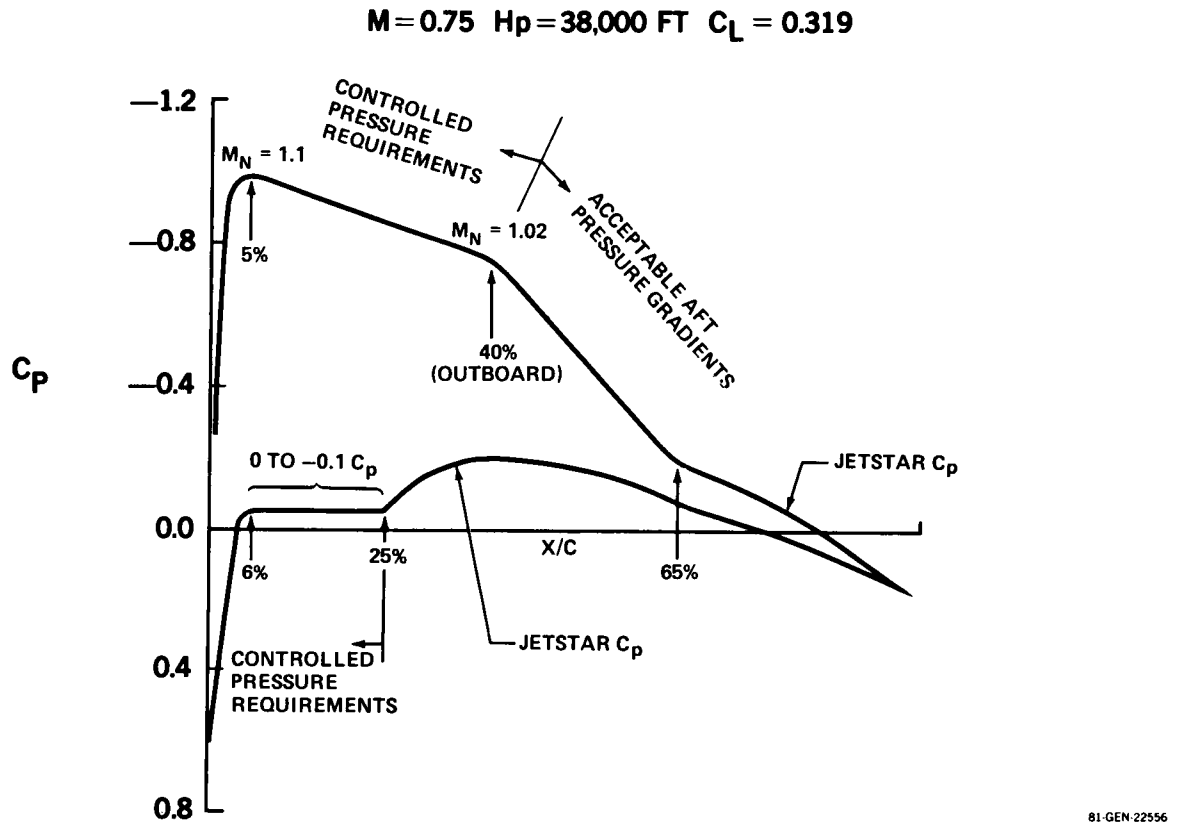

FIGURE 7. DESIRED LFC GLOVE PRESSURE DISTRIBUTION

PRECEDING PAGE BLANK NOT FILMED

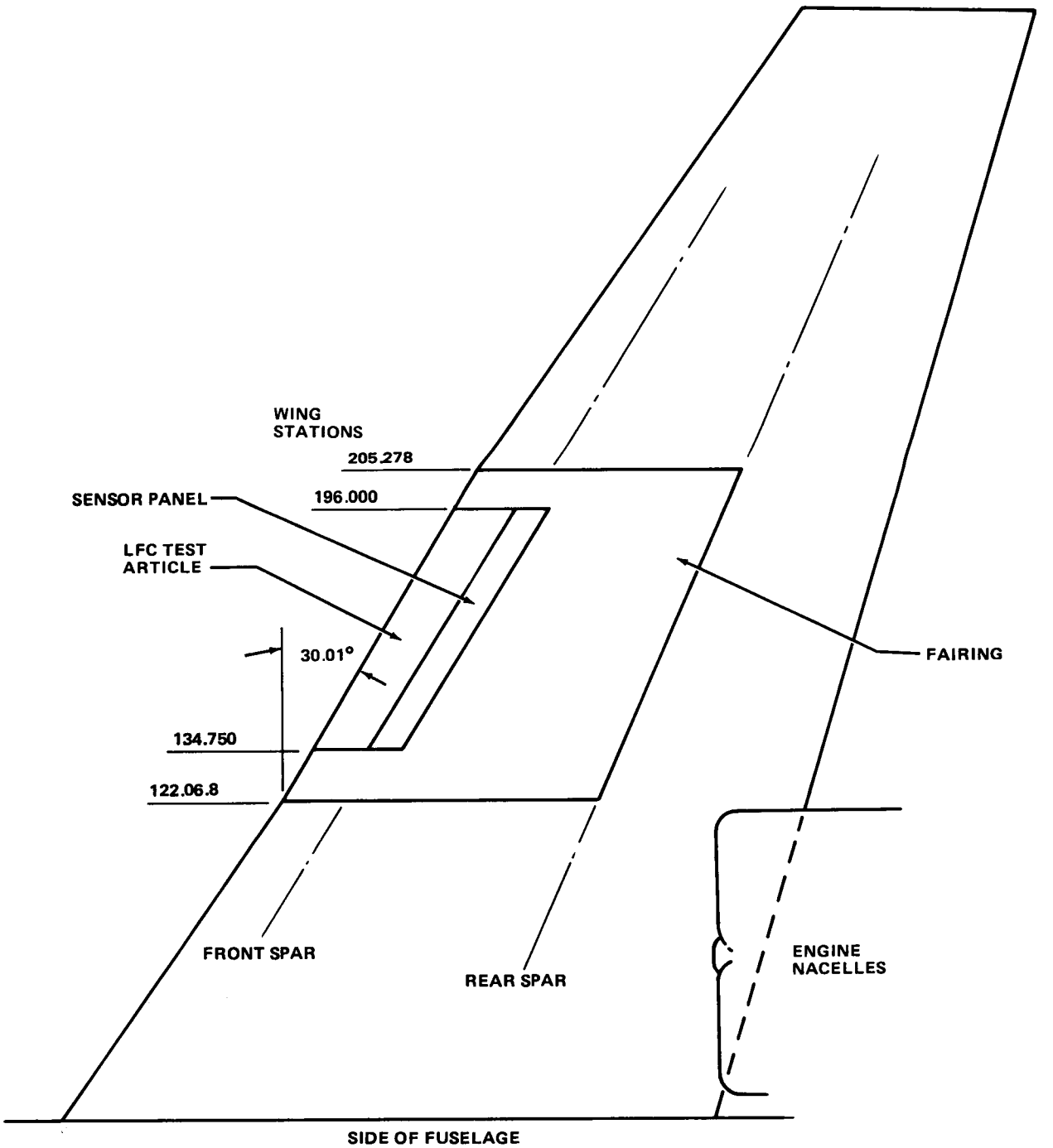

FIGURE 8. JETSTAR LFC TEST ARTICLE PLANFORM

The desired chordwise pressure distribution for the LFC glove region was a shock-free profile developed previously and described in Reference 4. This pressure distribution had a modest adverse gradient. The controlled pressure region on the upper surface was to be maintained streamwise to a distance from the leading edge corresponding to the 40-percent chord point of the outboard defining station. Within this region the resulting isobars should be parallel to the leading edge, insofar as possible, without violating the design criteria of forming the test article with straight line elements. In addition to the desired pressure profile, it was agreed that the attachment line Reynolds number (R_θ) should be within the range of 100 to 130.

The planform of the LFC flight test article was chosen to be compatible with the existing wing structure of the JetStar and to span the leading edge discontinuity which was previously covered by the wing mounted "slipper" fuel tanks. This results in the LFC test section having an inverse taper, where the outboard chord is larger than the inboard chord, ahead of the front spar. Chordwise, the glove was limited to the rear spar (65-percent chord) on the upper surface and to 25-percent chord on the lower surface. Spanwise, the LFC test region was located between wing stations 134.750 and 196.500. These stations were also the defining stations for the glove aerodynamic shape (i.e., between 0.42 and 0.62 semispan, respectively). Inboard and outboard transition fairings to the basic JetStar wing profile terminated at wing stations 122.068 and 205.278, respectively. The resulting leading edge sweep for this planform is 30.01 degrees, as indicated in Figure 8.

The flight conditions for development of the LFC leading edge glove design were established as:

Mach Number	0.75
Altitude	38,000 ft
Aircraft Weight	29,000 lb
Aircraft C_L	0.319

Initial Leading Edge Shape Development

Initial development of a leading edge shape at DAC began by application of the two-dimensional Tranen inverse Garabedian program (Reference 5) to define airfoils at the inboard and outboard defining wing stations, which met the desired pressure profile criteria. Because these airfoils were not readily compatible with the JetStar wing profiles, the more powerful and comprehensive Douglas/Jameson program was applied to the aerodynamic design of the glove shape (Reference 6). The Jameson program encompasses three-dimensional, transonic full-potential flow analysis and has a unique inverse capability which solves for the wing shape (geometry) to satisfy a prescribed pressure distribution. This program was then used to modify and adjust 3-D pressure distributions and leading edge test section shape so that a most satisfactory pressure distribution for LFC would be obtained within the established constraints of the modified JetStar wing.

An earlier parametric study, which correlated attachment line normal velocity derivative values with airfoil thickness and normal leading edge radius, was intended to assist in achieving the desired attachment Reynolds number (R_θ). However, it became evident during initial development of the leading edge shape that the pressure profile and geometric constraints were incompatible and would not allow any practical modifications of the leading edge shape to accommodate a specified value of R_θ. Thus, consideration of attachment line Reynolds number was essentially relegated to evaluation after the other constraints were satisfied.

Two major problem areas became evident in the aerodynamic shape development for the LFC leading edge flight test article. The first problem occurred because of the incompatibility between the desired LFC upper surface pressure profile, which required a slightly unfavorable gradient, and the extended favorable gradient of the basic JetStar upper surface inboard and outboard of the LFC test region. This situation was aggravated by the unusual planform with discontinuities in leading edge sweep angle. An illustration of the upper surface pressure incompatibility is shown in Figure 9, where the desired pressure profile for the LFC glove region is shown between the inboard and outboard pressures for the basic JetStar wing.

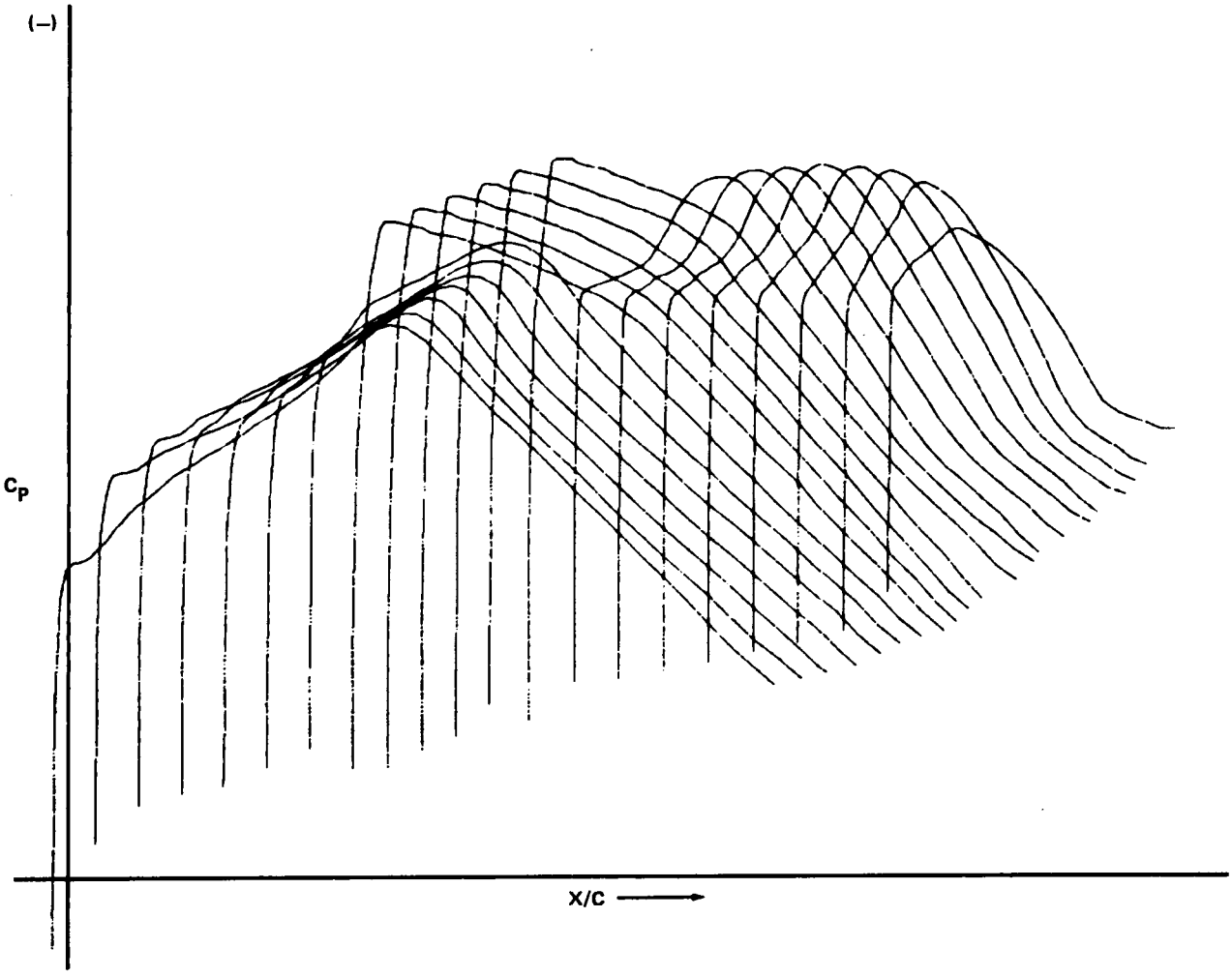

FIGURE 9. UPPER SURFACE PRESSURE DISTRIBUTION – JETSTAR WITH DESIRED LFC GLOVE PRESSURES

The second difficulty concerned the analytical modelling of the JetStar nacelles. These nacelles are located above the wing near the trailing edge where they significantly influence upper surface wing pressures. The 3-D transonic Jameson flow analysis program is limited to a detailed wing definition with a fuselage cross-flow correction based upon an infinite fuselage representation. Hence, nacelle geometry could not be directly included in the compressible wing flow analysis for the LFC leading edge flight article. To overcome this limitation, an analytical procedure was devised which modified the actual wing twist to account for the effect of nacelles on upper surface pressures. This method correlated well with data from tests of a Citation 650 wind tunnel model which had a similar fuselage-mounted nacelle configuration and provided detailed wing pressure data, with and without nacelles on the model. Briefly, the procedure used to correlate the Citation data and estimate the effect of nacelles was:

1. Compute the basic Jameson solution and correlate this with nacelles-off wind tunnel data.

2. Compute the Giesing vortex lattice solution with simulation of nacelles (Reference 7).

3. Compute the inverse Giesing solution, nacelles off, corresponding to the preceding forward solution with nacelles on.

4. Determine the effective twist distribution, from the preceding step, which produces an effect equivalent to that of the nacelles in Step 2.

5. Apply the effective twist to the basic Jameson input.

6. Compute the Jameson solution for the modified input and correlate this with the nacelles-on wind tunnel data.

Based upon results of the foregoing correlation, the leading edge glove shape for the JetStar wind tunnel model was developed. This development was accomplished cooperatively with GELAC in order to most efficiently integrate the leading edge test article shape into the basic JetStar wing. Thus, preliminary GELAC geometry was selected as the initial trial for developing the leading edge glove shape. The analytical procedure that was followed is outlined below.

1. The forward DAC Jameson solution was computed using the JetStar wing geometry with the GELAC preliminary LFC glove shape and estimated effective wing twist to account for the fuselage-mounted nacelles. This solution provided a reference for subsequent leading edge shape development. The upper surface isobar pattern is shown in Figure 10.

2. An inverse DAC Jameson solution was computed specifying the desired LFC pressure distribution within the leading edge test region (Figure 9). The isobar pattern for this solution is shown in Figure 11. The

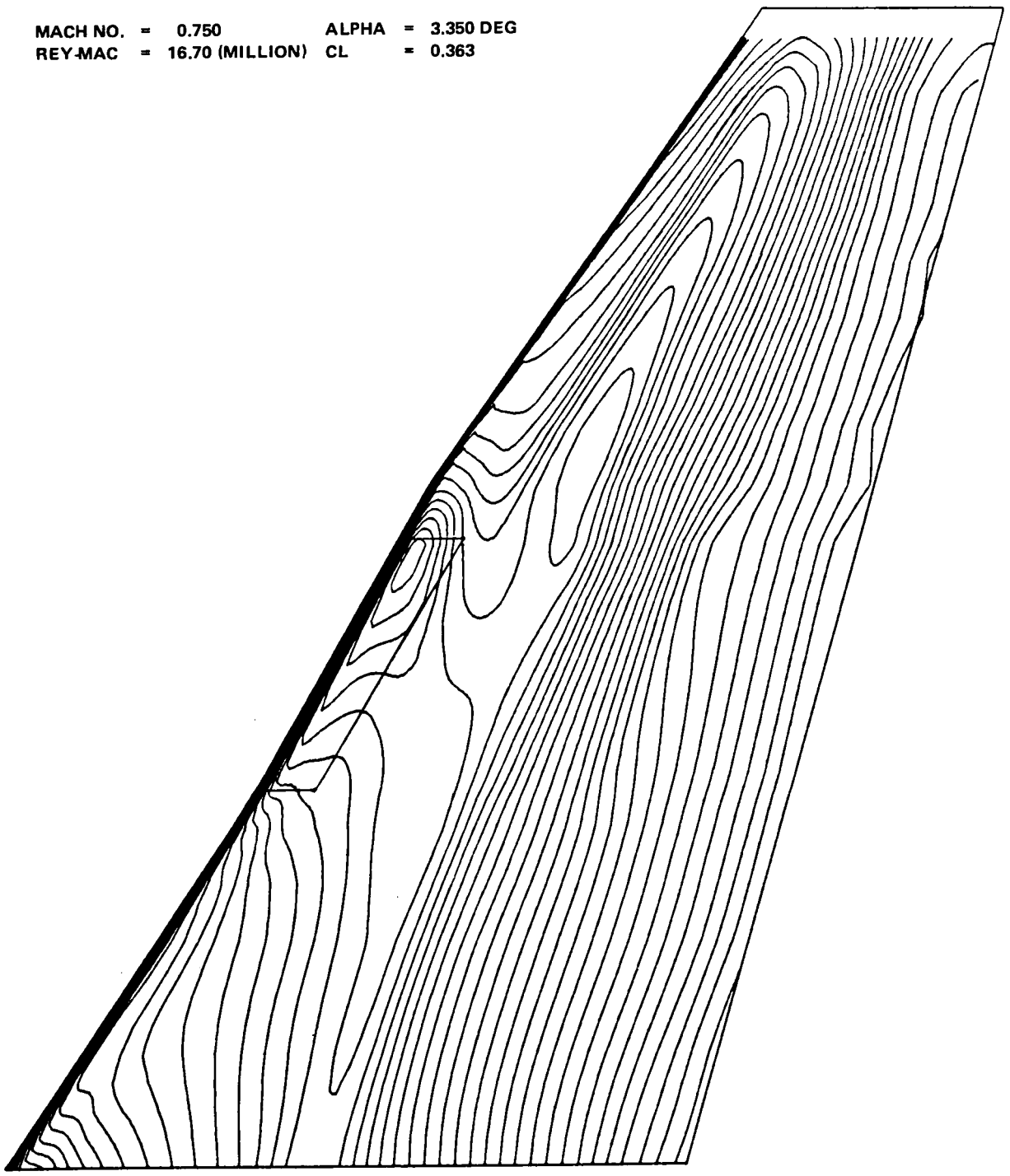

FIGURE 10. UPPER SURFACE ISOBARS – PRELIMINARY GLOVE SHAPE

MACH NO. = 00.750 ALPHA = 3.350 DEG
REY-MAC = 16.70 (MILLION) CL = 0.359

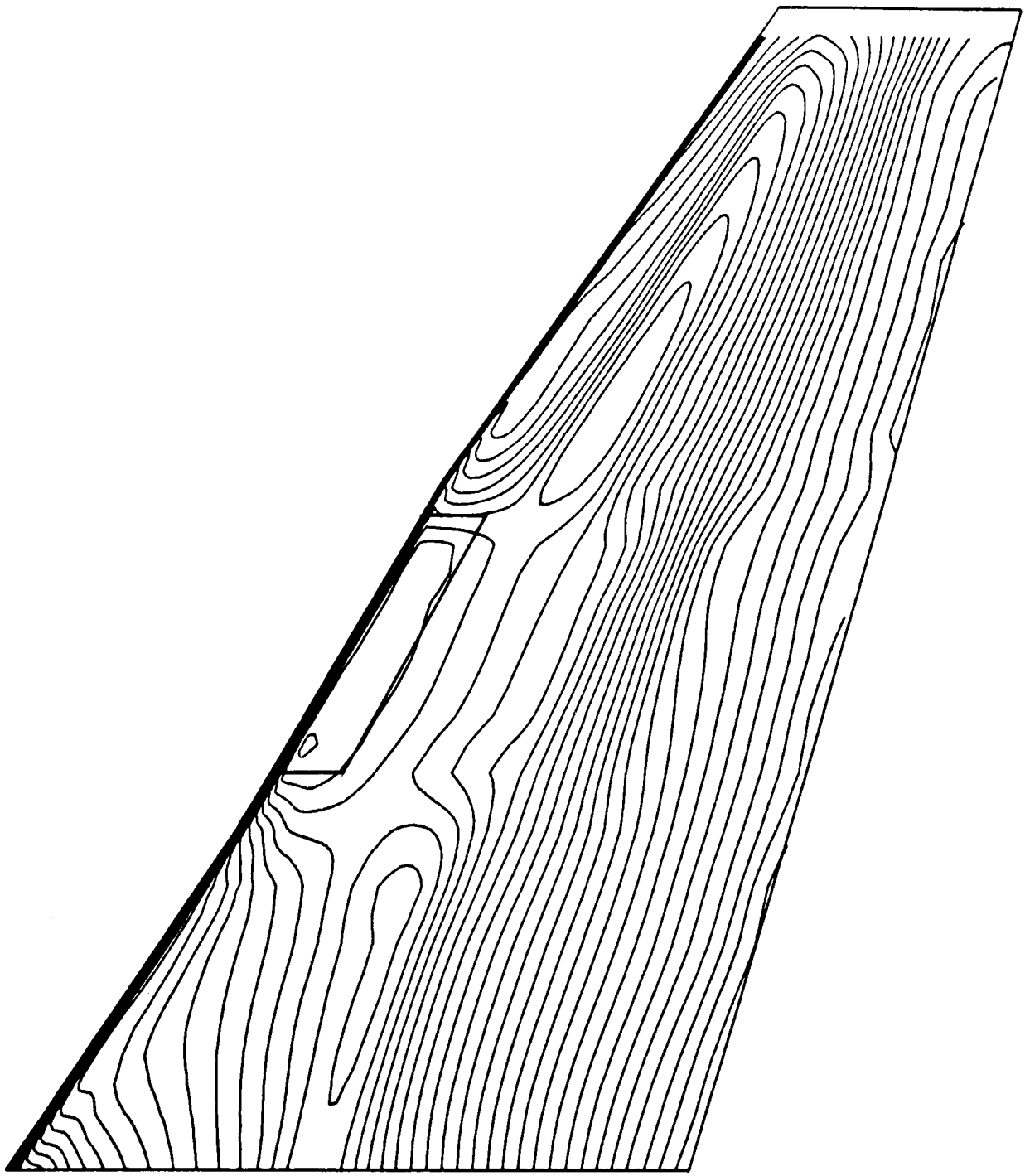

FIGURE 11. UPPER SURFACE ISOBARS – LFC TEST ARTICLE – DESIRED PRESSURE DISTRIBUTION

resulting wing contour, however, severely undercut the basic JetStar upper wing surface. Thus, the specified pressure distribution could not be achieved within the LFC test region using an external glove on the JetStar wing planform.

3. The inverse Jameson analysis was then applied to obtain wing geometry for modified pressure distributions in the LFC test region. After several adjustments a roof-top LFC pressure distribution was specified which resulted in a leading edge glove shape compatible with the basic JetStar wing contour. Figure 12 shows the upper surface isobars for this case. However, since surface geometry cannot be constrained using the inverse solution process, the resulting wing surfaces typically involve complex curvature, which is not desirable structurally. Thus, additional compromise was necessary to establish a leading edge glove surface having straight line elements.

4. A forward Jameson solution was then computed using straight line elements between the inboard and outboard defining stations for the LFC test region airfoil shape obtained in the preceding step. The resulting effect on the upper surface isobar pattern is shown in Figure 13. It is quite evident that the requirement for straight line elements on the LFC glove imposed a sensitive and difficult constraint upon the LFC glove shape development.

At this point in the aerodynamic development of the LFC glove shape, the defining airfoil sections corresponding to the flat roof-top solution were input into the Garabedian two-dimensional, transonic, potential flow analysis (Reference 8). This was done to evaluate the three-dimensional effects upon pressure distribution for the same airfoil section shape. The two-dimensional pressure distributions for the inboard and outboard defining airfoils are shown in Figure 14. The two-dimensional solution indicates a relatively strong shock in each case, while the three-dimensional solution did not show any evidence of a significant shock on the upper surface (Figure 9).

It is significant to note the discrepancy between the two- and three-dimensional pressure distributions for the same airfoil section geometry. Obviously, the design of the LFC leading edge glove shape could not be developed using simple sweep methods. This comparison emphasizes the three-dimensionality of the LFC leading edge glove aerodynamic design task and the sensitivity of the interaction between the flow in the test region and the basic JetStar inboard and outboard wing panels.

Subsequently, additional aerodynamic analysis by GELAC, using their FL022 program, and DAC using the Douglas/Jameson program, were conducted with frequent exchanges of data and results. Eventually, in order to establish the leading edge glove shape to be tested on the JetStar 10 percent scale wind tunnel model, GELAC and DAC aerodynamicists worked jointly at DAC to develop mutually acceptable leading edge glove geometry. Minor modifications were

MACH NO. = 0.750 ALPHA = 3.350 DEG
REY-MAC = 16.70 (MILLION) CL = 0.362

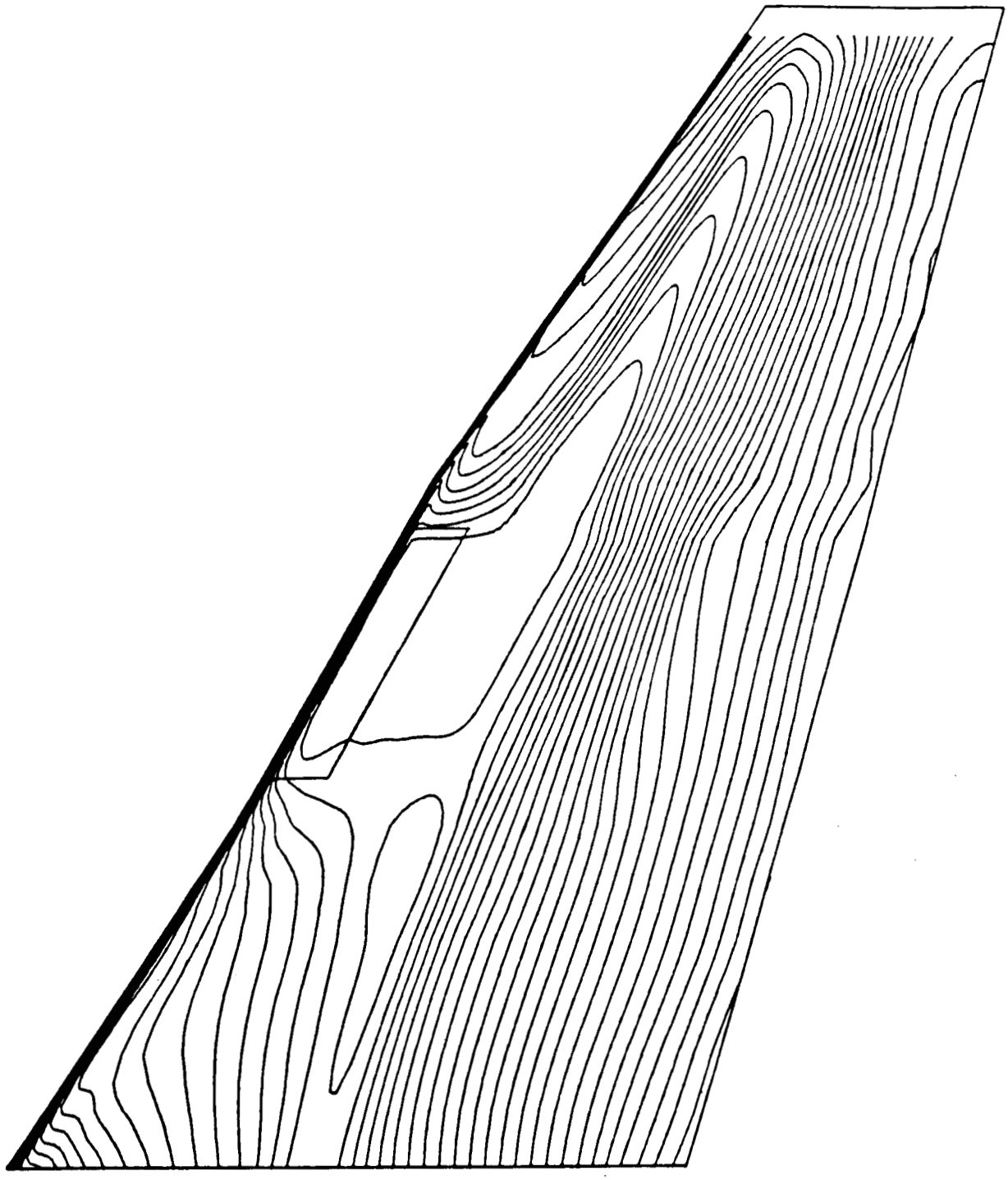

FIGURE 12. UPPER SURFACE ISOBARS – LFC TEST ARTICLE – MODIFIED FLAT ROOF-TOP PRESSURE DISTRIBUTION

MACH NO. = 0.750 ALPHA = 3.250 DEG
REY-MAC = 16.70 (MILLION) CL = 0.353

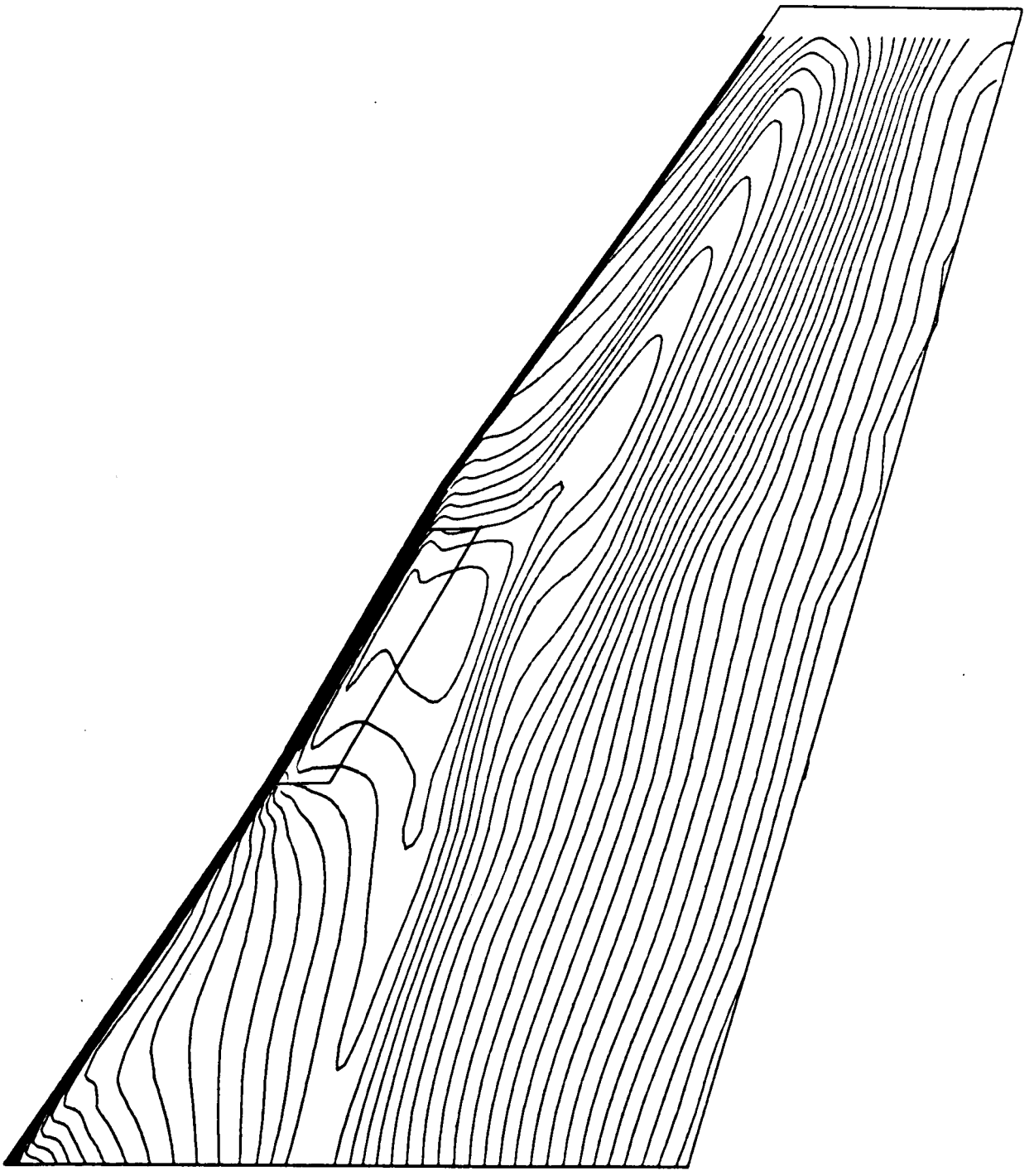

FIGURE 13. UPPER SURFACE ISOBARS – LFC TEST ARTICLE – MODIFIED ROOF-TOP GEOMETRY WITH STRAIGHT-LINE ELEMENTS

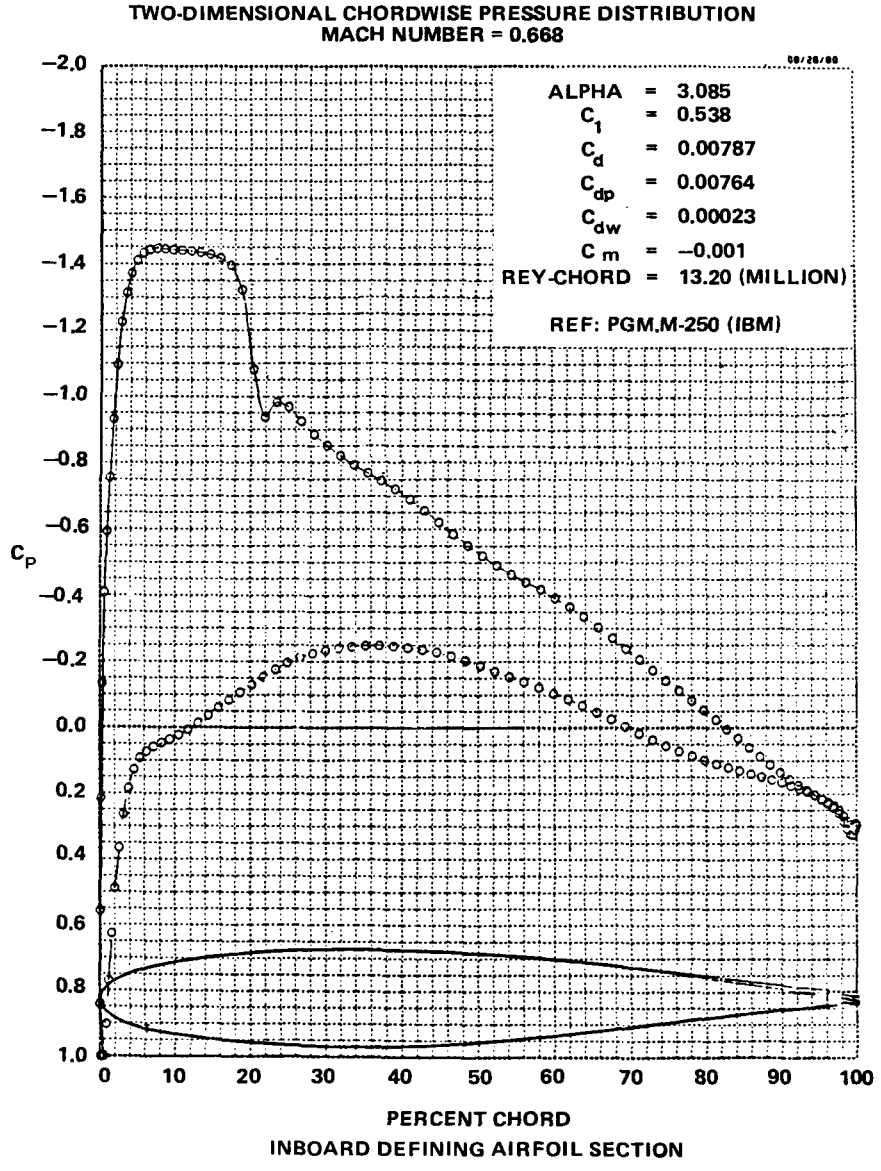

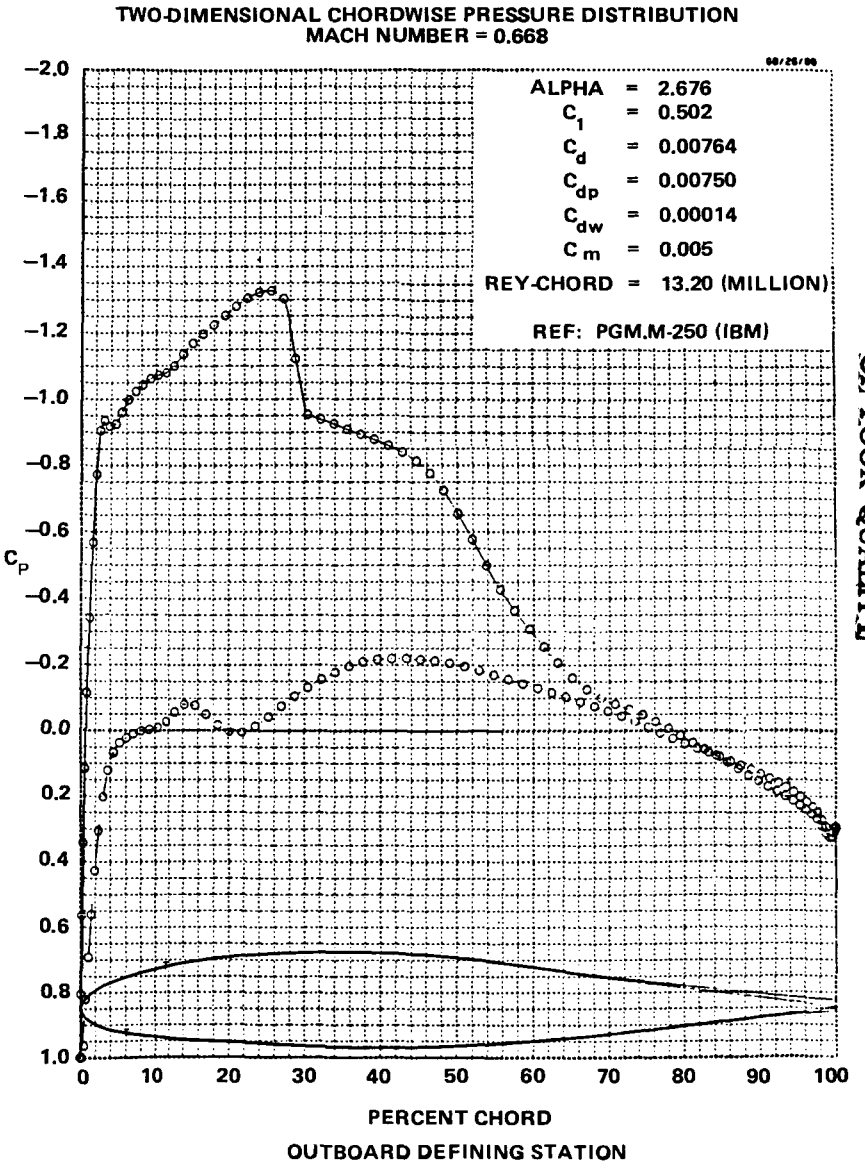

FIGURE 14. GARABEDIAN TWO-DIMENSIONAL SOLUTION FOR MODIFIED FLAT ROOF-TOP GEOMETRY

ORIGINAL PAGE IS
OF POOR QUALITY

made to facilitate lofting of the JetStar wind tunnel model wing glove and to accommodate lower surface adjustments pertinent to the GELAC LFC configuration. Upper and lower surface pressure distributions for this geometry are shown in Figure 15 and the isobar patterns are in Figure 16.

Having established the shape for the LFC leading edge flight test article on the 10 percent wind tunnel model, several off-design conditions were investigated to evaluate effects of changes in lift coefficient and Mach number. Jameson solutions were obtained for the following flight conditions:

Mach No.	Pressure Altitude (ft)	Lift Coefficient (wing-body)
0.75	38,000	0.358 (Design Cond)
0.75	35,000	0.265
0.75	40,000	0.415
0.72	38,000	0.374

At these off-design flight conditions, there were no adverse effects evident on the upper surface pressure distributions throughout the LFC leading edge test region.

5.2 JETSTAR WIND TUNNEL MODEL TEST

Wind tunnel tests of the 10 percent scale JetStar model were conducted at CALSPAN. The purpose of this test program was twofold. First, it was necessary to evaluate the flying qualities of the JetStar with the wing glove modification and with the asymmetric extension of the Douglas leading edge shield on the starboard wing. The second purpose was to confirm the wing pressures on the glove and substantiate the analytical flow prediction methods which were used to account for the nacelle effects on the wing pressures. Although the wind tunnel test was accomplished as a GELAC task, DAC provided technical support relative to the glove shape development.

It was determined from the wind tunnel test data that flight characteristics of the JetStar would be acceptable. Adequate control was available with existing JetStar lateral and directional control systems to operate the aircraft with the DAC leading edge shield extended on the starboard wing only. Also, the low-speed high-lift data indicated that, as intended, the extended shield had essentially no effect upon maximum lift.

The initial glove shape on the model produced a relatively irregular pressure distribution, which was improved by in-tunnel rework of the LFC glove region. Further modification of the glove shape improved the pressure distribution in the LFC test region. A shape was developed which was satisfactory and considered final. Further tests of the final shape were then run to determine the sensitivity to off-design conditions and the effects of the model nacelles on wing pressures.

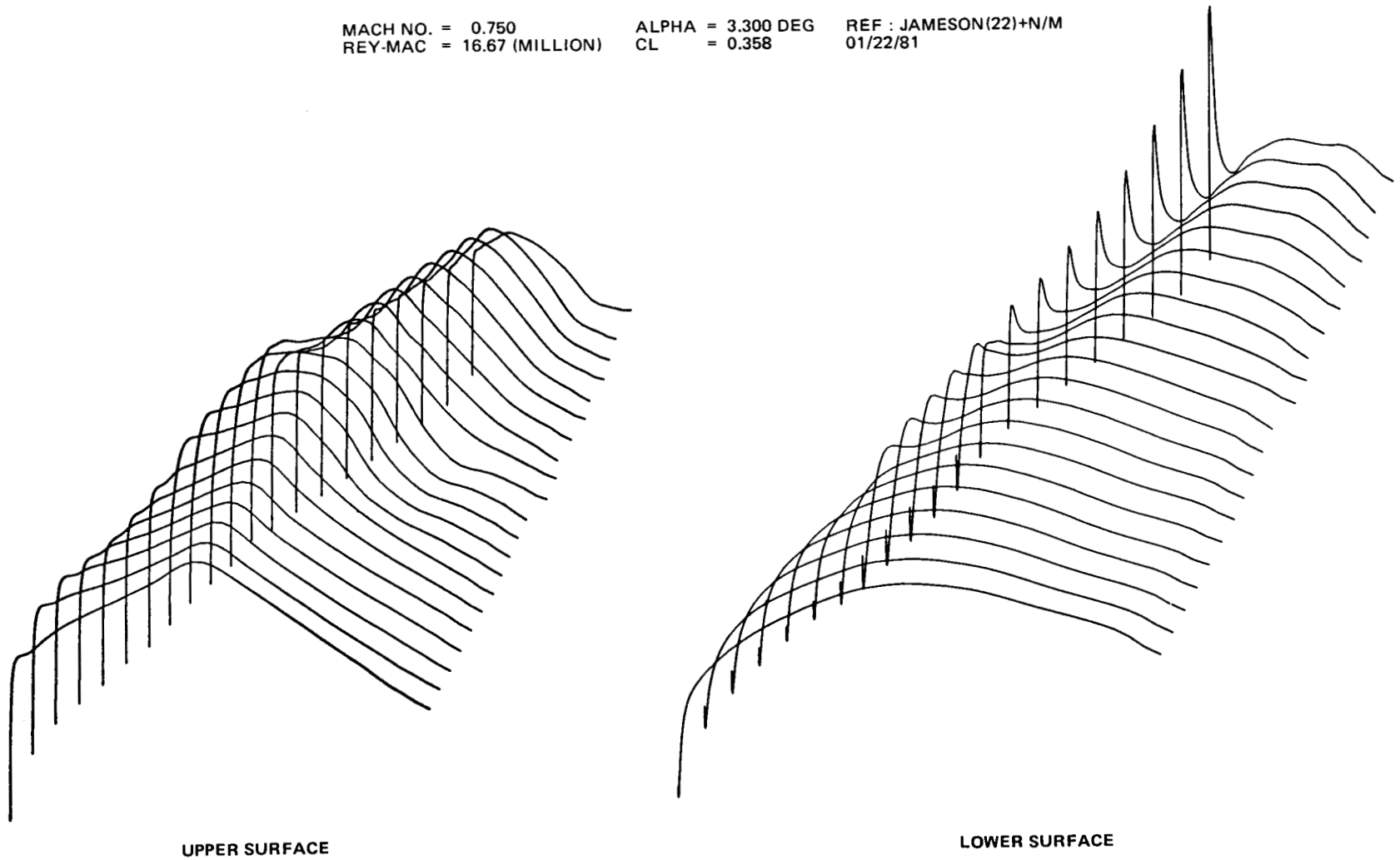

FIGURE 15. SURFACE PRESSURE DISTRIBUTION – LFC TEST ARTICLE – MOD 7Q SHAPE ON JETSTAR WING

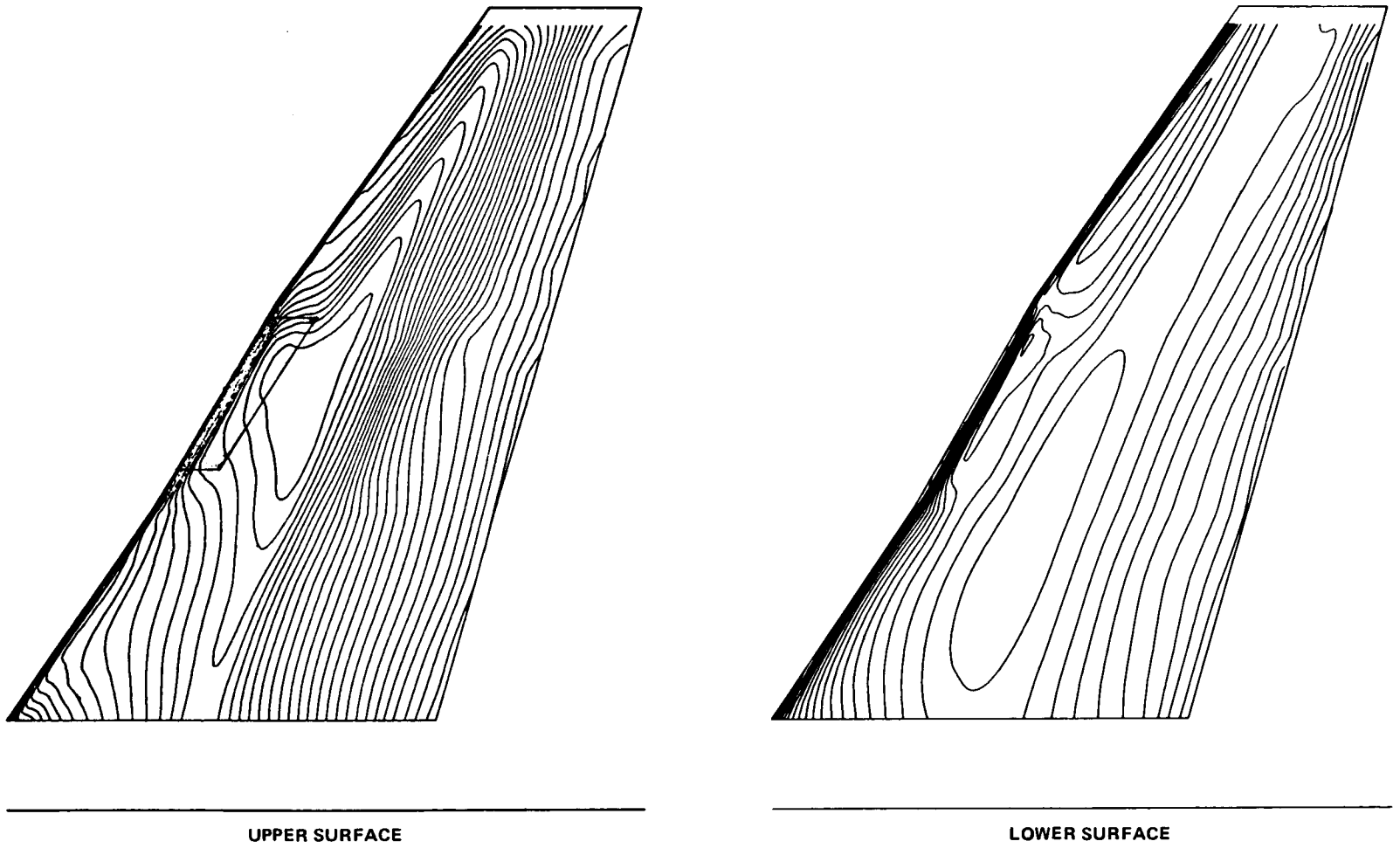

FIGURE 16. SURFACE ISOBARS – LFC TEST ARTICLE – MOD 7Q SHAPE ON JETSTAR WING

To substantiate, at least partially, the DAC Jameson transonic flow analysis, the experimental pressures measured on the recontoured LFC glove shape were compared with the corresponding analytical result for the analytically smoothed shape. This comparison is presented in Figure 17 and shows the agreement between experimental and analytical results for the nacelles-off configuration.

Final LFC Glove Shape Development

Development of the final LFC glove shape and prediction of the wing pressures on the JetStar LFC leading edge test article, with nacelles on, is outlined in the paragraphs below. This task was best accomplished by applying the experimentally determined incremental pressures, due to the nacelles, to the analytically determined pressures from the Douglas/Jameson program for the wing-body configuration.

The first step in adapting the JetStar wind tunnel model test results to the flight test article was the measurement of the recontoured glove shape. Analytical smoothing techniques were then applied to the recontoured shape and straight line elements specified between the glove shape defining airfoil sections. The result of this smoothing and a comparison with the corresponding JetStar airfoil sections are shown in Figure 18. This glove shape was designated MOD 8.

Pressure distributions for the MOD 8 glove shape, nacelles-off, were obtained using the DAC/Jameson program and are the basis for estimating surface pressures on the JetStar wing with the LFC glove.

The method developed initially, using an effective twist to adjust the DAC/Jameson analysis for the effects of fuselage-mounted nacelles above the wing, was less than satisfactory for the JetStar wing-fuselage-nacelle configuration. An alternative procedure, based upon the JetStar model wind tunnel test data, was devised to estimate upper surface pressures on the LFC leading edge flight test article.

Analysis of the CALSPAN wind tunnel test data for the JetStar with nacelles on and nacelles off showed that the nacelles had a relatively small effect on the pressure profiles in the leading edge test region when compared at constant angle of attack. Influence of the nacelles on upper surface pressures becomes significant downstream of approximately 16 percent chord. A representative example of the nacelle effect on wing pressures is shown in Figure 19. The inboard section of the LFC test article ends at approximately 12.5 percent chord while the outboard section extends to approximately 18 percent chord.

Incremental pressures due to the presence of the JetStar nacelles were obtained from the JetStar CALSPAN test data by comparing nacelles-on and nacelles-off wing pressures at constant angle of attack. These data verified the suppression of the flow over the wing upper surface due to the nacelles. The increments were reasonably consistent, in terms of pressure coefficient (C_p), over the span of the LFC test area and the nominal range of lifting conditions for the flight test program. The effect of Mach number on the nacelle increments was found to be small for the expected flight test Mach number variations. Thus, a single curve was established for the average

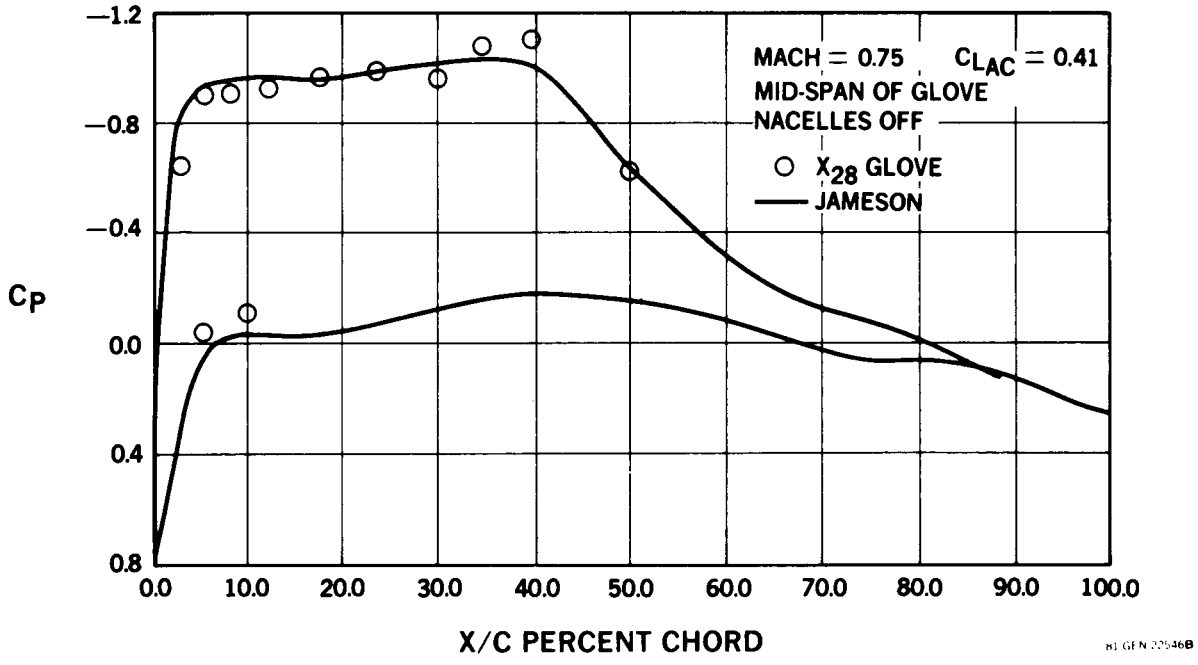

FIGURE 17. COMPARISON OF ANALYTICAL AND EXPERIMENTAL PRESSURES ON LFC GLOVE – 10 PERCENT SCALE JETSTAR MODEL GLOVE CONFIGURATION X_{28} AND JAMESON ANALYTICAL RESULT

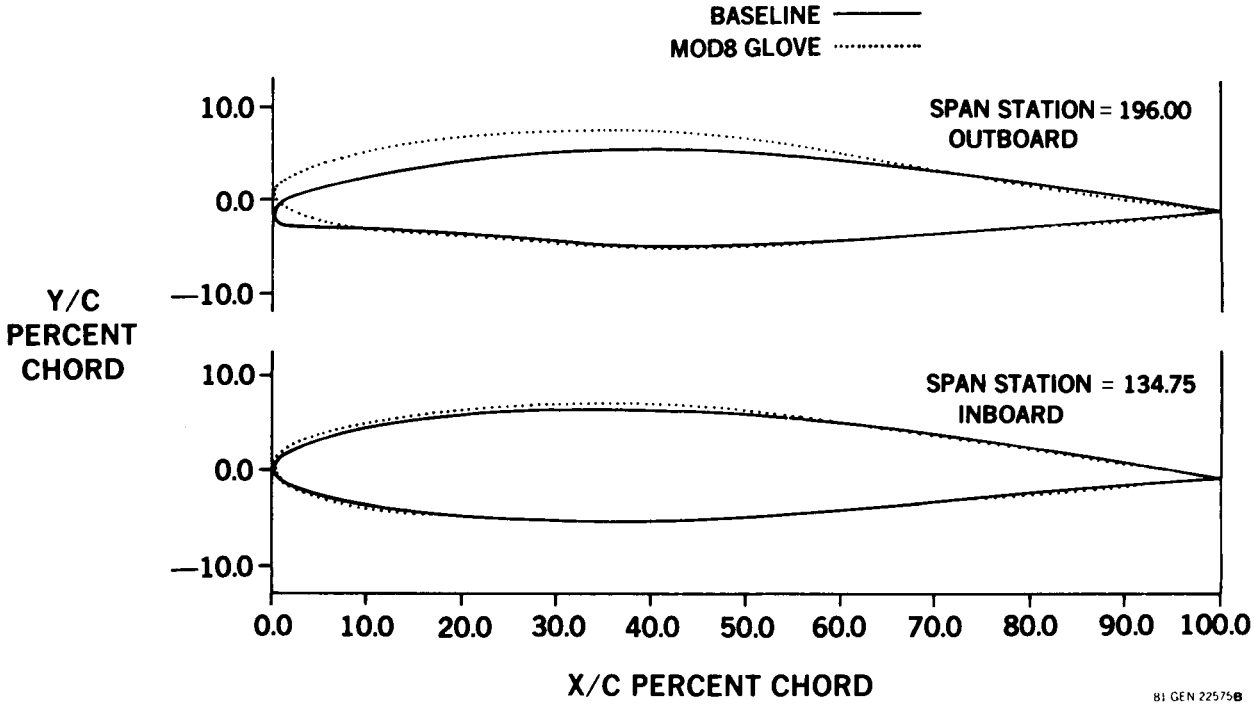

FIGURE 18. COMPARISON OF BASIC JETSTAR WING SECTIONS AND MOD 8 LFC GLOVE DEFINING AIRFOIL SHAPES

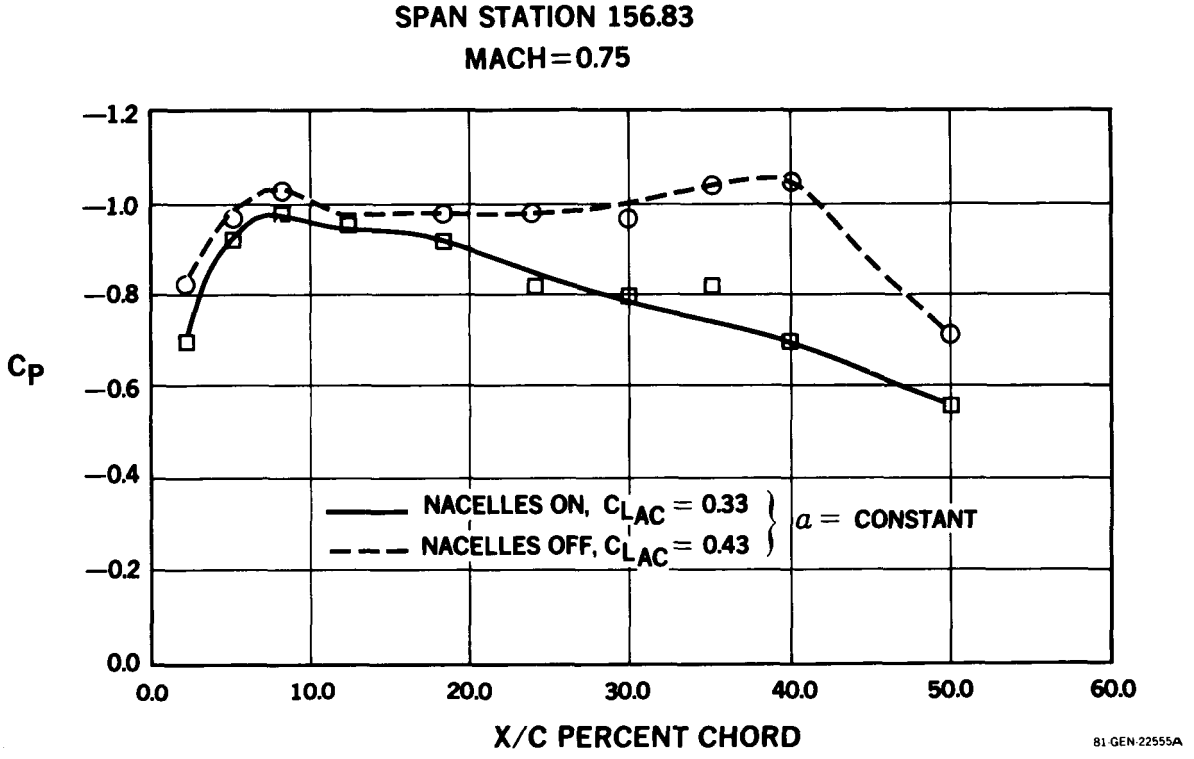

FIGURE 19. REPRESENTATIVE EXAMPLE OF NACELLE EFFECT ON WING PRESSURES – JETSTAR MODEL TEST

effect of the JetStar nacelles on the LFC test region upper surface chordwise pressures. The resulting curve of $\Delta C_{p\ nacelles}$ vs chord station is shown in Figure 20.

Predicted wing pressures, nacelles on, for the JetStar MOD 8 glove shape were obtained by applying the incremental pressures due to the nacelles (Figure 20) directly to the computed pressures for the nacelles off case. The resulting predicted pressures for the JetStar LFC glove, at design flight condition, are presented in Figures 21a through 21e. Five span stations encompassing the LFC glove test region are shown.

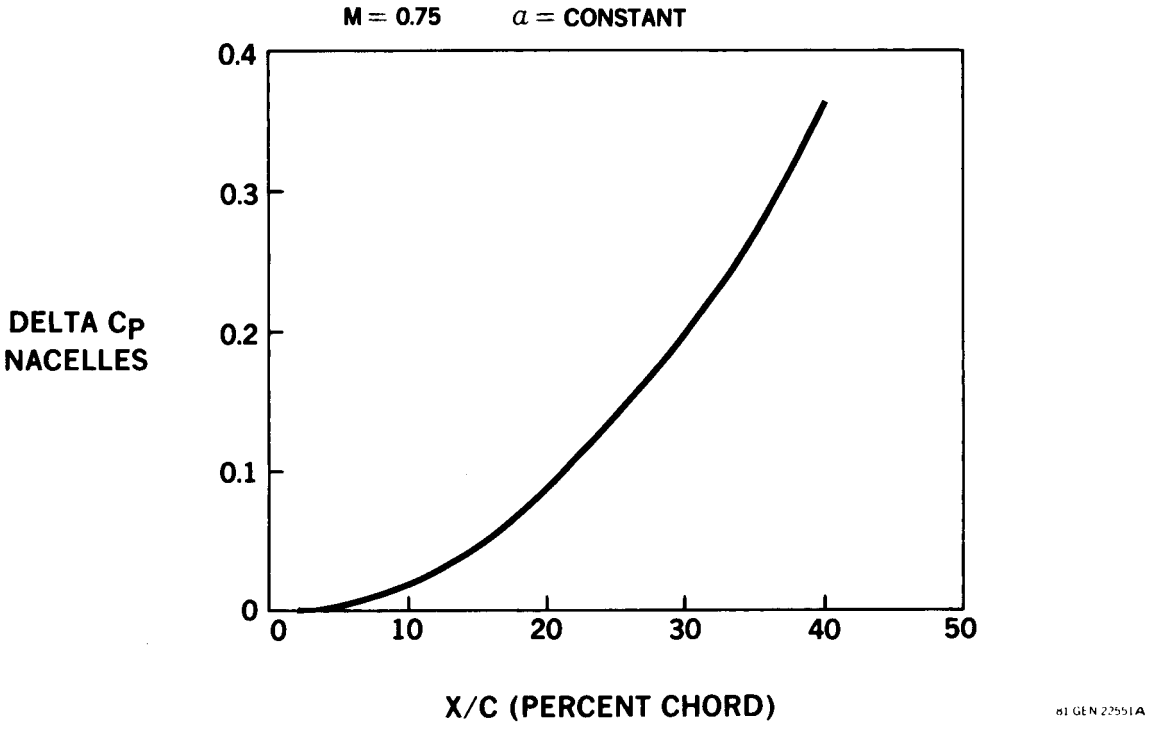

FIGURE 20. SUMMARY OF INCREMENTAL PRESSURE COEFFICIENT DUE TO NACELLES – JETSTAR MODEL TEST

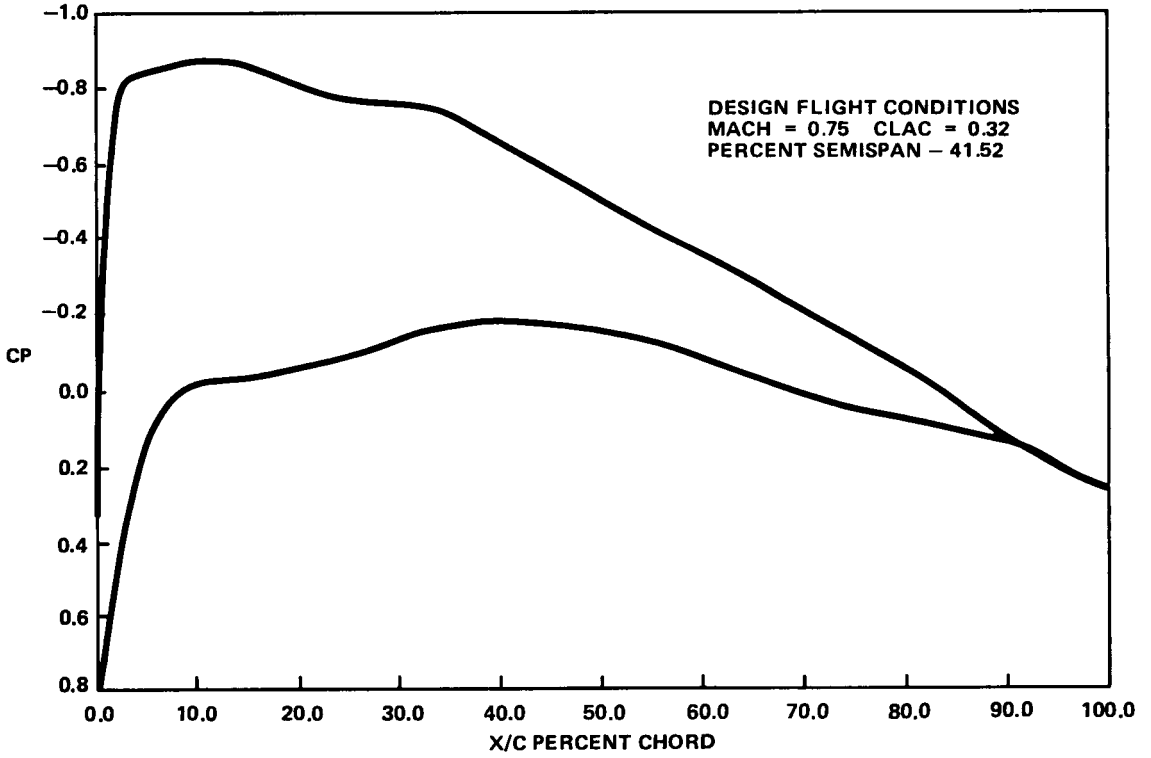

FIGURE 21a. PREDICTED PRESSURE DISTRIBUTION, NACELLES ON – LFC TEST ARTICLE MOD 8 SHAPE (41.54 PERCENT SEMISPAN)

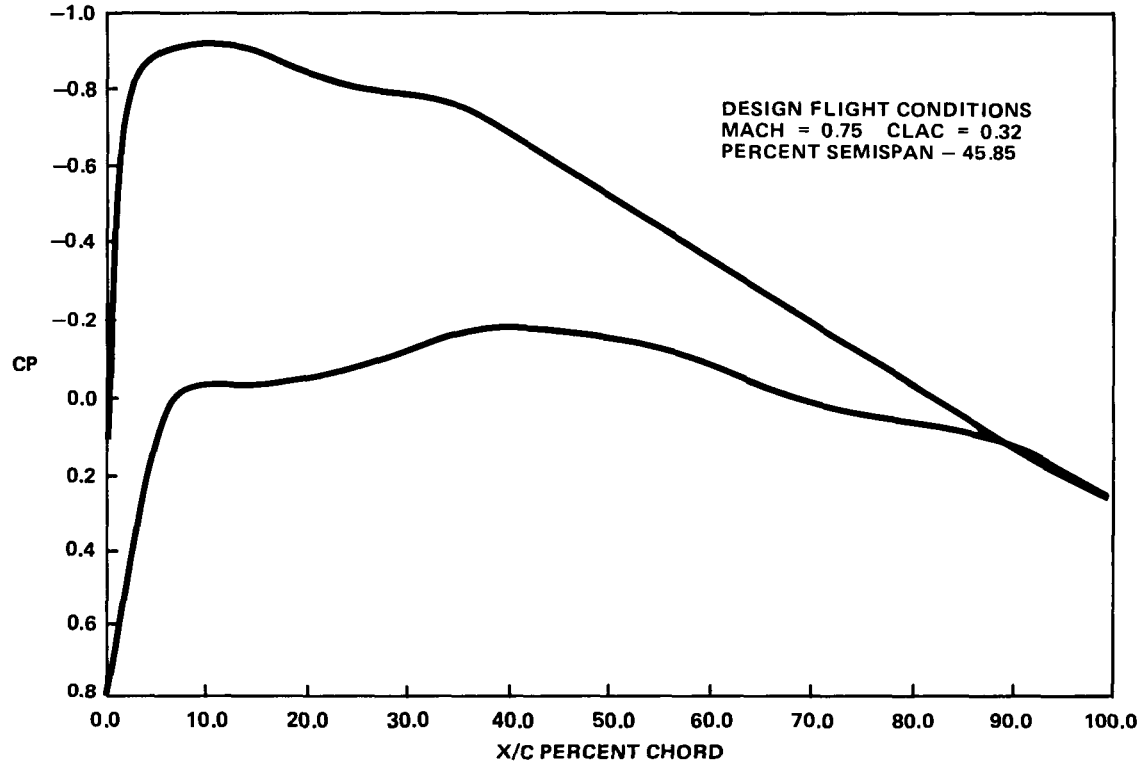

FIGURE 21b. PREDICTED PRESSURE DISTRIBUTION, NACELLES ON – LFC TEST ARTICLE – MOD 8 SHAPE (45.85 PERCENT SEMISPAN)

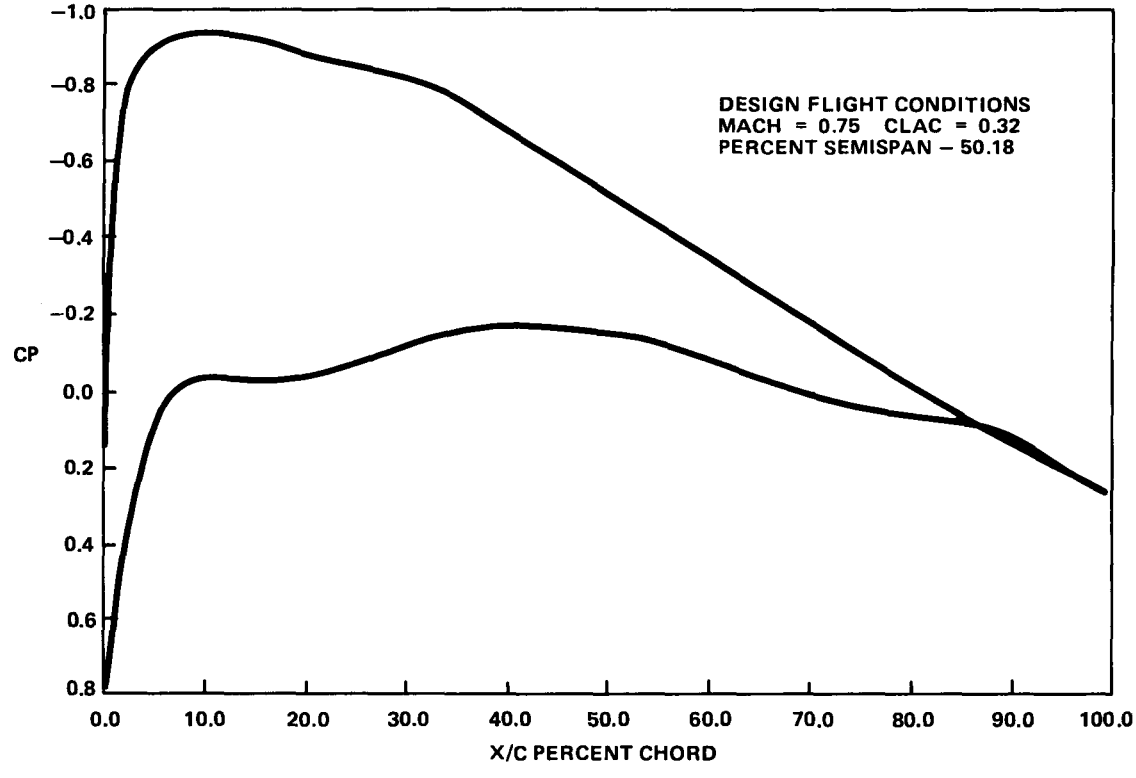

FIGURE 21c. PREDICTED PRESSURE DISTRIBUTION, NACELLES ON – LFC TEST ARTICLE – MOD 8 SHAPE (50.18 PERCENT SEMISPAN)

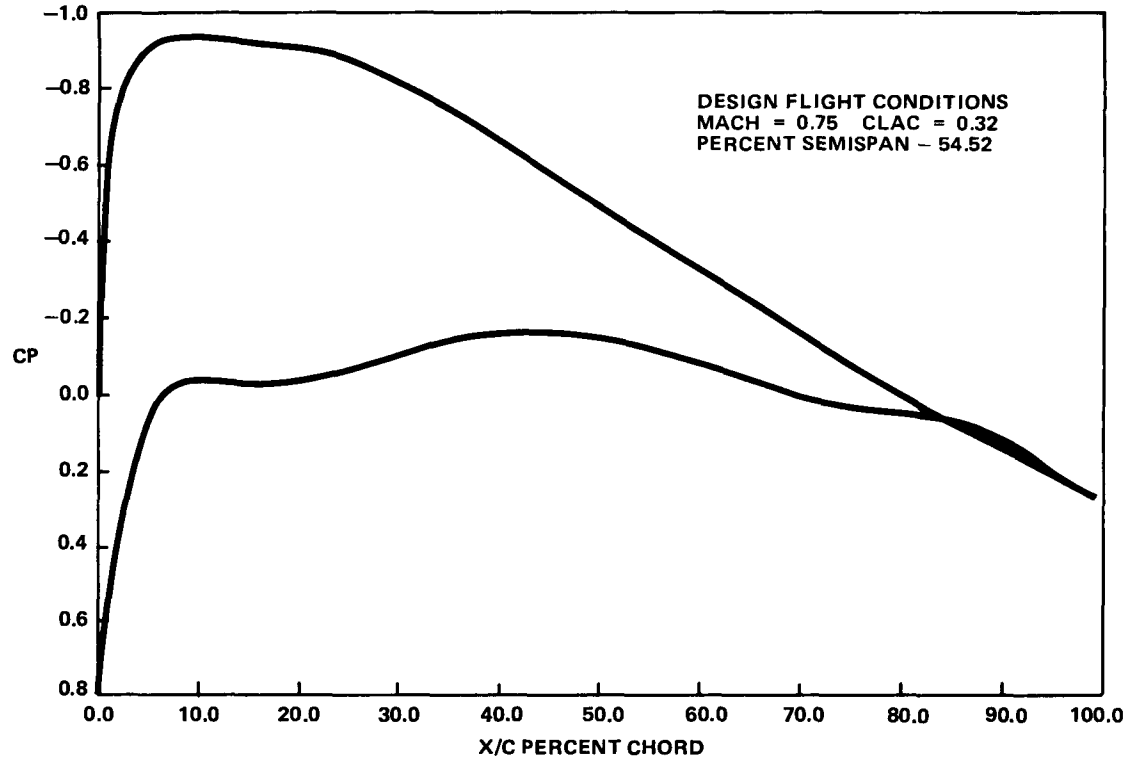

FIGURE 21d. PREDICTED PRESSURE DISTRIBUTION, NACELLES ON – LFC TEST ARTICLE – MOD 8 SHAPE (54.52 PERCENT SEMISPAN)

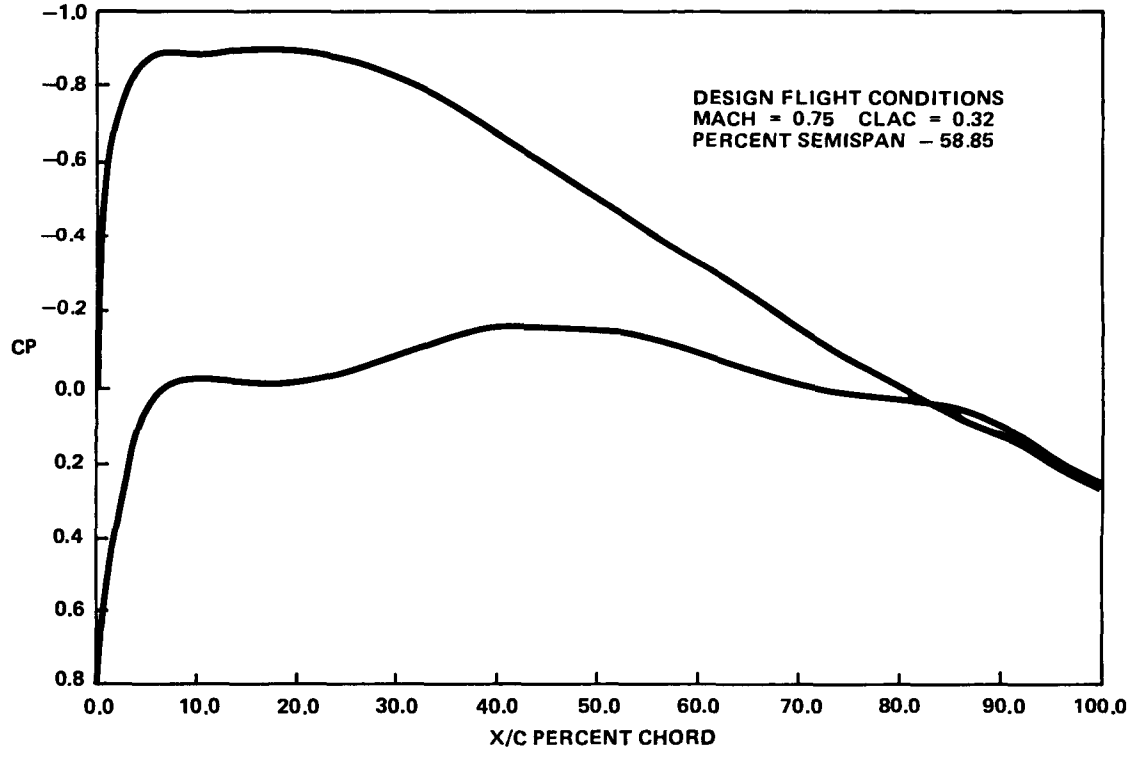

FIGURE 21e. PREDICTED PRESSURE DISTRIBUTION, NACELLES ON – LFC TEST ARTICLE – MOD 8 SHAPE (58.85 PERCENT SEMISPAN)

The predicted pressure distribution for the MOD 8 leading edge shape, at midspan of the test region, with nacelles on, is shown in Figure 22 and compared with CALSPAN test data for the recontoured leading edge shape. This comparison indicates the validity of the procedure developed to predict flight condition wing pressures on the JetStar LFC glove. The key to this method is the match- ing of analytical and measured pressure coefficients in the leading edge region where effects of the nacelles are minimal. Also shown for comparison in Figure 22 is the upper surface portion of the originally specified pressure profile (Figure 7). This shows that the MOD 8 shape substantially achieves the desired profile for the LFC leading edge glove flight test article.

At the design Mach number, the effects of lift coefficient variation on wing pressures were evaluated using the method outlined above. The resulting off-design pressure profiles of the LFC leading edge glove at midspan are given in Figure 23. The differences presented here correspond to a 15 percent change in lift from the design value and represent the expected range of flight test lift coefficients. Reference nacelles-off Jameson calculations for the off-design cases verified that the pressure profiles remain well behaved in both the increased and decreased lifting conditions.

5.3 LFC LEADING EDGE GLOVE DEFINING AIRFOILS

Coordinates for the leading edge glove defining airfoils are tabulated in Tables 1 and 2. These are the streamwise airfoils developed for the inboard and outboard wing stations of the leading edge test article, wing stations 134.750 and 196.000, respectively. Geometric wing surface development for the Douglas/Jameson and GELAC/FL022 transonic potential flow computation was based upon spanwise straight line elements between these defining airfoils. It should be noted that the LFC leading edge test article surface lofted by GELAC was developed using straight line elements which were adjusted and distributed to provide straight line elements along the front spar plane, the trailing edge of the upper surface fairing, and the leading edge. This adjustment resulted in a more-or-less "accordion" effect on the arrangement of the straight line elements on the test article and upper surface fairing. However, such an anomaly between the analytical and lofted surfaces does not significantly affect the end result.

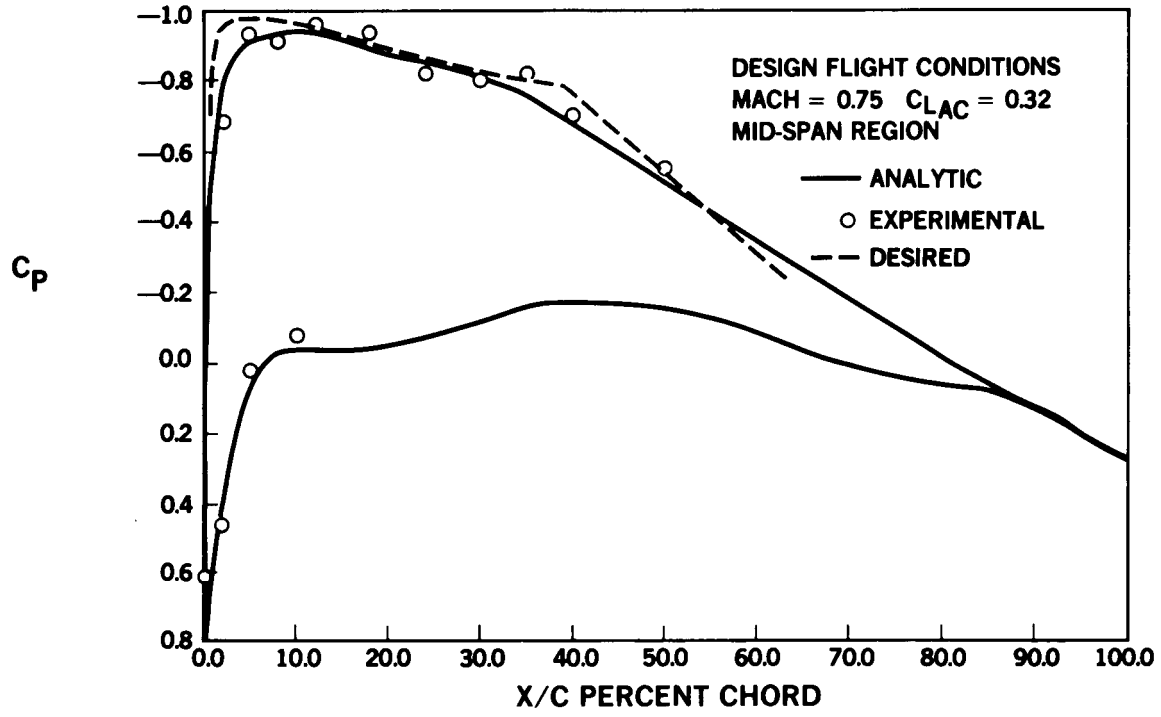

FIGURE 22. COMPARISON OF PREDICTED PRESSURE DISTRIBUTION WITH JETSTAR MODEL TEST DATA AND DESIRED LFC PRESSURE DISTRIBUTION

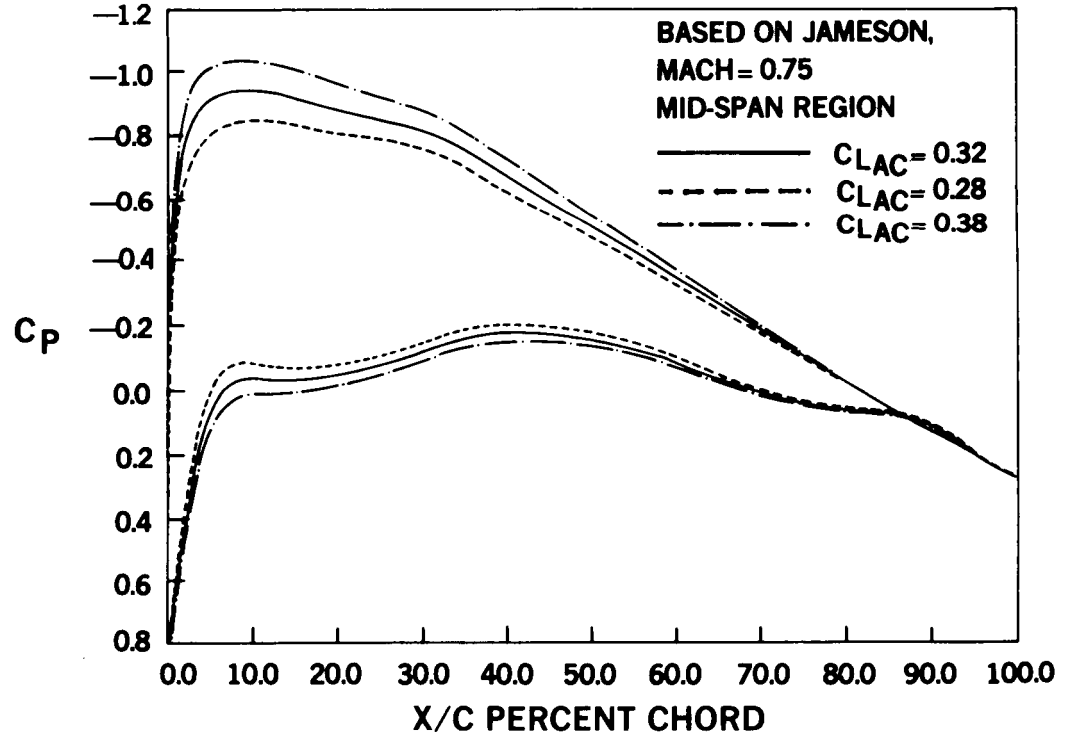

FIGURE 23. PREDICTED OFF-DESIGN PRESSURE PROFILES AT LFC TEST ARTICLE MIDSPAN

TABLE 1

LEADING EDGE GLOVE DEFINING AIRFOIL COORDINATES

Inboard Station, Y = 134.750
Wing Reference System Dimensions - Inches

Upper Surface			Lower Surface		
X	Y	Z	X	Y	Z
190.38484	134.75000	-1.514761	61.81308	134.75000	-0.160770
190.25812	134.75000	-1.494420	62.18457	134.75000	-0.739580
189.87845	134.75000	-1.433550	62.80798	134.75000	-1.321460
189.24742	134.75000	-1.332370	63.68053	134.75000	-1.928860
188.36751	134.75000	-1.191330	64.79874	134.75000	-2.558210
187.24223	134.75000	-1.010940	66.15866	134.75000	-3.177430
185.87598	134.75000	-0.791960	67.75562	134.75000	-3.743440
184.27419	134.75000	-0.535280	69.58366	134.75000	-4.225750
182.44305	134.75000	-0.241940	71.63570	134.75000	-4.618770
180.39000	134.75000	0.086850	73.90332	134.75000	-4.937550
178.12302	134.75000	0.449980	76.37726	134.75000	-5.206000
175.65106	134.75000	0.847340	79.04730	134.75000	-5.445730
172.98387	134.75000	1.276320	81.90274	134.75000	-5.670590
170.13194	134.75000	1.727690	84.93224	134.75000	-5.885790
167.10643	134.75000	2.198410	88.12378	134.75000	-6.092600
163.91927	134.75000	2.684690	91.46475	134.75000	-6.286730
160.58296	134.75000	3.183120	94.94203	134.75000	-6.469140
157.11070	134.75000	3.688750	98.54170	134.75000	-6.648670
153.51619	134.75000	4.197890	102.25008	134.75000	-6.789760
149.81325	134.75000	4.693830	106.05281	134.75000	-6.877440
146.01677	134.75000	5.184080	109.93492	134.75000	-6.908570
142.14223	134.75000	5.702610	113.88106	134.75000	-6.884440
138.20486	134.75000	6.242170	117.87556	134.75000	-6.809370
134.22025	134.75000	6.802980	121.90269	134.75000	-6.683940
130.20325	134.75000	7.328960	125.94661	134.75000	-6.506060
126.16934	134.75000	7.793400	129.99113	134.75000	-6.290230
122.13414	134.75000	8.175890	134.02020	134.75000	-6.040780
118.11351	134.75000	8.466430	138.01785	134.75000	-5.763280
114.12325	134.75000	8.665220	141.96837	134.75000	-5.460970
110.17923	134.75000	8.776960	145.85597	134.75000	-5.139720
106.29712	134.75000	8.807160	149.66528	134.75000	-4.807130
102.49226	134.75000	8.761170	153.38109	134.75000	-4.475810
98.77992	134.75000	8.646290	156.98860	134.75000	-4.151320
95.17476	134.75000	8.473270	160.47346	134.75000	-3.847870
91.69124	134.75000	8.254240	163.82191	134.75000	-3.565980
88.34323	134.75000	7.998540	167.02066	134.75000	-3.307770
85.14398	134.75000	7.709660	170.05719	134.75000	-3.071990
82.10609	134.75000	7.385670	172.91954	134.75000	-2.856340
79.24150	134.75000	7.022990	175.59642	134.75000	-2.660680
76.56146	134.75000	6.621090	178.07736	134.75000	-2.482090
74.07654	134.75000	6.182790	180.35251	134.75000	-2.320940
71.79660	134.75000	5.712140	182.41296	134.75000	-2.176420
69.73068	134.75000	5.213290	184.25064	134.75000	-2.047210
67.88696	134.75000	4.689540	185.85820	134.75000	-1.933840
66.27271	134.75000	4.144100	187.22934	134.75000	-1.837130
64.89430	134.75000	3.576980	188.35872	134.75000	-1.757480
63.75708	134.75000	2.985290	189.24176	134.75000	-1.695190
62.86542	134.75000	2.365480	189.87506	134.75000	-1.650530
62.22290	134.75000	1.722290	190.25609	134.75000	-1.623660
61.83231	134.75000	1.072910	190.38329	134.75000	-1.614670
61.69547	134.75000	0.439770			

TABLE 2

LEADING EDGE GLOVE DEFINING AIRFOIL COORDINATES

Outboard Station, Y = 196.000
Wing Reference System Dimensions - Inches

Upper Surface			Lower Surface		
X	Y	Z	X	Y	Z
207.83446	196.00000	0.232441			
207.72511	196.00000	0.244480	97.18173	196.00000	0.282150
207.39778	196.00000	0.280620	97.50664	196.00000	-0.194810
206.85371	196.00000	0.340940	98.04840	196.00000	-0.671740
206.09512	196.00000	0.425540	98.80484	196.00000	-1.146900
205.12502	196.00000	0.534580	99.77304	196.00000	-1.612260
203.94713	196.00000	0.668240	100.94923	196.00000	-2.054550
202.56615	196.00000	0.826740	102.32884	196.00000	-2.458010
200.98759	196.00000	1.010310	103.90648	196.00000	-2.810030
199.21761	196.00000	1.219160	105.67593	196.00000	-3.106740
197.26324	196.00000	1.453280	107.63019	196.00000	-3.354660
195.13222	196.00000	1.713790	109.76147	196.00000	-3.566390
192.83287	196.00000	1.998320	112.06126	196.00000	-3.754580
190.37434	196.00000	2.302690	114.52045	196.00000	-3.927870
187.76634	196.00000	2.626770	117.12924	196.00000	-4.092030
185.01906	196.00000	2.968770	119.87750	196.00000	-4.251240
182.14345	196.00000	3.327530	122.75417	196.00000	-4.409100
179.15074	196.00000	3.703110	125.74806	196.00000	-4.546060
176.05287	196.00000	4.085480	128.84729	196.00000	-4.668390
172.86186	196.00000	4.453490	132.03955	196.00000	-4.792230
169.59120	196.00000	4.977190	135.31236	196.00000	-4.902650
166.25397	196.00000	5.686000	138.65298	196.00000	-4.961520
162.86230	196.00000	6.375350	142.04822	196.00000	-4.972320
159.42908	196.00000	6.951250	145.48470	196.00000	-4.934420
155.96815	196.00000	7.468950	148.94875	196.00000	-4.851070
152.49304	196.00000	7.898280	152.42677	196.00000	-4.724700
149.01743	196.00000	8.223820	155.90500	196.00000	-4.556390
145.55495	196.00000	8.446380	159.36966	196.00000	-4.357450
142.11942	196.00000	8.578700	162.80711	196.00000	-4.132640
138.72441	196.00000	8.638350	166.20370	196.00000	-3.886220
135.38351	196.00000	8.639830	169.54604	196.00000	-3.623690
132.10988	196.00000	8.590620	172.82089	196.00000	-3.348800
128.91643	196.00000	8.491130	176.01532	196.00000	-3.064820
125.81573	196.00000	8.337170	179.11676	196.00000	-2.771990
122.81999	196.00000	8.124470	182.11296	196.00000	-2.478740
119.94106	196.00000	7.851910	184.99193	196.00000	-2.195070
117.19026	196.00000	7.523130	187.74245	196.00000	-1.922500
114.57861	196.00000	7.145800	190.35352	196.00000	-1.663500
112.11633	196.00000	6.730290	192.81496	196.00000	-1.417860
109.81322	196.00000	6.286480	195.11696	196.00000	-1.186650
107.67841	196.00000	5.822450	197.25049	196.00000	-0.970860
105.72031	196.00000	5.343440	199.20714	196.00000	-0.771730
103.94673	196.00000	4.851730	200.97919	196.00000	-0.590230
102.36458	196.00000	4.347630	202.55954	196.00000	-0.426610
100.98015	196.00000	3.831970	203.94214	196.00000	-0.281850
99.79887	196.00000	3.307890	205.12138	196.00000	-0.157380
98.82547	196.00000	2.781330	206.09261	196.00000	-0.054170
98.06380	196.00000	2.259260	206.85207	196.00000	0.026960
97.51685	196.00000	1.747440	207.39674	196.00000	0.085400
97.18680	196.00000	1.248520	207.72447	196.00000	0.120650
97.07501	196.00000	0.764180	207.83392	196.00000	0.132430

5.4 LFC SUCTION FLOW REQUIREMENTS

Initial Boundary Layer and Suction Analysis

Initially, suction flow analysis was conducted using the simple but convenient X-21 boundary layer stability criteria for the attachment-line, cross-flow, and Tollmein-Schlichting stability criteria (Reference 9). This suction analysis method was readily available and had been previously found to be conservative with respect to suction requirements obtained using the more comprehensive SALLY advanced stability analysis code (Reference 10).

Preliminary suction requirements were determined for the MOD 7Q LFC leading edge glove shape using X-21 criteria for the design flight condition and several off-design conditions. The required chordwise suction distribution, in terms of the suction velocity, was determined for the inboard and outboard spanwise stations of the LFC test region. The spanwise variation in suction required over the upper surface of the LFC test region was relatively small and the X-21 boundary layer stability criterion at the attachment line was satisfied. Thus, no suction was required at the leading edge. These suction distributions began at approximately 0.5 percent chord, increased to a peak suction coefficient (C_Q) of -0.0005 at 4 percent chord, and then decreased to a sustaining C_Q level of -0.0001 at 9 percent chord. The higher suction levels were associated with the region where crossflow is the dominant instability. Subsequent analysis showed that suction applied at the attachment line does prove to be very beneficial. (It should be noted that the X-21 criteria were developed for a "local" boundary layer condition and applied to a "marching" solution procedure while later advanced stability codes consider integrated effects within the boundary layer.)

Attachment Line Flow Analysis

During checkout and preparation for use of the advanced boundary layer stability analysis computer code, which was provided by NASA, two items of concern arose. It was noted that the results of boundary layer stability analysis were very sensitive to: (1) location of the attachment line; and (2) the value of the pressure coefficient at the attachment line. Therefore, analyses were carried out to assure the most accurate prediction of these critical parameters for the final LFC flight test article suction analysis.

A study of attachment line pressure coefficient was conducted to determine and validate the spanwise variation, as calculated by the Jameson analytical method. Results of the study showed that in three-dimensional flow, the case of the finite wing, the attachment line pressure coefficient is reduced relative to simple sweep theory. Validity of the calculated Jameson leading edge pressures was substantiated using both the Garabedian and Neumann two dimensional codes, References 5 and 11, respectively. The two-dimensional calculations, at very low Mach number (the Neumann code is incompressible), agreed very well. Since these two codes were developed using different

formulations, the consistency of the results indicates compatibility and validity of both formulations. It was thus concluded that the Jameson computation is reliable for determining pressures near the leading edge of the LFC test region.

Location of the attachment line on the MOD 8 leading edge test article was determined for JetStar lift coefficients of 0.25, 0.33, and 0.40 at M = 0.75. This range of lift coefficients corresponds to the anticipated range of flight test conditions. The resulting spanwise variation of attachment line location is shown in Figure 24. These results were used to position and size the number 1 suction flute for the DAC leading edge LFC panel.

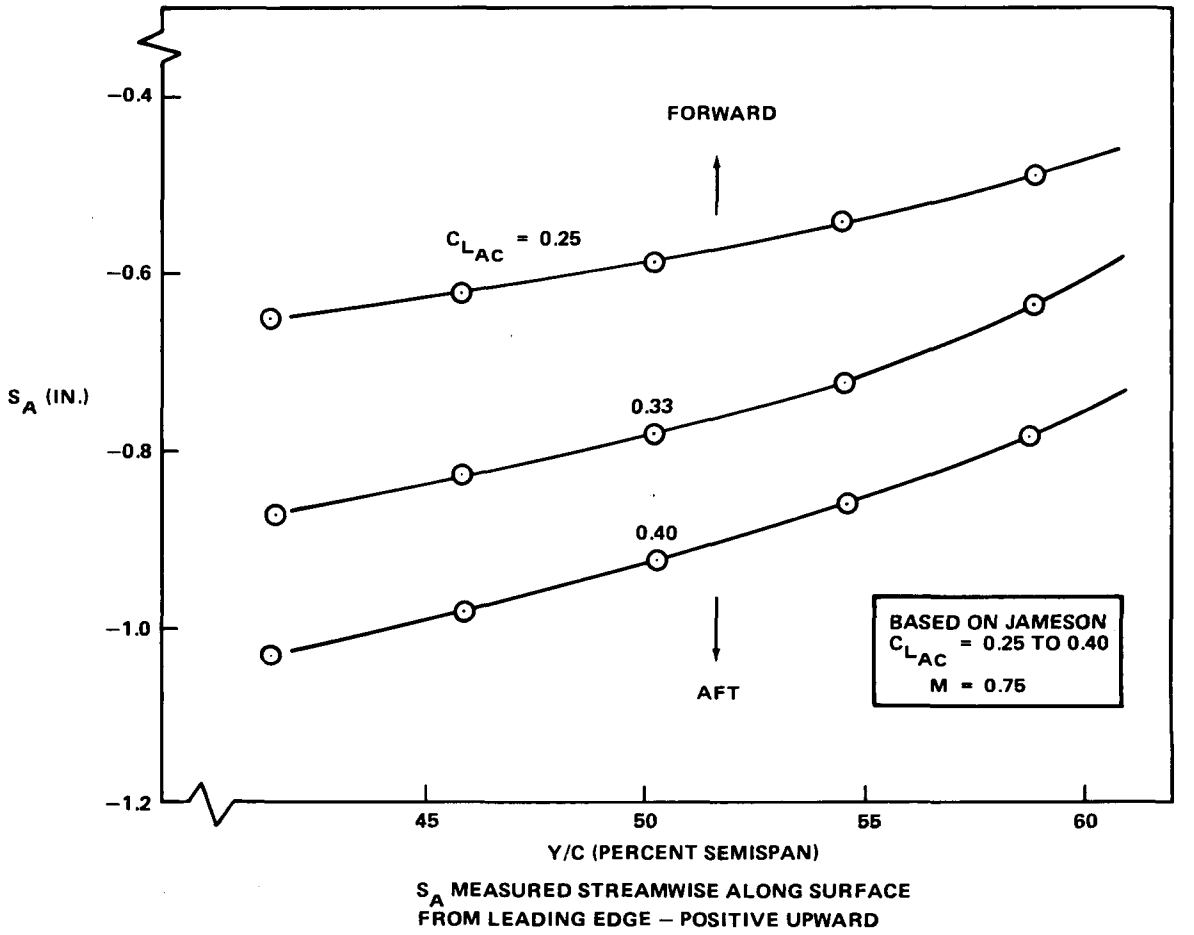

FIGURE 24. ATTACHMENT LINE LOCATION – MOD 8 LFC GLOVE – FLIGHT TEST ARTICLE

Final LFC Leading Edge Glove Suction Distribution

Suction requirements for the MOD 8 leading edge shape were established using the MARIA boundary layer stability code, which considers only the cross-flow instability (Reference 12). A comprehensive computer-graphic display of the MARIA output was developed which greatly enhanced the interpretation and usefulness of the MARIA code as a design tool. Pressure and suction distributions are displayed along with a carpet plot of amplification factor (N-factor) versus chord station (x/c) for each wave length.

Results of the MARIA boundary layer stability analysis for a midspan station of the MOD 8 leading edge glove, at design flight condition without suction, are shown in Figure 25. The range of amplification factor values, indicative of cross-flow instability in the boundary layer, is between 7 and 9. This range of values was based upon prior correlation with the SALLY code which treats both the cross-flow and Tollmein-Schlichting (streamwise) instabilities. The condition shown in Figure 25 was judged to be a marginally stable cross-flow situation in which transition would be expected to occur at 7 to 10 percent chord.

The effects of suction distribution variation on the amplification factor envelope at the design flight condition are illustrated in Figure 26. This example is for a preliminary case in the development of the suction distribution for the LETA and it does not correspond to the suction distribution finally specified for the test article at design flight condition. A very dramatic effect of suction applied at the leading edge and encompassing the attachment line is shown. The nominal case, based upon the earlier analysis, had no suction at the leading edge, a primary suction level of $C_Q = -0.0005$ from $x/c = 0.01$ to 0.07, and a sustaining level of $C_Q = -0.0001$ thereafter. For this case (1), only a slight reduction in amplification factor relative to the case without suction was obtained. Increasing the primary suction to $C_Q = -0.0009$ (2) did not appreciably reduce the amplification factor envelope. However, extending the primary suction (at the nominal value of $C_Q = -0.0005$) forward to the attachment line (3) resulted in substantial reduction of the amplification factor envelope. This result demonstrated the importance of suction applied at the attachment line and its effectiveness in reducing the cross-flow instability development in the boundary layer downstream. It became evident that modest suction applied upstream of a region subject to strong cross-flow in the boundary layer is more effective in controlling growth of the cross-flow instability than large amounts of suction applied after the instability has developed significantly. A logical misconception arising from X-21 criteria, that suction along the attachment line was not necessary when the attachment line Reynolds number (R_θ) was less than 100, has resulted in previous suction distributions which did not consider use of suction at the attachment line.

DESIGN FLIGHT CONDITION

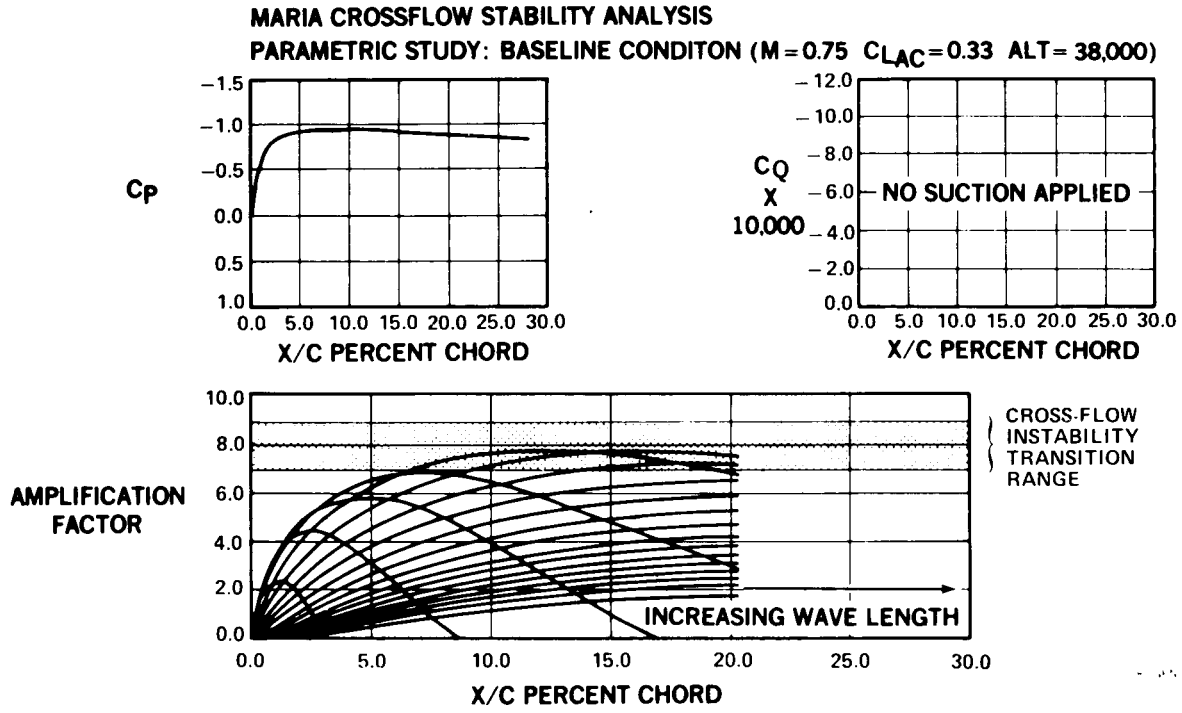

FIGURE 25. BOUNDARY LAYER STABILITY – MOD 8 LFC GLOVE – SUCTION OFF

DESIGN FLIGHT CONDITION

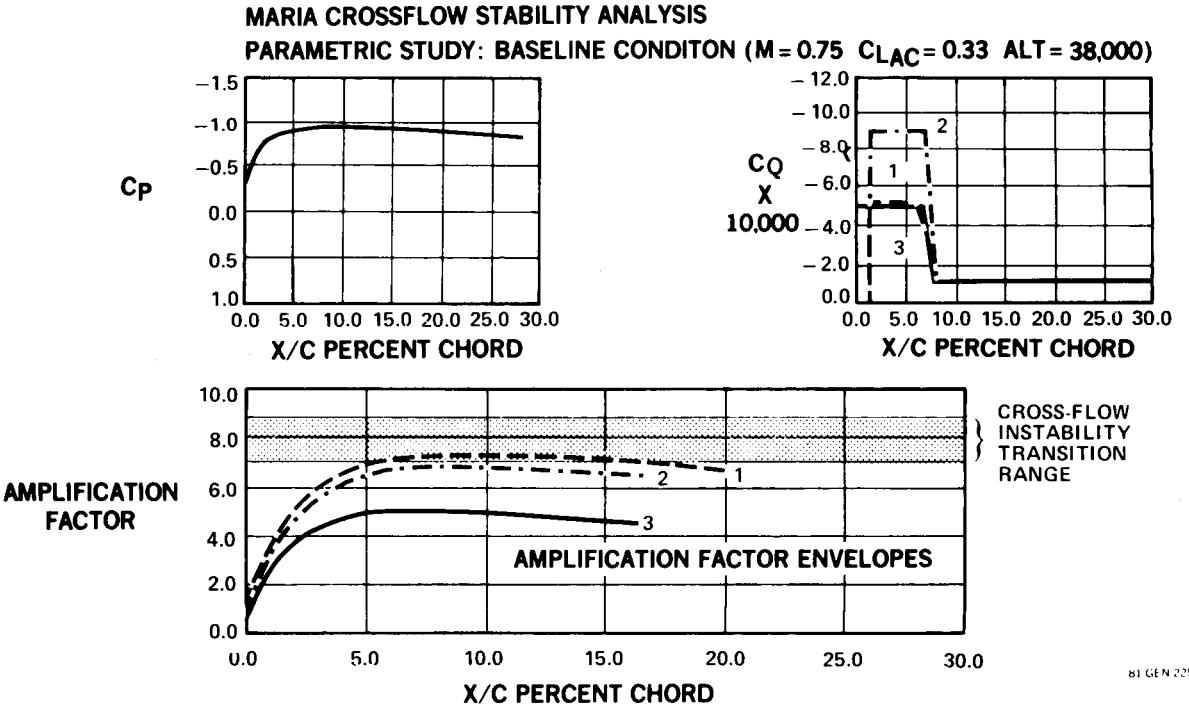

FIGURE 26. BOUNDARY LAYER STABILITY – MOD 8 LFC GLOVE – EFFECTS OF SUCTION DISTRIBUTION

Off-design flight test conditions were investigated to assure, based upon MARIA code results, that a flight condition could readily be achieved where transition would certainly occur near the leading edge of the LFC test region. At a Mach number of 0.77 and an altitude of 32,000 ft, the peak value of the amplification factor was found to be 12 without suction, which is considerably above the transition threshold value. In this instance, transition would be expected to occur at 3 to 4 percent chord. The effect of primary suction, applied over the first 4 percent of chord at a modest level of C_Q = -0.0004, reduces this peak amplification factor from 12 to 8. This result again emphasized the importance of suction applied along the attachment line and indicated that the JetStar LFC glove flight test would provide a valid test of the perforated titanium surface and DAC LFC configuration.

The basic suction distribution selected for the LFC Leading Edge Glove at design flight condition was defined as follows:

(1) C_Q = -0.0005 in the region extending from the attachment line through Flute No. 7, which extends to x/c = 0.035 at the inboard end of the test panel and to x/c = 0.044 at the outboard end. (This is the primary suction level applied in the region where the cross-flow instability predominates.)

(2) C_Q = -0.0001 in the region covered by Flute No. 8 through 15. The trailing edge of Flute No. 15 is at x/c - 0.111 inboard and at x/c - 0.147 outboard. (This is the sustaining suction level applicable in the region of the Tollmein-Schlichting instability dominance.)

This suction distribution is shown in Figure 27. The continuous suction levels, used for analytical purposes, are given along with the equivalent suction values which occur as an intermittent distribution as the flow crosses the perforated strips. It should be noted that the suction flutes are tapered; thus, the equivalent suction values were determined by the ratio, total surface area/porous area, for each flute.

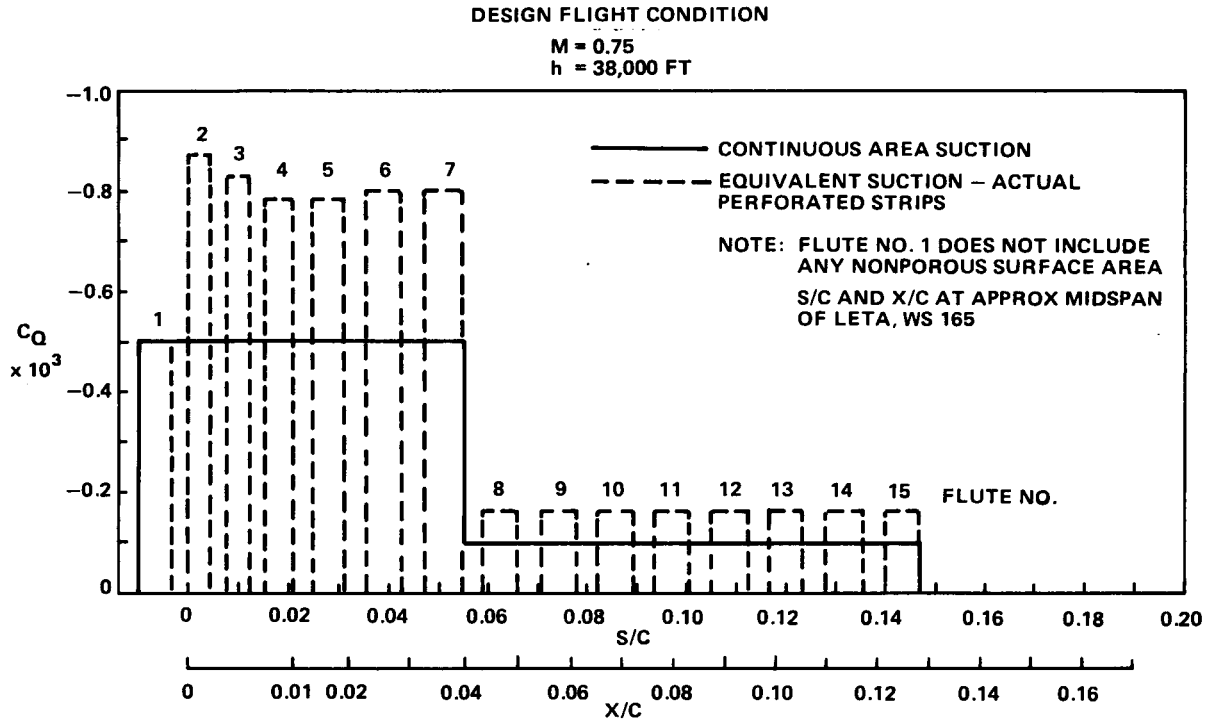

FIGURE 27. BASIC SUCTION DISTRIBUTION

At the design flight condition a check was made using the more comprehensive SALLY boundary layer stability analysis code (Reference 10) to assure that the MARIA analysis was adequate for determining occurrence and location of transition on the JetStar LFC glove. (The MARIA analysis is simplified; (1) to consider only growth of the cross-flow instability, and (2) uses a specialized approximation, based upon results from the SALLY code, to quickly solve for cross-flow disturbance amplification factors.) Analytical results using the SALLY code indicated that transition would occur at approximately 3.7 percent chord (amplification factor greater than 9) without suction. The corresponding results for the basic suction distribution are plotted in Figure 28. These calculations show that at design conditions a maximum amplification of 5 occurs in the cross-flow sensitive region and the growth of the Tollmein-Schlichting disturbances is not critical until approximately 20 percent chord. Extension of suction aftward would be necessary to sustain a laminar boundary layer beyond 20 percent chord. The SALLY stability analysis confirms the conclusion developed using the MARIA code as a preliminary analysis method.

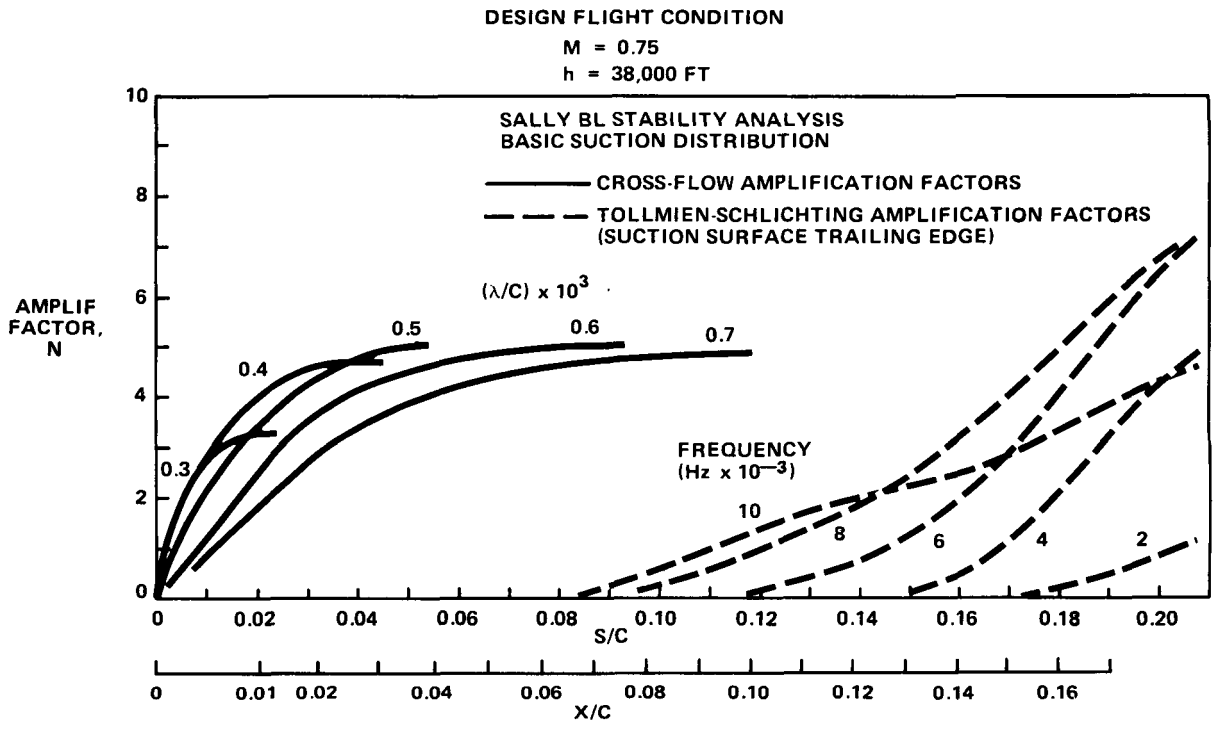

NOTE: S/C AND X/C SCALES REFER TO APPROXIMATELY MIDSPAN OF LETA (WS 165)

FIGURE 28. DOUGLAS LFC LEADING EDGE SUCTION PANEL BOUNDARY LAYER STABILITY

LFC Leading Edge Suction Panel Interface Flow Conditions

Flow conditions, suction flow quantity, and flute exit pressure were estimated for each flute of the LFC suction panel. These estimates were based upon the surface pressures and basic suction distribution at the design flight test condition. It should be noted that surface pressures and the analytically determined suction distributions are for continuous suction quantities and this must be reconciled with the intermittent porosity of the actual suction surface. The suction surface is essentially a series of perforated strips, extending spanwise along the LFC leading edge panel and alternating chordwise with non-porous strips of bonded surface between the perforated titanium skin and the fluted fiberglass substructure. Figure 29 shows the arrangement of perforated strips on the unrolled suction surface. Also shown in Figure 29 are the predicted isobars on the test article surface at the design flight condition. This figure illustrates the extent of chordwise and spanwise pressure variation expected over the perforated suction areas.

SUCTION FLUTES AND ESTIMATED ISOBAR PATTERN
DESIGN FLIGHT CONDITION
M = 0.75
h = 38,000 FT

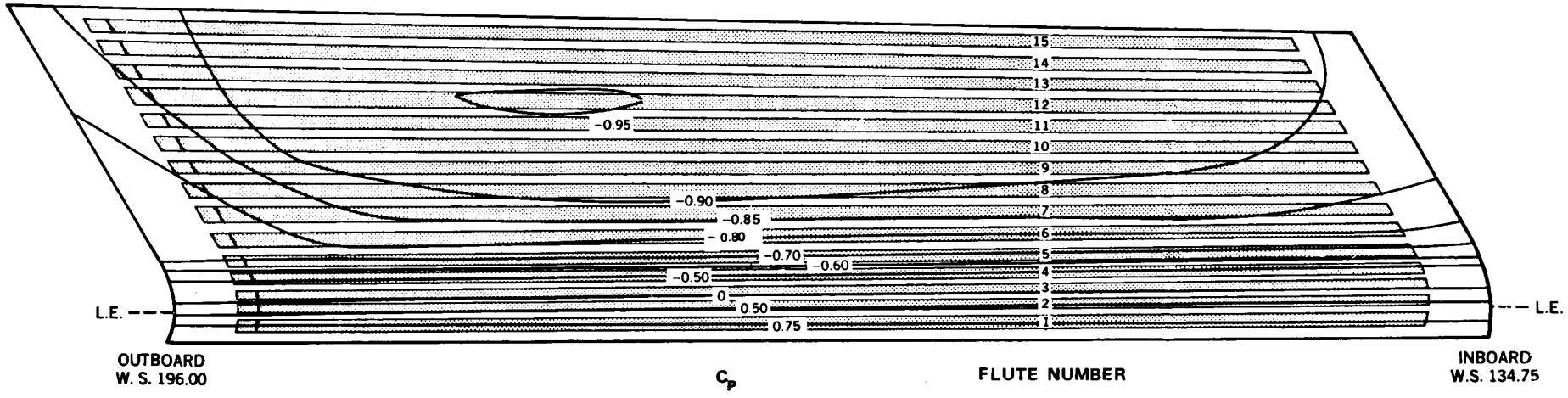

ATTACHMENT LINE C_p = 0.75

NOTE: ILLUSTRATION IS THE FLAT PATTERN SURFACE

FIGURE 29. PERFORATED STRIP ARRANGEMENT

The considerations and procedure used to estimate flow parameters for the suction panel are summarized below:

(a) Chordwise pressure variation (gradient) across the width of the perforated (porous) strip - a consequence of the chordwise pressure distribution.

(b) Spanwise pressure variation along the length of the flute - the result of three-dimensional effects within the LFC leading edge test region.

(c) Application of sufficient suction through the perforated strip area to provide the equivalent (integrated) suction required by the basic chordwise suction distribution.

(d) Assurance that actual suction levels meet requirements in all porous areas, considering spanwise external pressure variations along the suction flutes.

(e) Assurance that outflow does not occur considering chordwise pressure gradient.

(f) Nominal porosity of 14.5 SCFM/ft^2 at 14 psf pressure differential across the perforated titanium suction surface. Flow is linear with pressure differential in the region of interest and corrected to flight test ambient conditions. This relation is given in Figure 30.

(g) M 0.20 in the exit duct from each flute.

Flute pressure and suction flow quantity were initially determined for each flute at design flight test condition (pressure distribution) and basic suction distribution. Flute pressure was adjusted until the required suction flow was obtained at the critical spanwise location in accordance with Item (c), assuming the nominal porosity for the perforated suction area, Item (f). Then, if necessary, the flute pressure was reduced further to comply with Items (d) and (e). With the flute pressure thus established, the resulting total flow through the perforated suction area was calculated using the nominal porosity and the pressure differential between the flute and external surface. Finally, the velocity of the total flow through the flute exit duct was evaluated to affirm that the Mach number in the exit duct was less than 0.20, Item (g). Thus, the flow quantity and interface pressure were estimated for each flute. These parameters are tabulated in columns 3 and 4 of Table 3 for the Baseline - Nominal Flow through the suction surface.

Flow conditions for the LFC leading edge suction panel were adjusted following bench testing of the suction panel. Actual suction areas for each flute were determined by inserting a light probe into the flute, then observing and measuring the width of the open suction area. Flow measurements then established the surface porosity index for the suction area of each flute. The measured surface porosity for each flute is listed in Column 5 of Table 3. These values were then used to establish the adjusted interface flow conditions tabulated in Columns 6 and 7 of Table 3 for the baseline - nominal and baseline - 150 percent Nominal flows. The resulting interface pressures are generally less than the previous estimate, as noted, and the total flow is reduced slightly because the average porosity is less than the reference value. This is due to the fact that the pressure differential needed to meet minimum suction requirements and prevent inflow-outflow is achieved at lower values of flow through the surface.

The nominal suction flow distribution, which resulted from the foregoing analysis and adjustments, is plotted in Figure 31. This baseline-nominal flow is greater than the basic suction distribution noted for reference on the figure. Excess suction is a consequence of compliance with the foregoing conditions (a) through (f). Thus the baseline-nominal flow provides suction in excess of the basic suction distribution everywhere along the flutes except at the critical spanwise location, and even there whenever outflow must be prevented.

The same procedure was then applied for 150 percent of the basic suction distribution, i.e., $C_Q = -0.00075$, from the attachment line to $x/c = 0.04$ and $C_Q = -0.00015$ downstream from $x/c = 0.04$. Interface flow conditions for this case are listed in Columns 6 and 7 of Table 4. Although the reference suction levels are increased 50 percent, the actual flow quantities are increased by a lesser amount because of the conservative conditions used to establish the baseline - nominal flow. The reduction in flute pressure necessary to achieve 150 percent of nominal flow at the critical spanwise location results in a lesser percentage increase in the suction flow elsewhere along the flute. The suction distribution for this second case is also shown in Figure 31.

An evaluation was made of the velocity through the perforations and the corresponding hole Reynolds number, based upon the 150 percent nominal suction flow case. The perforated surface flow characteristics plotted in Figure 30, the surface pressure distribution shown in Figure 29, and the interface (flute) pressures given in Table 4, Column 7 were used to determine the largest pressure differential across the perforated titanium. It was found that the largest pressure differences are expected to occur at the inboard leading edge of flute number 3, where a hole Reynolds number of 185 was computed at a velocity of 409 ft/sec through the hole. At the baseline-nominal flow, the same critical condition occurred and the maximum hole Reynolds number decreased to 147. Although these hole Reynolds numbers seem large, they are less than half of the value demonstrated during the swept wing wind tunnel test without causing any adverse effect (i.e., transition).

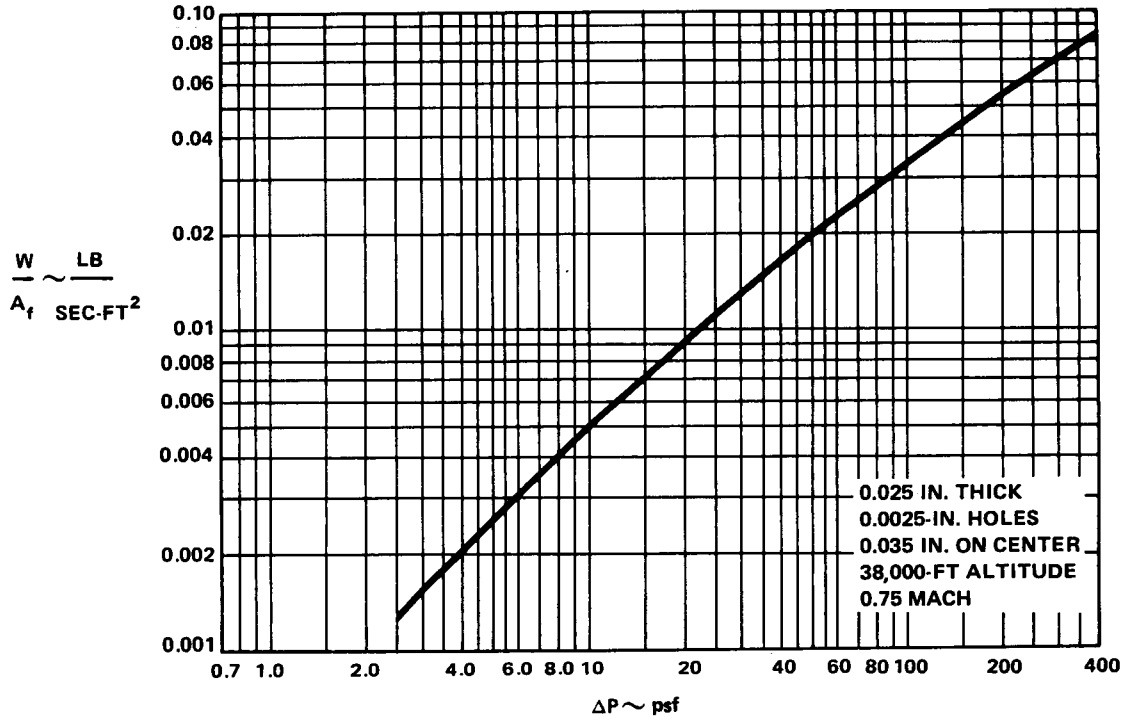

FIGURE 30. PRESSURE DROP CHARACTERISTICS OF EB PERFORATED TITANIUM

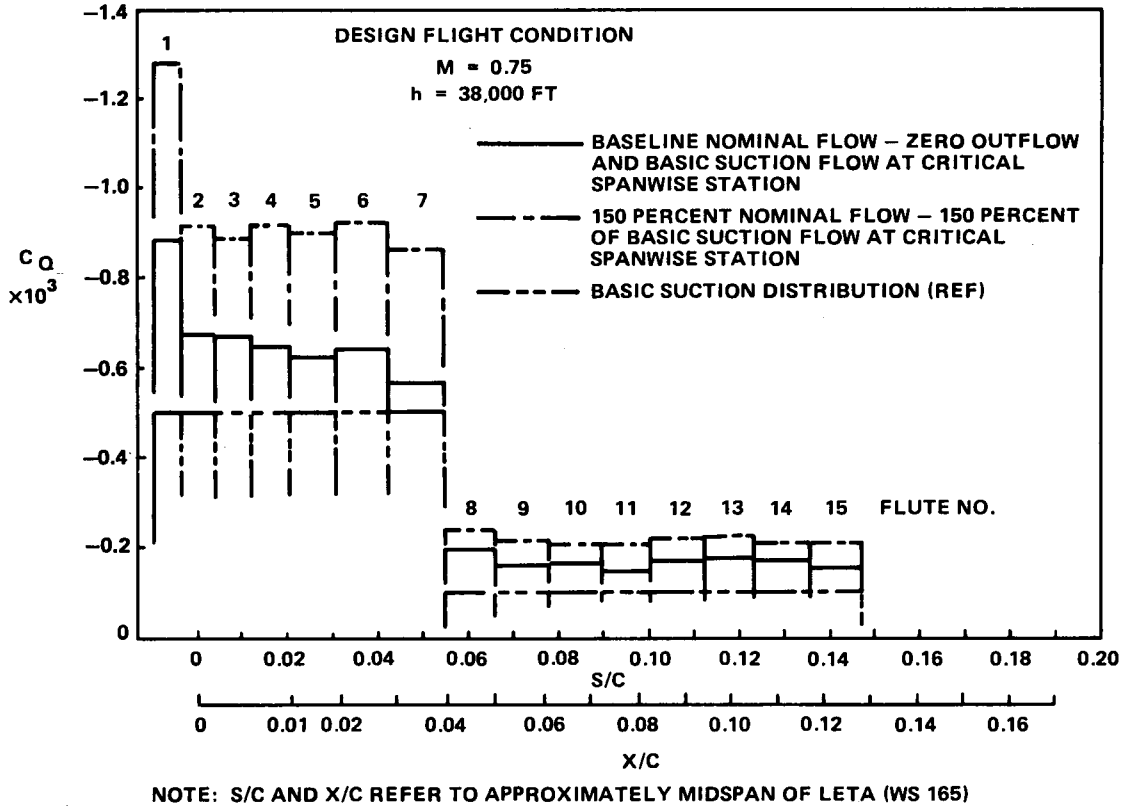

NOTE: S/C AND X/C REFER TO APPROXIMATELY MIDSPAN OF LETA (WS 165)

FIGURE 31. NOMINAL AND 150-PERCENT FLOW DISTRIBUTIONS

TABLE 3
ADJUSTED INTERFACE FLOW CONDITIONS
Baseline - Nominal Flow

SUCTION FLUTE NO.	DUCT ID IN.	FLOW[1] LB/SEC	PRESSURE[1] PSF	FLUTE[2] POROSITY	FLOW[3] LB/SEC	PRESSURE[3] PSF
1	0.75	0.00418	521	14.0	0.00408	513
2	1.00	0.00389	453	14.0	0.00360	446
3	1.00	0.00380	370	12.0	0.00342	358
4	1.00	0.00373	320	15.0	0.00370	315
5	1.00	0.00419	286	14.1	0.00410	280
6	1.00	0.00480	262	16.1	0.00479	260
7	1.00	0.00454	255	14.8	0.00451	250
8	0.75	0.00153	269	13.9	0.00147	268
9	0.75	0.00131	269	13.7	0.00119	268
10	0.75	0.00145	267	12.0	0.00125	265
11	0.75	0.00150	266	6.9	0.00112	261
12	0.75	0.00150	266	12.7	0.00130	265
13	0.75	0.00150	266	13.2	0.00136	265
14	0.75	0.00150	266	12.2	0.00130	265
15	0.75	0.00150	266	8.0	0.00116	262
	Total Flow	0.04092		Total Flow	0.03835	

(1) Revised 12-8-82 for nominal porosity of 14.5 SCFM/FT2 at 14 PSF ΔP.
(2) Measured flute porosity, 7-12-83 bench test at NASA DFRF.
(3) Flow conditions adjusted for individual flute porosity values.

TABLE 4

ADJUSTED INTERFACE FLOW CONDITIONS

Baseline - 150 Percent Nominal Flow

SUCTION FLUTE NO.	DUCT ID IN.	FLOW[1] LB/SEC	PRESSURE[1] PSF	FLUTE[2] POROSITY	FLOW[3] LB/SEC	PRESSURE[3] PSF
1	0.75	0.00600	499	14.0	0.00590	489
2	1.00	0.00521	434	14.0	0.00490	428
3	1.00	0.00504	353	12.0	0.00460	332
4	1.00	0.00534	301	15.0	0.00528	295
5	1.00	0.00603	267	14.1	0.00593	261
6	1.00	0.00693	241	16.1	0.00690	240
7	1.00	0.00668	234	14.8	0.00665	228
8	0.75	0.00196	265	13.9	0.00179	264
9	0.75	0.00175	265	13.7	0.00165	264
10	0.75	0.00180	264	12.0	0.00160	261
11	0.75	0.00192	262	6.9	0.00155	254
12	0.75	0.00192	262	12.7	0.00167	260
13	0.75	0.00192	262	13.2	0.00170	260
14	0.75	0.00192	262	12.2	0.00160	259
15	0.75	0.00192	262	8.0	0.00157	255
	Total Flow	0.05634		Total Flow	0.05329	

(1) Revised values 12-8-82 for nominal porosity of 14.5 SCFM/FT2 at 14 PSF ΔP.

(2) Measured flute porosity, 7-12-83 bench test at NASA DFRF.

(3) Flow conditions adjusted for individual flute porosity values.

5.5 LFC SURFACE WAVINESS CRITERIA

Waviness criteria for the LFC leading edge flight test article were adapted from available X-21 results (Reference 13) and information provided by Mr. A.L. Braslow of NASA. Specification of waviness criteria for fabrication of the LFC flight test article was simplified to the values shown in Figure 32. For the wavelengths less than 10 inches, a height-to-wavelength ratio of 0.001 is specified while for longer wavelengths, a maximum wave height of 0.010-inches is specified. Multiple wave criteria, computed according to Reference 13, are shown for the design flight condition at 38,000 feet and for an off-design altitude of 30,000 feet. The specified waviness tolerances for the flight test article are more severe than the multiple wave criteria at design test altitude.

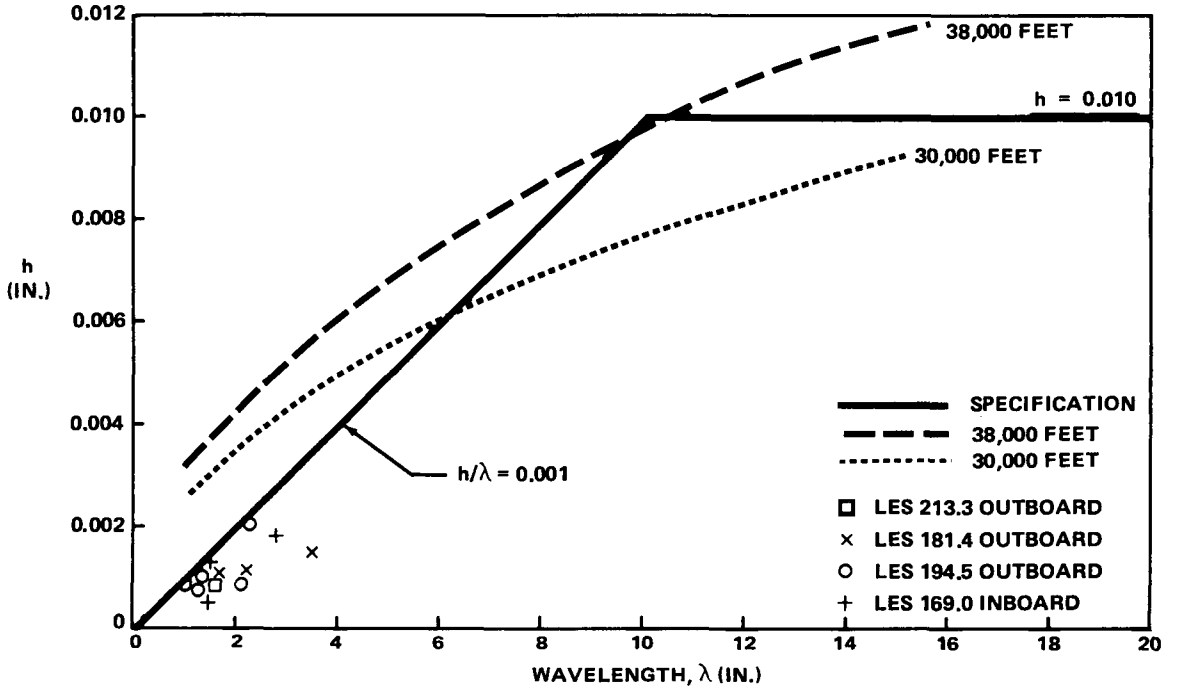

FIGURE 32. LFC FLIGHT TEST ARTICLE SPECIFICATION WAVINESS LIMITS – MULTIPLE-WAVE CRITERIA

Waviness measurements were made on a 20-inch span leading edge test specimen, which was used for envirnomental testing of PGME flow and surface clearing at very low temperatures, and the corresponding portion of the swept wing model female tool. These measurements were made using a 3-point waviness gauge described in Reference 13, at a room temperature of 70°F and in a cold chamber at a temperature of -70°F. These data showed that:

1. Contour of the tooling used to form and cure the fluted substructure and outer surface was accurately reproduced in the finished part.

2. There was no evidence of changes in surface contour due to change in temperature, within the range of -70°F to +70°F.

3. The technique for measuring waviness with a 3-point gauge and dial indicator was repeatable and reliable.

Waviness measurements of the LFC leading edge suction panel, after bonding of the perforated titanium skin to the substructure, are noted on Figure 32. These measurements were all within the limits specified and encompass the entire span of the suction panel.

SECTION 6
LOW-SPEED SWEPT WING MODEL TEST

A wind tunnel test was conducted in the DAC Low-Speed Wind Tunnel using a two-dimensional swept wing model which had been developed and tested previously (See Section 8.2 of Reference 4). The objectives of this test were (1) to evaluate the aerodynamic and surface suction system characteristics of a leading edge panel having the same configuration as that developed for the LFC leading edge glove flight test article, and (2) to evaluate methods for detecting transition from laminar to turbulent flow using unobtrusive acoustic sensing techniques. A brief description of the model and summary of results follows.

6.1 MODEL DESCRIPTION AND INSTALLATION

The model used in this test was a 30-degree swept wing section which spanned the tunnel test section and had a 6-foot chord, normal to the leading edge. A simple three-segment flap, hinged at 0.85 chord, was provided to adjust the pressure distribution. Sidewall fairings were installed to better simulate the flow over a high aspect ratio wing.

The leading edge and upper surface panels of the basic model were removable and incorporated the active LFC surfaces to be tested. The existing Dynapore upper surface panel, which extended from the front spar to 0.70 chord, was used in this test. A new leading edge panel, having the perforated titanium surface bonded to a fluted fiberglass substructure similar to that designed for the LFC flight test article, was the primary configuration component for this test.

The new leading edge panel consisted of a perforated titanium skin, 0.025-inch thick with nominal 0.0025-inch-diameter holes spaced 0.025 inch apart in an orthogonal array, bonded to the lands of a fluted fiberglass substructure. The substructure formed the spanwise suction ducts. The resulting LFC surface consisted of spanwise strips of distributed suction between the supporting bonded strips. A cross section of the leading edge panel is shown in Figure 33. This figure illustrates the subsurface static port sleeves located in the spacer flutes and the optional subsurface diffuser-baffle in a suction flute. A photo of the leading edge installed in the tunnel is shown in Figure 34.

Interior suction fittings were provided on the leading edge panel to simulate the flight test article suction system. Two suction fittings were provided for each suction flute, a primary fitting at the inboard end of the flute and an alternative fitting near the midspan of the flute.

Suction for the test was provided through the primary manifold by a 50 H.P. centrifugal blower. Suction lines were connected from the ends of each flute of the original Dynapore upper surface panel to secondary manifolds in groups of 4 flutes per manifold. The suction ducts from the leading edge panel were brought out of the model through openings in the outer structural ribs. Flow through each secondary manifold was controlled by a simple gate valve and measured with Meriam Type 50 MW20 laminar flow meters.

ORIGINAL PAGE IS
OF POOR QUALITY

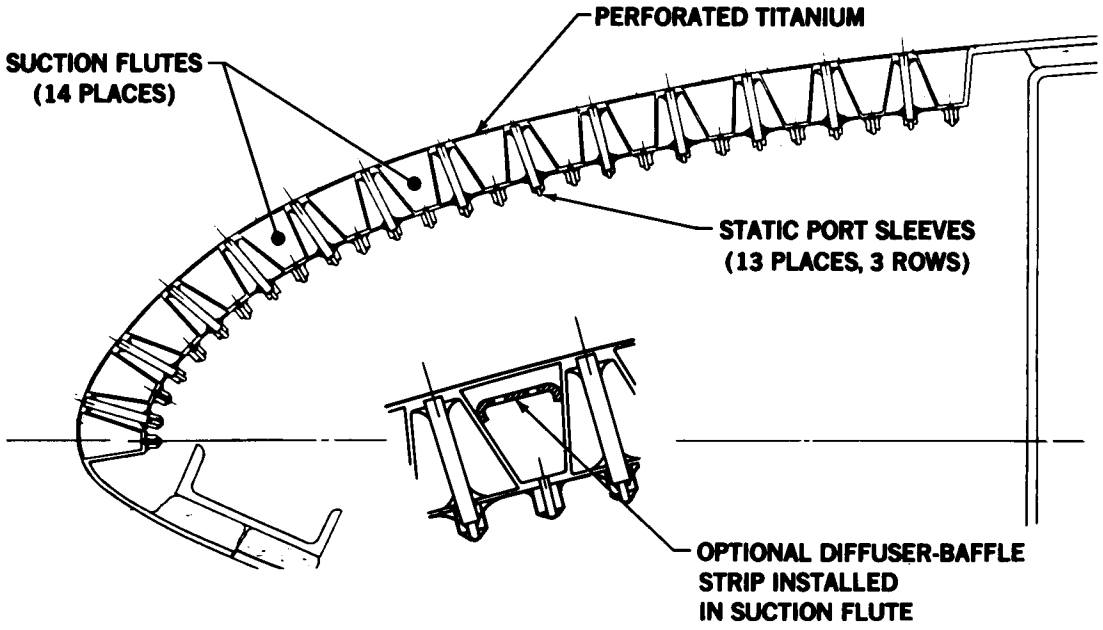

FIGURE 33. SWEPT-WING MODEL LEADING EDGE PANEL CROSS SECTION

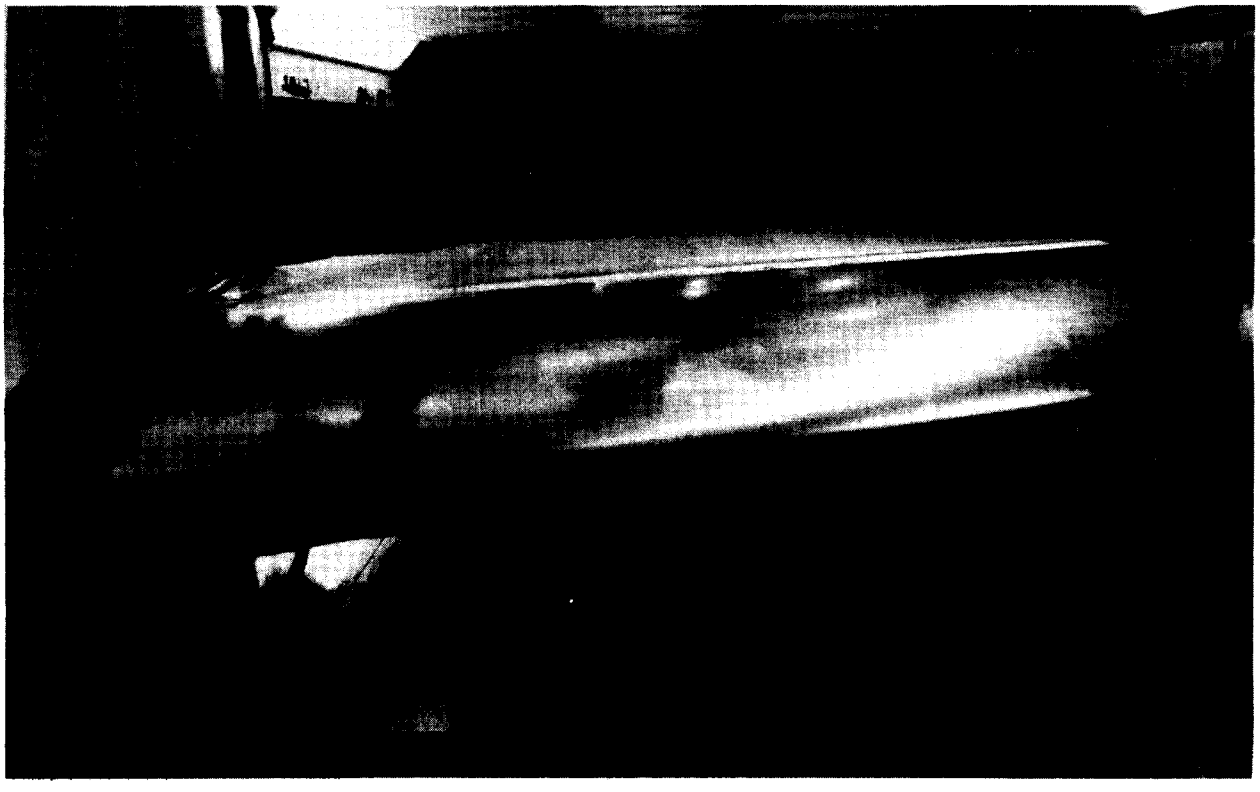

FIGURE 34. SWEPT-WING MODEL IN DAC TUNNEL

Instrumentation for this test included the following:

1. Subsurface Static Pressure Taps - These pressure sensors were installed in the spacer flutes between the suction flutes. Static pressure was measured through the porous surface. Three chordwise rows of static pressure taps were located at the tunnel centerline and 15 inches on either side of the centerline. There were 13 subsurface pressure taps in each row.

2. Flute Pressure - Flute pressure was measured in each of the 30 suction flutes. Four additional spanwise flute pressures were measured in flute numbers 4, 8, and 12.

3. Boundary Layer Total Pressures - Boundary layer total pressures were measured at 3 spanwise stations. Three-tube total pressure rakes were located at 70 percent chord on the tunnel centerline and 15 inches on either side of the tunnel centerline.

4. Acoustic Sensors - Three Kulite microphones, provided by NASA, were located approximately 3 inches inboard of the tunnel centerline in the spacer flutes downstream of suction flute No. 6, 9, and 12.

   A B&K 4136 1/4-inch condenser microphone was exposed internally to selected subsurface static pressure sensors.

   Acoustic data was recorded and analyzed using an oscilloscope and an audio analyzer.

   A hand-held total pressure probe connected to a medical stethoscope provided a distinctive auditory signal which was the most reliable method of identifying and locating boundary layer transition.

5. Flow Control and Measurement - Suction flow was controlled by valves and measured through Meriam laminar flow meters. In addition, a Parker-Hannefin remote control valve and a prototype automatic control valve were installed for evaluation as part of the test program.

6.2 TEST RESULTS AND ANALYSIS

Aerodynamic testing confirmed previous test results for the swept wing model. Laminar flow was achieved on the upper surface past 70 percent chord with the nominal suction distribution. Nominal suction consisted of C_Q = -0.0005 in the cross-flow region, from the leading edge (attachment line) to approximately 6 percent chord, followed by a sustaining suction level of C_Q = -0.0001 applied downstream to the front spar joint. This sustaining level precludes transition in the region where Tollmein-Schlichting instability prevails. Suction on the Dynapore upper surface panel was maintained at essentially the same values required in previous testing. Increased suction (C_Q = -0.0004) was necessary aft of the front spar juncture to recover from (1) the 4-inch

chordwise gap in applied suction, and (2) surface anomalies associated with the juncture between the suction panels. Furthermore, in the aft region of the upper surface panel, cross-flow conditions again become dominant in the adverse gradient of the pressure recovery region. Typically, this recovery region required C_Q values ranging from -0.0011 to -0.0013. With suction off, transition occurred at 8 percent chord for a Reynolds number of 8.5×10^6. This transition location was the same as obtained previously on the reference nonporous leading edge panel (Reference 4).

Effects of surface pressure distortion (spanwise gradient) were investigated using differential deflection of the trailing-edge flap segments. Laminar flow was achieved by increasing the suction applied in order to maintain critical suction at the spanwise location of minimum surface pressure.

Results showed that a large increase in suction is required to extend laminar flow if instability of the laminar boundary layer is allowed to develop and approach a condition of imminent transition. The amount of suction required to extend laminar flow is quite dependent upon the condition of the laminar boundary layer at the point where suction is applied, or resumed in the case of interrupted suction.

Minimum suction allows moderate instability growth where amplification factors may increase to values in the 4 to 5 range and then alternate as the flow progresses downstream. Hence, in a region where suction cannot be applied practically, such as a juncture between suction panels, additional suction is required ahead of the interruption in order to prevent amplification factors from reaching a critical value (approximately 9) before suction can be resumed. Thus, a small amount of additional suction applied ahead of the interruption may be the equivalent of much larger suction applied downstream from the interruption. Therefore, it is imprudent to assume that laminar flow can be extended arbitrarily by introducing a minimal level of suction. Such a minimum suction would be appropriate only for the laminar boundary layer which has been conditioned upstream by a carefully adjusted suction distribution. Increased suction would be required to extend a mature laminar boundary layer that was about to transition to turbulent flow.

Deliberate attempts to cause transition due to oversuction were unsuccessful in this test, at least to the limits of the test equipment. Application of suction to a local suction coefficient value of -0.0050, which was 10 times the nominal primary suction level, did not have any adverse effect on the extent of laminar flow observed. Excessive suction was applied sequentially to Flute No. 2, 3, and 4. The maximum oversuction was achieved in Flute No. 2, which is essentially at the leading edge ($x/c = 0.003$ to $x/c - 0.005$). The hole Reynolds number computed for this case was 383.

Several auxiliary items were evaluated relative to features of the leading edge flight test article. Spanwise location of suction flute fittings, at midspan rather than at the inboard end of the suction flute, was found to be non-critical for the flow rates and flute lengths used in this test. Results also showed that the backup subsurface diffuser-baffle devices were not required in the suction flutes. Evaluation of remote control valves for the suction system did not reveal any characteristics which would preclude their use for the flight test program. To the extent determinable in this test, there were no adverse effects noted due to operation of either the prototype chamber valve or the Parker-Hannifin valve.

Considering results of testing of the LFC Swept Wing Wind Tunnel Model, it was concluded that the LFC leading-edge panel configuration for the leading-edge glove flight-test article is generally satisfactory with respect to aerodynamic characteristics. For the flute lengths and expected flow quantities, operation is satisfactory with suction applied at the inboard end of the flutes and it is not necessary to isolate the inner surface of the perforated titanium from the flow along the suction flutes.

Testing of acoustic transition detection devices and techniques took the major portion of the test time; it concluded with negative to indeterminate results. The Kulite sensors did not show any useful response or indication of transition through the perforated titanium surface. Detection of transition using a microphone and static pressure orifices was marginally successful when the pressure orifices were drilled to a conventional diameter for static pressure orifices (approximately 0.040 inch). However, this result was not acceptable with respect to the objective of acoustically detecting transition through the perforated surface.

SECTION 7
DETAIL DESIGN

Based on a formal preliminary design review, the LFC concept and basic systems operations were established. Some changes and compromises were necessarily incorporated during the detail design, but no significant changes or re-directions occurred. The changes that were made between preliminary design and final design were to simplify fabrication and improve assembly methods.

7.1 LEADING EDGE LFC SUCTION PANEL

The aerodynamic analysis performed on the final agreed airfoil shape, MOD 8, indicated that suction applied at the most forward location, including the attachment line, gives the greatest benefit for reducing the amplification factor. Therefore, the detail design incorporates a suction flute layout that provides for capturing, in one flute, the attachment line along the entire length and over its chordwise excursion throughout the angle of attack range of interest at cruise. The attachment line region or band tends to slope upward from the inboard end of the test section to the outboard end. As depicted in Figure 35, the first flute is designed wide enough to completely include this sloping band. The bottom edge of the second flute is oriented exactly along the leading edge as a reference line. Because the pressure isobars are closer together outboard than inboard, some tapered flutes are necessary aft of the leading edge to stay within the maximum C_p variance. A maximum C_p variance of 0.4 is used as the criterion to minimize the energy necessary to obtain the required pressure in each flute. In matching this criterion with the tapering test section, which has a longer chord outboard than inboard, all flutes other than 1, 4, and 5 are tapered. Flutes 2 and 3 increase slightly in width toward the inboard edge to best match the isobar pattern and C_p variation limit. The remaining flutes increase in width toward the outboard edge to best match the tapering test section. Figure 36 illustrates the relationship of the flute layout with the theoretical constant C_p lines. A typical cross section of the leading edge flute configuration is shown in Figure 37.

Each flute has one suction outlet fitting installed at the inner surface near the inboard end. These suction fittings (Figure 38) are bonded to the fiberglass backing face of the suction panel after matching slots have been cut into the flutes. Plastic nylon hoses are attached with clamps to the suction flute fittings. These hoses carry the suction air to the inboard interface of the test article where they are attached to the aluminum tubing that continues carrying the suction air to the chamber valve assembly in the JetStar cabin.

At the trailing edge of the suction panel and joined securely to it is a removable panel of fiberglass and non-perforated titanium that extends the surface aft to form a sensor panel. This panel extends spanwise for the full length of the test article and chordwise to several inches behind the spar. Various sensors to detect laminar flow or establish the conditions that exist on the suction panel can be mounted on this sensor panel.

PRECEDING PAGE BLANK NOT FILMED

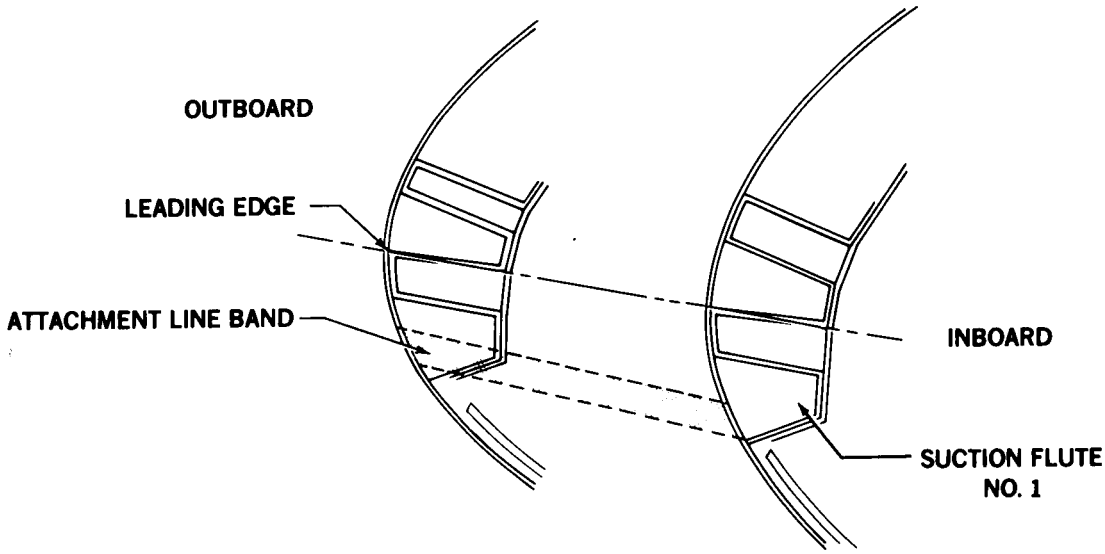

FIGURE 35. ATTACHMENT LINE BAND AND FLUTE NUMBER 1

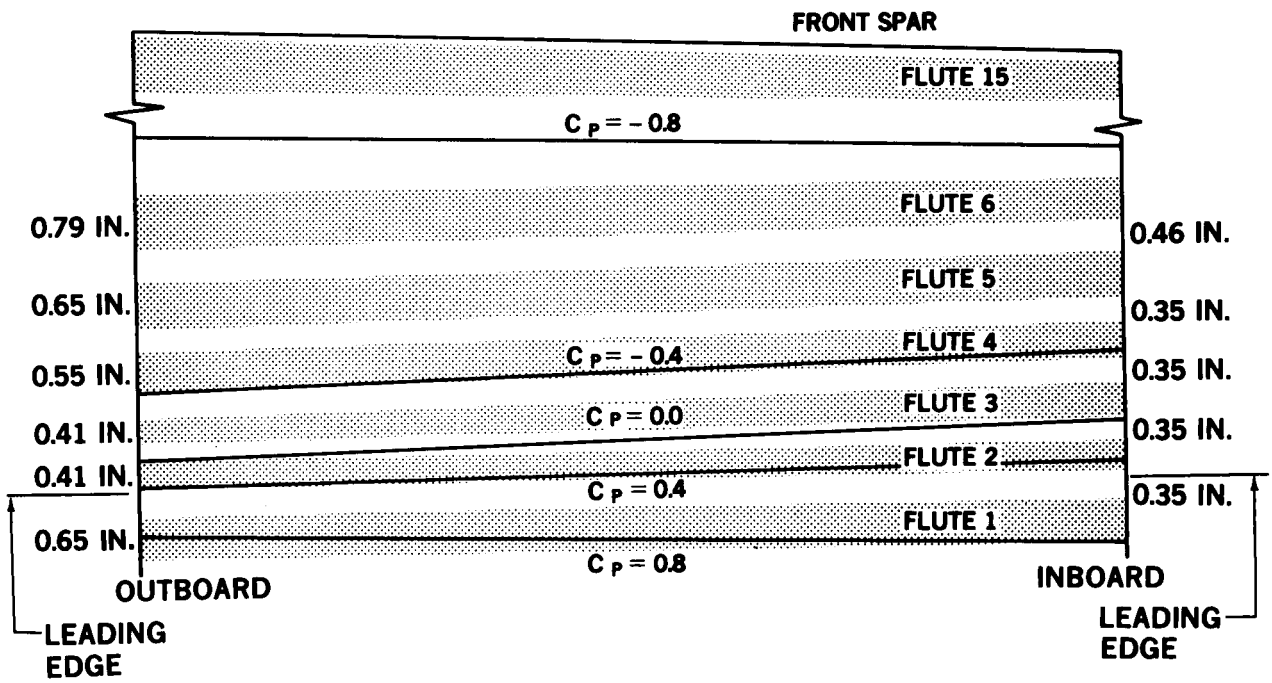

FIGURE 36. CONSTANT C_p LINES AND FLUTE CONFIGURATION

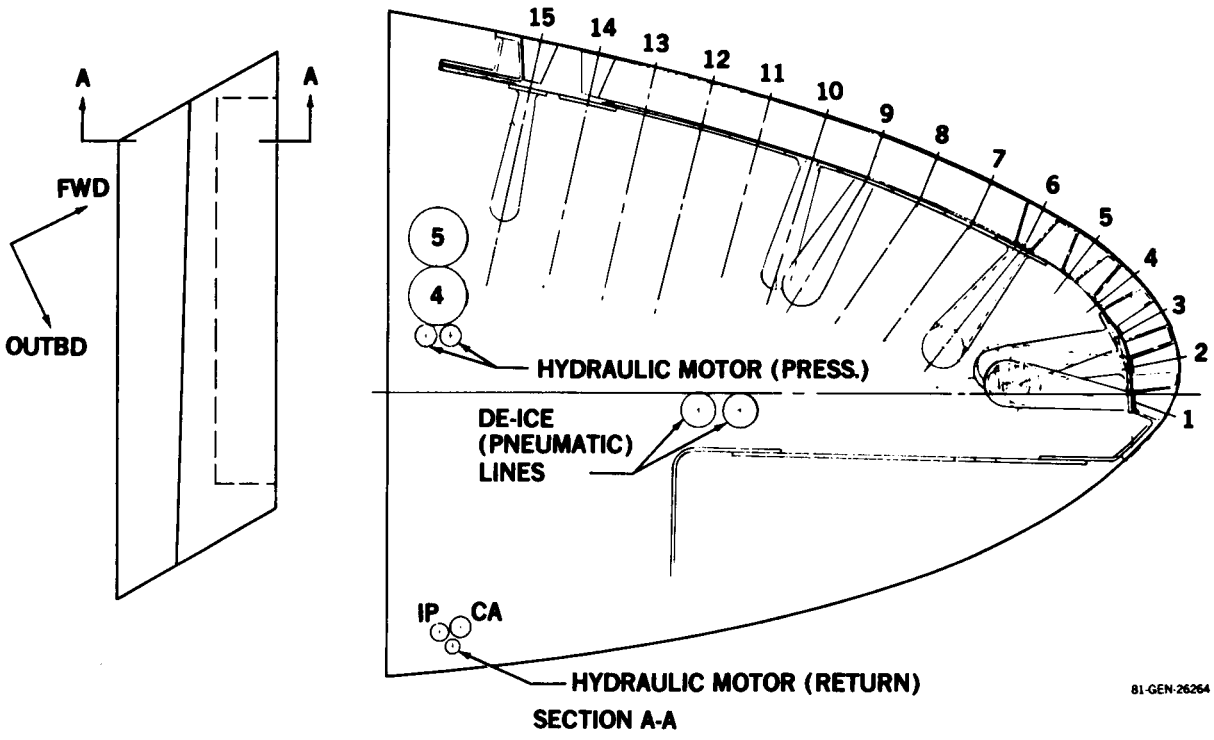

FIGURE 37. LEADING EDGE FLUTE CONFIGURATION

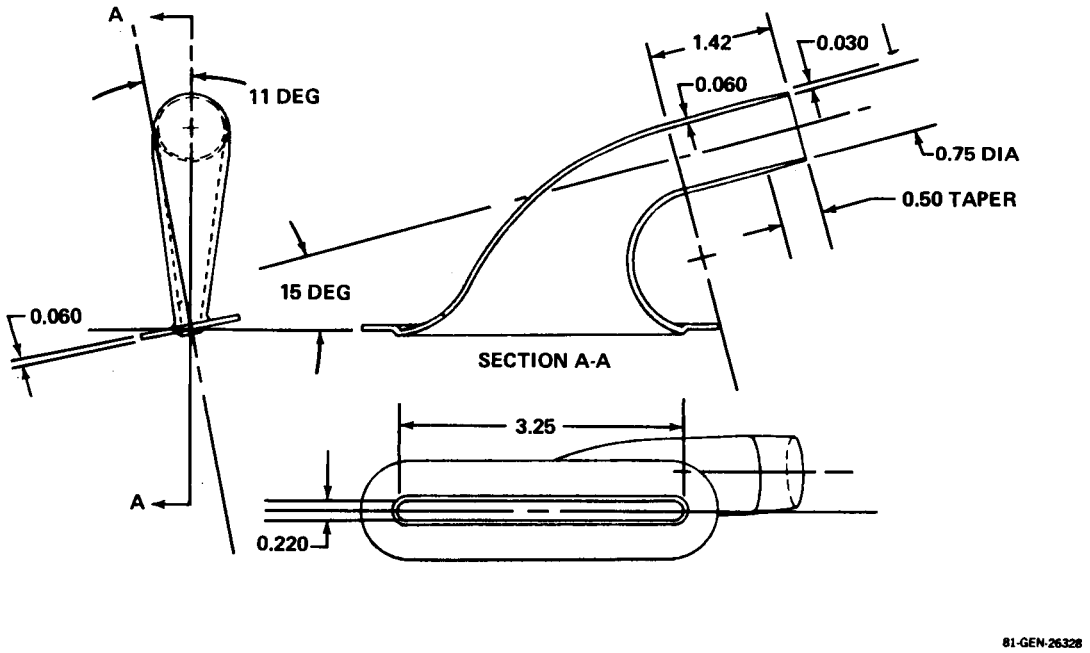

FIGURE 38. SUCTION FLUTE FITTING

7.2 LEADING EDGE SUPPORT STRUCTURE

As illustrated in Figure 2, the suction and sensor panel assembly that forms the upper surface is attached to the JetStar wing by means of ribs mounted on the front spar. The five main ribs and two closure ribs are connected at the bottom by several full length stringers and access panels to close the box. The ribs are attached to the spar through machined aluminum attach fittings. The unit is designed to have these attach fittings permanently mounted on the spar and for the ribs and access panels to be detachable.

7.3 HIGH-LIFT SHIELD SYSTEM

Two double ribs inboard and outboard are designed to support the shield actuating hinges, the actuators and linkages that operate the shield which, in the closed position, forms about 50 percent of the lower surface of the test article. An additional idler hinge that supports the shield at its mid-span is connected to an intermediate rib. This rib is attached to the front spar through a four-bar linkage that reduces load transfer between the wing and the test component by allowing acceptable relative deflections. A section through the inboard actuator station is shown in Figure 39. The shield is shown both in the closed position and the full open position.

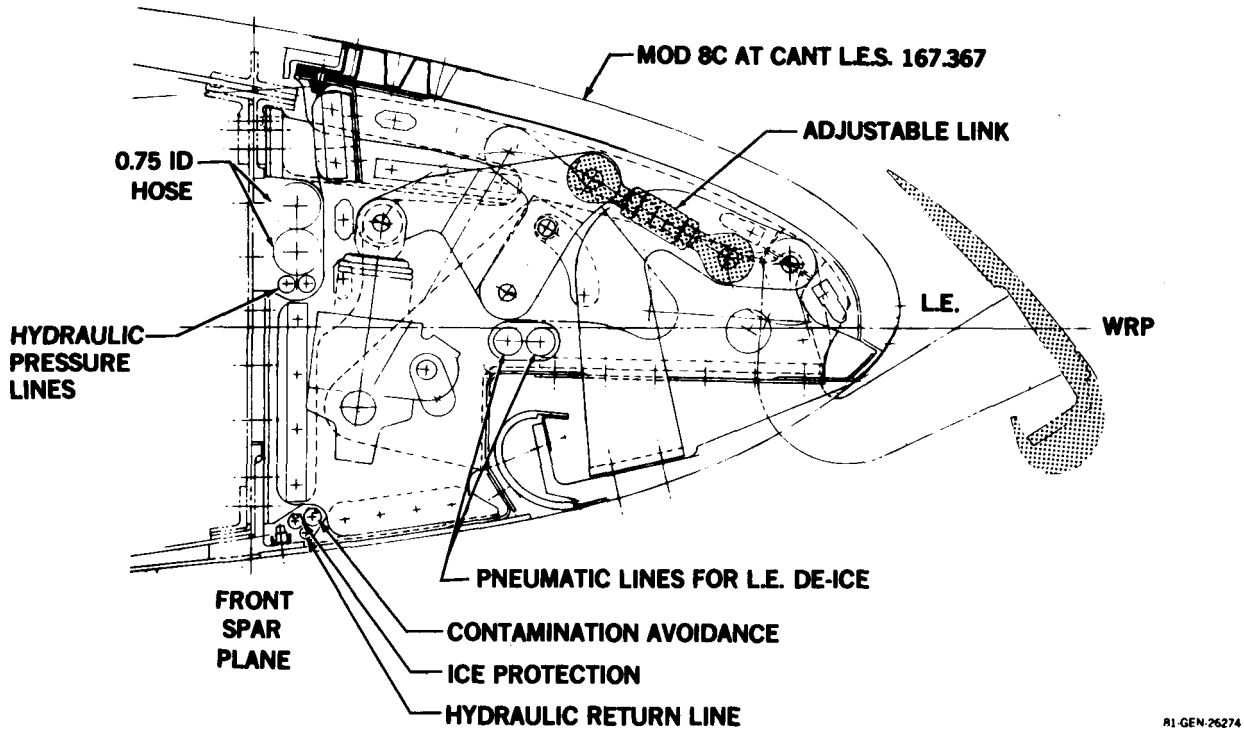

FIGURE 39. INBOARD ACTUATOR RIB LINKAGE INSTALLATION

In addition to supporting the actuator, bell crank, linkage, and hinge for the shield, each pair of machined ribs has mechanical stops incorporated to limit the travel of the actuation mechanism in the event of failure in the hydraulic drive motor shut-off circuit. The hydraulic drive motor is mounted on the wing spar outboard of the test article. A torque shaft connects the motor to the outboard actuator, which in turn is connected to the inboard actuator by a similar torque shaft. The linkages, shield, hinges, and override stops are designed to be fail-safe in the event of any single failure such as a broken hinge or torque shaft.

7.4 SUCTION/CLEARING SYSTEM

The maintenance of laminar flow control by distributed suction requires a fairly sophisticated system capable of providing the proper suction flow and corresponding pressure for each area on the airfoil surface. The structural design of the leading edge panel provides isolated flow channels or flutes that divide the panel into 15 spanwise strips of porous titanium through which air can flow in or out through the surface.

The flow through each flute is controlled individually by a motor-driven valve in a chamber valve assembly. The chamber, 25-inch long by 20-inch diameter, is located in the cabin of the JetStar and contains all 15 valves for controlling the flow in or out of the flutes. The operation of the chamber valve assembly in the suction mode requires a suction source with sufficient capacity to maintain the pressure in the chamber below the lowest requirement of any flute on the test section. At the same time, the suction source must provide the combined flow volume for all of the flutes. For design purposes, the requirement of the DAC test article is a total maximum flow of 0.056 pounds per second at a pressure of 230 pounds per square foot.

The valves are required to operate from zero flow to a maximum based on the suction requirements at the location of the perforated strip of each indivdual flute. The pressure requirement is dictated by the surface pressure over the perforated area of the flute. The pressure differential between the flute pressure and the surface establishes the flow through the porous surface depending on the pressure drop characteristic of the porous surface. The volume of flow required depends on the condition of the boundary layer as the air flows over that portion of the porous surface.

The capabilities built into the suction system allow for the possibility of exploring off-design conditions by providing for an excess of up to 150 percent of the calculated flow required at any one flute area. This excess capacity should allow investigation of off-design conditions, damage tolerance, waviness, and partial blockage of surface porosity.

7.5 ENVIRONMENTAL PROTECTION AND SURFACE CLEARING

Contamination Avoidance

The primary purpose of the shield is to deflect or catch airborne debris and thus prevent it from contaminating the leading edge of the test article during takeoff and landing. Such a device has been wind tunnel tested against insects and proved to be effective.

Since it may be critical to keep the leading edge free of virtually all contaminantes, including ice, a secondary protection system is incorporated on the shield. This secondary system consists of 12 spray nozzles mounted on the back of the shield, spaced and directed at the leading edge such that a liquid under pressure can be deposited on the leading edge in sufficient quantities to provide a continuous protective coating (see Figure 40). The liquid proven most effective and chemically acceptable is propylene glycol methyl ether (PGME) diluted to 60 percent solution with water. PGME is a freezing-point depressant which extends the usable operating temperatures to well below the freezing point. This would be important during operations where the freezing level occurs at a relatively low altitude such that the JetStar comes in contact with the below-freezing air before the CA operation including surface clearance is completed. This ability to operate at below-freezing temperature also allows the CA spray system to be used to clear any ice that may accumulate on the leading edge suction panel. In tests using PGME a finite time was required to clear all the liquid from the surface, and the time increased at colder temperatures.

Design of the CA spray system controls allows for intermittent operation. This permits the amount of liquid applied to the surface to be varied. (See Figure 41.) An early objective of the test operation should be to determine the minimum amount of liquid required to prevent contamination from influencing the achievement of laminar flow. The recommended operation includes the use of sufficient clearing air to keep a slight positive pressure beneath the surface and allow some outflow through the porous surface whenever liquid is on the surface.

OF POOR QUALITY

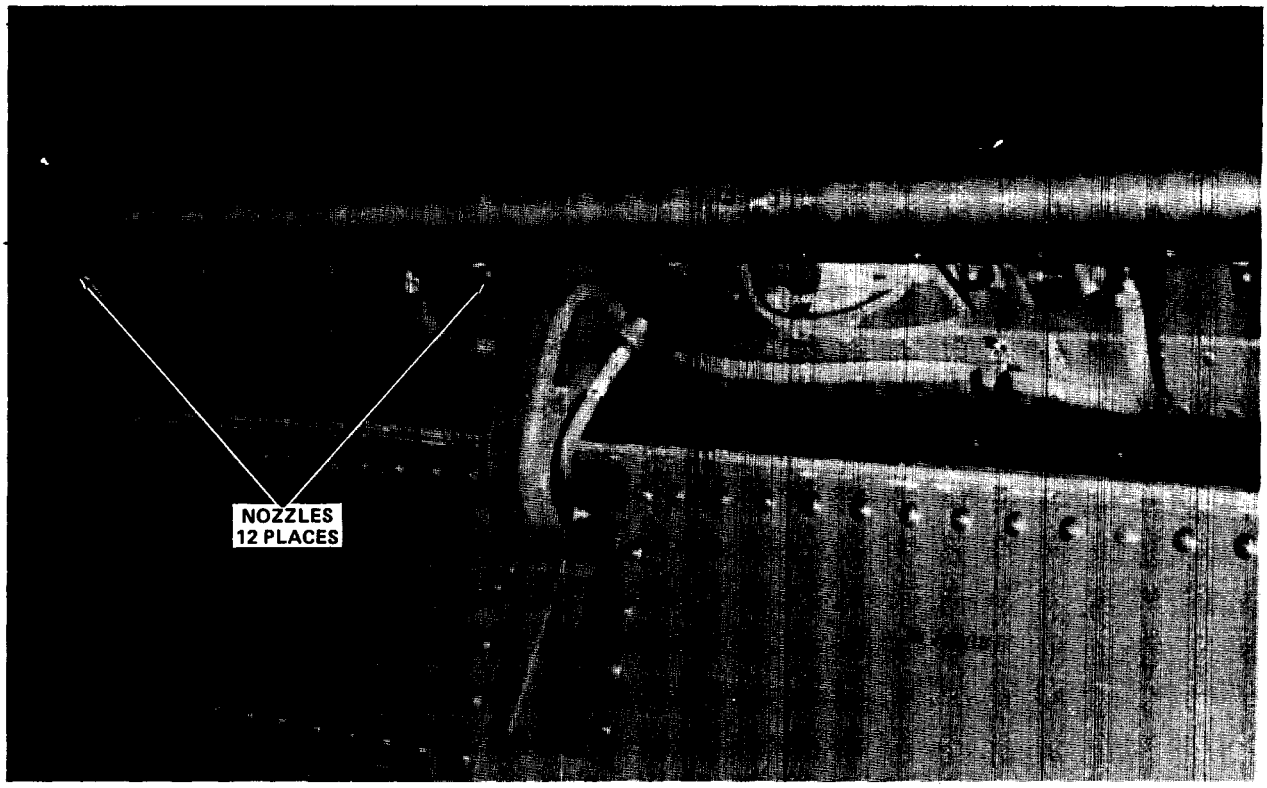

FIGURE 40. CA LIQUID SPRAY NOZZLES ON SHIELD

SHIELD ID SYSTEM

1. TKS CONTROL UNIT.
2. SYSTEM ON/OFF SWITCH.
3. LOW-PRESSURE WARNING LIGHT (AMBER).
4. ANTI-ICE LIGHT, NORMAL OPERATION (BLUE).
5. FLUID QUANTITY INDICATOR.
6. DIMMER SWITCH.

CA SPRAY SYSTEM

7. SYSTEM SELECTOR SWITCH.
8. CYCLE TIMER CONTROLS.
9. SHIELD EXTENDED LIGHT (GREEN).
10. FLUID SPRAY ON LIGHT (AMBER).
11. PURGE ON LIGHT (AMBER).
12. N_2 PRESSURIZATION SWITCH.
13. FLUID SUPPLY PRESSURE GAGE.
14. N_2 PURGE PRESSURE GAGE.

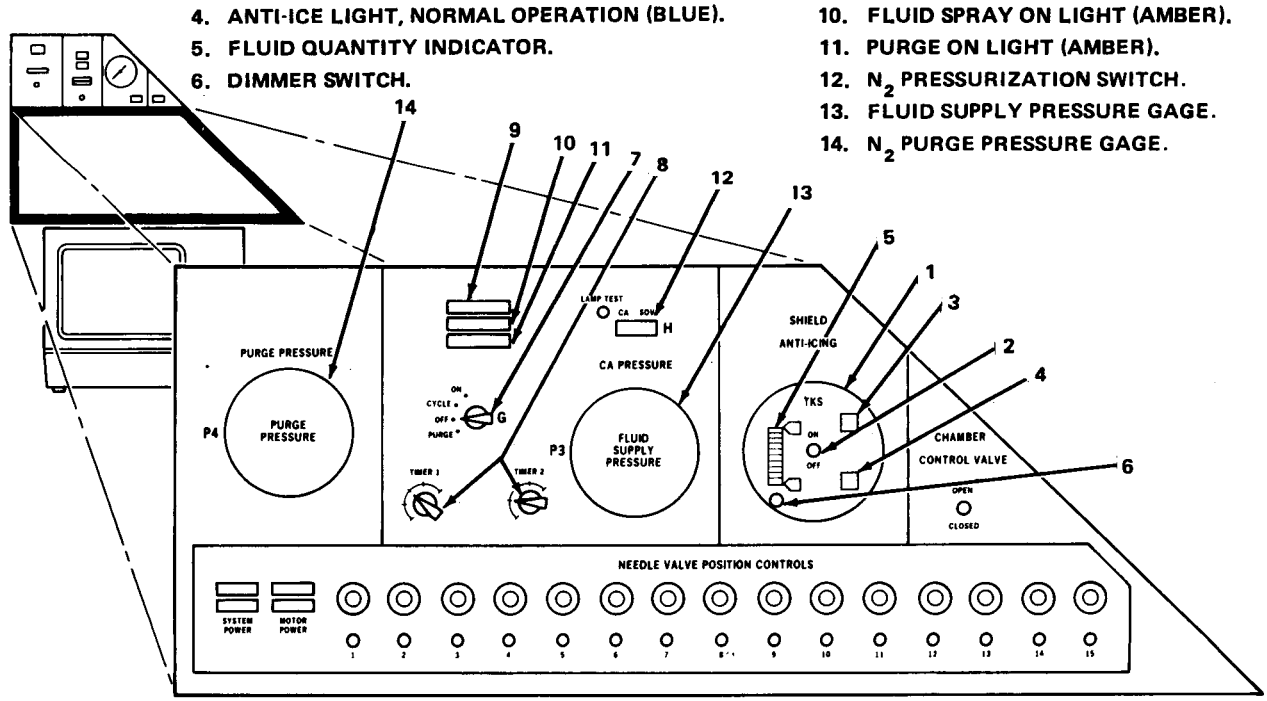

FIGURE 41. CONTROL FOR CA SPRAY AND IP SYSTEMS

Ice Protection

To provide protection against ice formation on the shield that would affect high-lift performance, a TKS Ltd. ice protection system, which secretes a freezing-point depressant through a porous panel, is inserted in the leading edge of the shield. The shield, being extended normally for takeoff and climb, will be in the position to catch any leading edge ice during an encounter with icing conditions. During such encounters the TKS system is operated and the glycol based freezing-point depressant fluid flows over the surface of the shield to prevent ice from accumulating. This may provide sufficient ice protection for the main wing leading edge and make use of the supplementary spray system unnecessary for this purpose. Figure 42 illustrates the TKS installation on the shield.

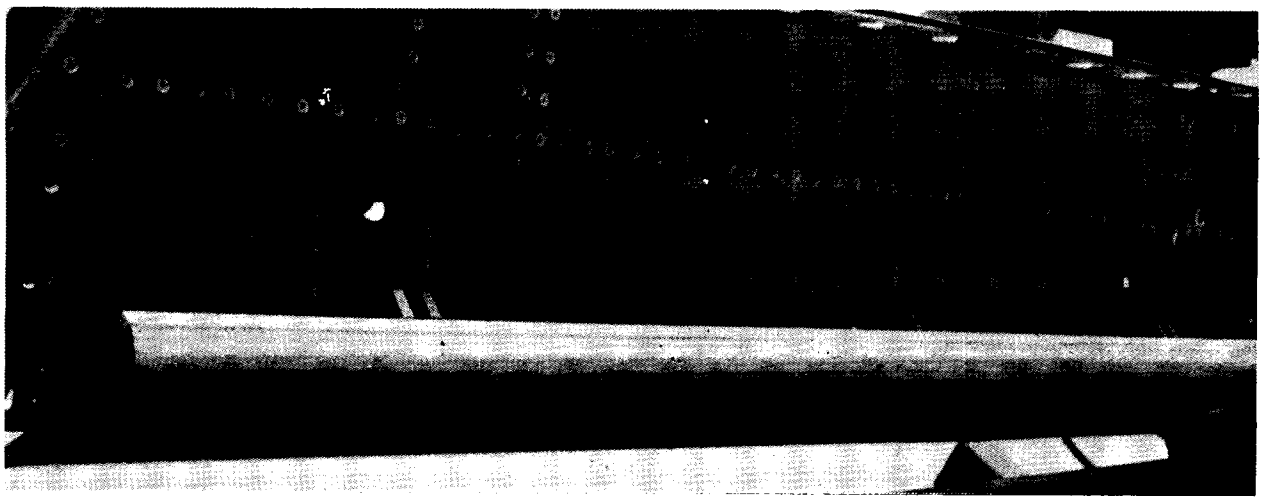

FIGURE 42. TKS IP INSTALLATION ON SHIELD LEADING EDGE

Surface Clearing

To supplement the natural tendency of any residual PGME and water mixture to evaporate or be swept aft and off the surface by the free stream airflow, clearing air is supplied to the flutes under pressure and can be forced out through the porous surface. Increasing the temperature of the clearing air increases the rate at which the surface can be cleared of liquid. Provision for varying the clearing air pressure in each flute as well as changing the temperature of the air supply is inherent in the system.

The suction system has the ability to allow for reverse airflow through the system and to control the pressure and flow rate of clearing air. The clearing air source is the cabin air conditioning and pressurization system from the ground to 12,000 feet altitude. Above 12,000 feet, the emergency pressurization system is available for this purpose. The pressurization air is diverted into the system ahead of the chamber valve assembly. The chamber serves as an air pressure accumulator and the valves are then used to control the flow of pressurized air into the various flutes as required to maintain from 0.5 to 1.0 psi above the ambient pressure on the perforated surface at the flute location. This pressure has been shown in tests to be sufficient to expel any residual liquid from the perforations. The air flowing out through the perforated surface also aids in evaporating the surface liquid.

ORIGINAL PAGE IS
OF POOR QUALITY

SECTION 8
STRUCTURAL TESTING

8.1 ELECTRON BEAM PERFORATED TITANIUM SURFACE

The DAC-designed LFC suction panel has an outer skin surface of 0.025-inch-thick titanium with an array of closely spaced holes. The holes were formed by an electron beam in an evacuated environment. The metallurgy was altered in the vicinity of the holes, but its effect on the structural properties was unknown. Also, because of the relatively small size of the EB perforated sheets available from suppliers, several sheets had to be welded together. TIG welding was used to assemble the EB perforated surface sheet for the flight test article. The extent to which this weld altered the metallurgy of the basic titanium material was unknown and thus required additional structural testing.

The titanium properties were evaluated at room temperature and consisted of standard tension and fatigue tests. For comparison, both plain titanium sheet and perforated titanium with and without a welded joint were tested. The results of the fatigue tests are summarized in Table 5. The concern was the highly perforated surface welded together from smaller pieces would encounter accelerated fatigue failure. Both the initial tests of plain, perforated, and welded perforated titanium and the recycled specimen tests went beyond 120,000 cycles without failure. Failure was induced only by increasing the stress levels well beyond that of the design limits. All other properties of the perforated titanium were essentially the same as the basic titanium sheet at $-65^{o}F$, room temperature, and $+160^{o}F$.

8.2 BOND STRENGTH

The fabrication of the LFC suction panel required bonding of perforated titanium to a fluted fiberglass substructure. In flight testing the suction panel, it will be exposed to the extremes of atmospheric temperatures in both wet and dry conditions. Structural testing of both the fiberglass and the bonded joints was carried out from -65°F to 160°F. In addition to normal exposure to water, the suction panel will be exposed to cleaning solvents and freezing-point depressants used in the contamination avoidance and ice protection systems. Testing of the fiberglass and bonded joints was accomplished in the presence of these materials as well, and results are presented later in this section.

The types of shear tests for the fiberglass included interlaminar shear, rail shear, and fastener shear-out as well as fastener bearing. For the combined fiberglass bonded to perforated titanium, both the double-lap shear and climbing drum peel tests were performed. The results of these tests are summarized in Table 6. Since existing standards for the materials to be used did not include the lower curing and bonding temperatures proposed, the values for mechanical properties used in the design were taken from the table.

A flat panel burst test assessed the structural integrity and bond strength of the EB perforated outer titanium sheet to the fiberglass fluted substructure. The tested specimen was a panel 4-1/2 by 7 inches configured as in Figure 43.

TABLE 5

SUMMARY OF EB PERFORATED TITANIUM FATIGUE TESTS

SPECIMEN NO. AND DESCRIPTION	R = MIN STRESS/MAX STRESS		CYCLES
1. Plain Ti	0 =	0/12,000	120,000
2. EB Perf Ti	0 =	0/12,000	120,000
3. Welded Perf Ti	0 =	0/12,000	120,000
4. EB Perf Ti	-0.75 =	-9,000/12,000	120,000
5. Welded Perf Ti	-0.75 =	-9,000/12,000	120,000
6. Plain Ti	-0.67 =	-16,000/24,000	120,000*
7. EB Perf Ti	-0.67 =	-16,000/24,000	120,000*
8. Welded Perf Ti	-0.67 =	-16,000/24,000	120,000*
9. EB Perf Ti	-2.8 =	-33,600/12,000	77,000 (failed)
10. Welded Perf Ti	-2.8 =	-33,600/12,000	49,000*** (failed)
11. Plain Ti	-2.5 =	-29,800/11,900	120,000
12. Plain Ti**	-2.66 =	-60,480/22,720	6,000 (failed)

*Recycling of specimens from Tests 1, 2, and 3.

**Continuation of test 11 at higher stress level.

***Failure occurred approximately 0.22 inch from center of weld bead along a row of perforations.

Note: The negative sign indicates compressive stress.

TABLE 6

MECHANICAL PROPERTIES TEST RESULTS

TEST METHODS	MECH PROP (LB/IN^2)	COND	TEMPERATURE		
			-65°F	RT	+160°F
Tension FG	Tens. Stress	Dry	68,000 (59,300)	58,300 (47,200)	50,000 (41,400)
		Wet	67,000 (50,600)	52,000 (41,100)	46,000 (28,900)
Compression FG	Comp. Stress	Dry	80,000 (83,400)	65,000 (62,900)	46,000 (50,900)
		Wet	78,000 (71,800)	51,500 (53,700)	35,000 (40,700)
Interlaminar Shear FG	Shear Stress	Dry	16,200 (8,840)	14,500 (8,350)	9,200 (7,390)
		Wet	16,000	12,100	6,400
Rail Shear FG	Shear Stress	Dry	16,840 (22,600)	12,660 (16,000)	11,100 (13,800)
		Wet	17,130	10,940	10,290
Fastener Shearout FG	Shear Stress	Dry	22,200	19,000	14,200
		Wet	23,200	14,000	9,400
Fastener Bearing FG	Bearing Stress	Dry	82,000 (84,600)	57,000 (68,400)	43,000 (48,400)
		Wet	62,000	37,000	26,000
Double Lap Shear Ti to FG	Shear Stress	Dry	3,650	3,800 (2,950)	2,450
		Wet	3,650	3,360	2,300
Climbing Drum Peel Ti to FG	Average Load (Lb)	Dry	79	88	103
		Wet	71	66	75

( ) Properties for NARMCO N588/7781 (ECDE-1/0-550) Fiberglass Epoxy - MIL-HDBK 17A

The specimen was first tested to a suction pressure of -12 psi without any sign of failure. It was then tested to a positive pressure until failure occurred along the edge bond of the skin to the substructure at 108 psi. This is well in excess of the maximum capability of the clearing air supply system, even with a pressure control system malfunction.

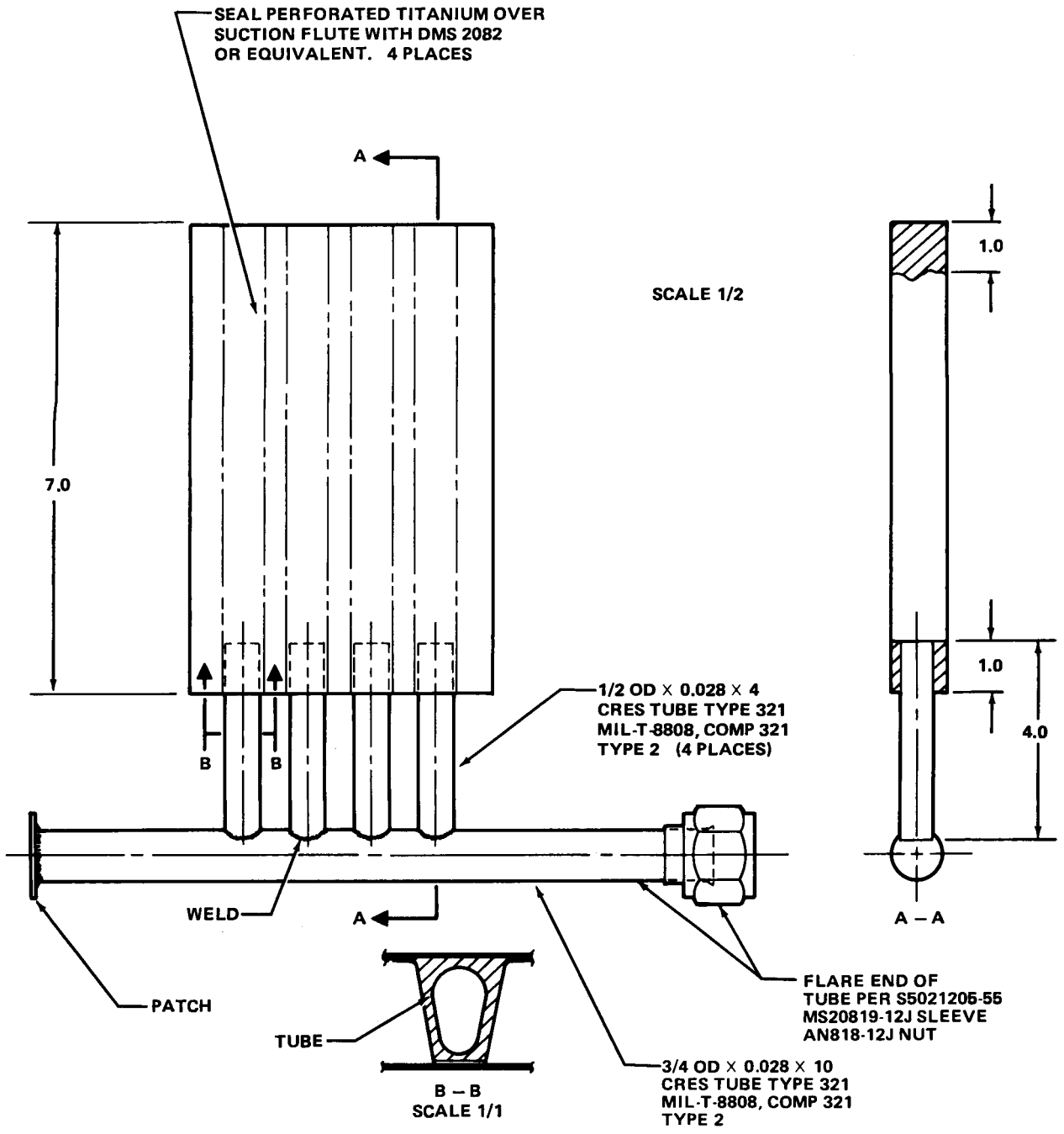

FIGURE 43. BURST SPECIMEN

Adhesive Tolerance to PGME

The fabrication of the suction panel with figerglass fluted substructure and perforated titanium surface requires a superior bonding adhesive between the figerglass and titanium. Both AF31 and FM73 adhesives were extensively tested and found to have adequate bond strength under dry and wet conditions. The anticipated use of a chemical cleaning solvent such as EGME or PGME as a surface clearing or contamination avoidance fluid required that the bond be tested after exposure to these solvents. Considerable deterioration in the FM73 bond occurred after moderate exposure to either of the solvents. AF31 proved to be least affected by exposure to PGME which is the primary contamination avoidance fluid.

The AF31 adhesive that was selected has a phenolic base whereas FM73 has an epoxy base. The epoxy base adhesives tend to break down and lose strength in the prolonged presence of glycol type solvents, while the phenolic base adhesives have a much greater resistance to glycol. Although some decrease in strength of the AF31 was noted under prolonged exposure to PGME at elevated temperature, the relatively short exposure time during a given flight test and the complete drying of the test article between exposures to PGME do not constitute any hazard over the anticipated life of the test article.

8.3 NOSE BOX TEST

A fluted fiberglass curved substructure with a bonded perforated titanium surface skin representing the LFC flight test article suction panel structure was tested in compression and torsion. Loads were applied in two separate tests to the one common specimen. The tested unit is shown in Figure 44. The specimen cross section is representative of the actual flight test article contour. The specimen is 20 inches long with flat plates attached to the ends. These flat plates distribute the test axial compression and torque loads to the ends of the specimen.

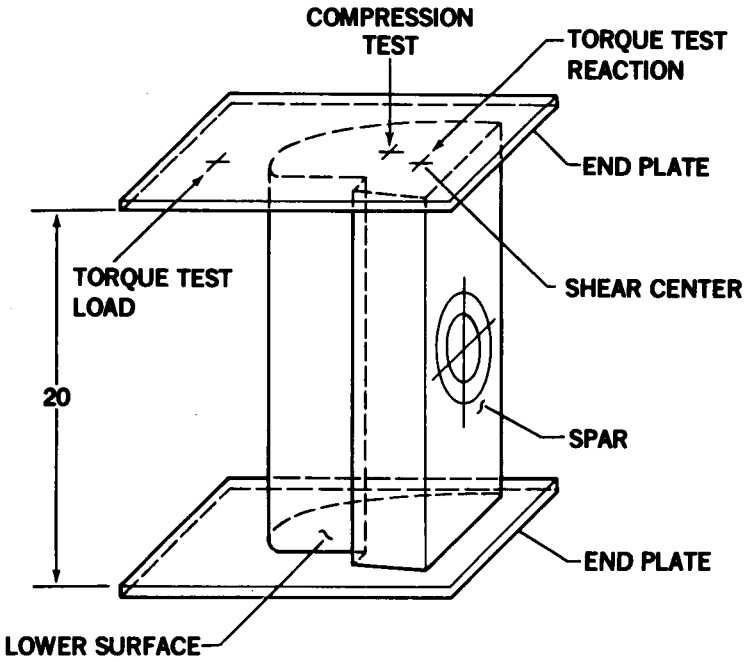

FIGURE 44. AXIAL COMPRESSION/TORSIONAL SHEAR TEST SPECIMEN

The compression test load was based on the JetStar wing, maximum vertical deflection of +3.3 inches between wing stations 196 and 135 (61 inches in length) at 40 percent chord (GELAC SRD 72-73-843). The test compressive load was applied to the C.G. of the test section. Its intensity was representative of the wing bending moment load intensity along the upper surface of the leading edge during flight. The test torque load was based on a wing twist of 0.4 degrees between W.S. = 196 and W.S. = 135 (61 inches in length), about the 40 percent wing chord. This torque was applied about the shear center of the leading edge test specimen. These tests were to help substantiate the structural design and to determine if any local irregularities of the titanium skin surface (between the fluted substructure) occur due to the design loads. Excessive irregularities of 0.003 to 0.004 inch would be sufficient to trigger turbulent flow. Strain gages were installed at flutes number 3 and 10, on the inner and outer surface, midway between the flat end plates. (The flutes are numbered from 1 starting at the leading edge and increasing toward the front spar.)

A maximum compressive load of 65,000 pounds and a maximum torque of 17,000 in-lb was applied without failure of the test specimen. These loads during non-destructive testing represent approximately 70 percent of the estimated specimen strength. Predicted stress levels of the outer titanium sheet and the inner fiberglass sheet compared favorably with test results. A check for surface irregularities (waviness) of the EB perforated titanium outer skin of the fluted corrugated panel was made at 0, 25, 50, 75, and 100 percent of the maximum applied loads. Figure 45 is a plot of three-pronged dial indicator readings of the surface waviness during the compression and torsion tests. There was no visible or measurable change in waviness or deformation of the EB perforated titanium surface during or at the conclusion of either test.

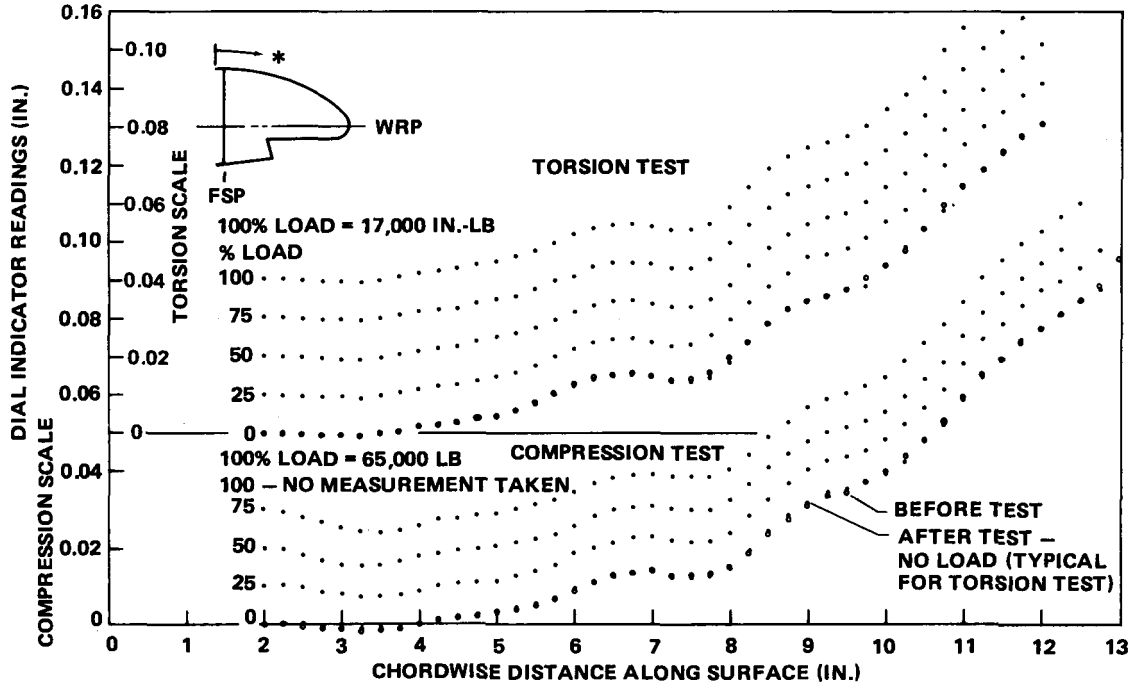

FIGURE 45. WAVINESS MEASUREMENTS UNDER LOAD – 20-INCH LEADING EDGE SPECIMEN

SECTION 9
STRUCTURAL ANAYSIS

9.1 REQUIREMENTS

The overall structural requirements were provided by Lockheed, Reference 14. Deployment of the shield was limited to a maximum speed of 250 KEAS or Mach 0.4. It was necessary to avoid overloading the existing structure of the JetStar at the attachments of the main ribs of the leading edge flight test article to the front spar.

9.2 DESIGN LOADING CONDITION

Critical flight and shield operational loads were estimated for the following:

- Airloads on the entire leading edge test article including the sensor panel.
- Airloads on the leading edge shield in deployed, intermediate, and stowed positions.
- Airloads on the closure ribs due to load transfer from the adjacent JetStar fairings.
- Induced load in the leading edge structure due to JetStar wing bending.
- Fail-safe loading conditions were also determined.

To reduce load transfer due to wing deflections, the center rib was supported by a four-bar linkage system, and a continuous spanwise shear attachment to the front spar was avoided.

To avoid overloading in the event of an actuator or drive shaft failure, the hydraulic pressure to the actuator was limited to 650 psi. With this limit, the strength and stiffness of the shield system was sufficient to stall the other actuator and prevent overloading.

As a precaution, a factor of 2.0 was used to determine the ultimate design loads from limit loads.

9.3 AEROELASTIC ANALYSIS

The design criteria were taken from FAR 25, which requires the shield design to be free of flutter and divergence at all speeds up to 1.2 V_D and, in addition, be free of flutter at all speeds up to V_D following a failure in any of the mechanical load paths. Figure 46 shows the V_D envelope.

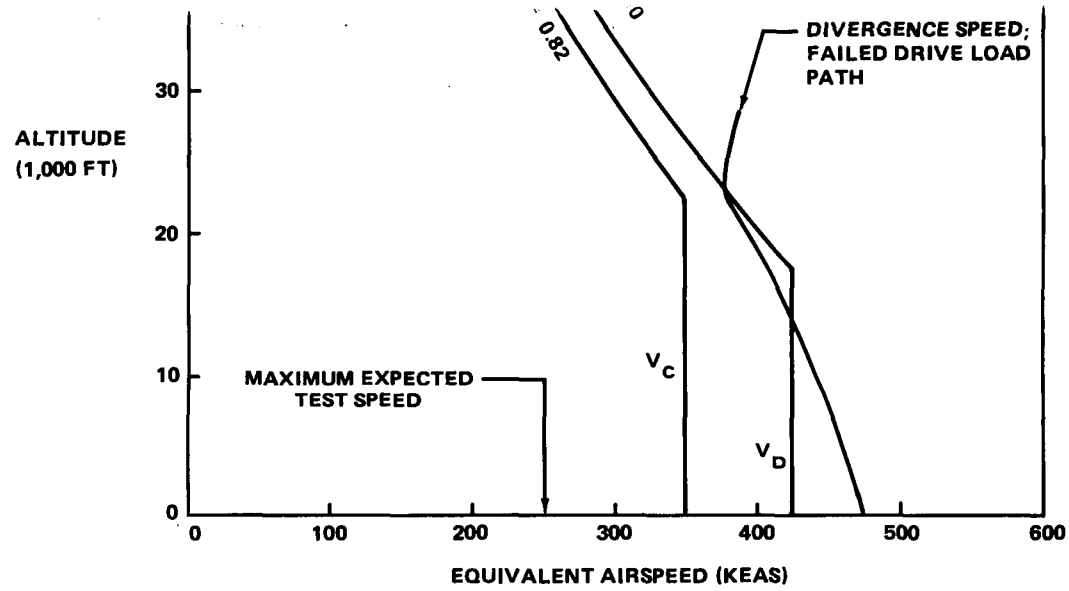

FIGURE 46. JETSTAR FLUTTER ENVELOPE – SHIELD EXTENDED

The results of the analyses show that the shield has high flutter speed margins, but is subject to static divergence following a loss of the mechanical load path between either actuator and the shield; for example, by failure of either adjustment link. However, the minimum divergence speed was still 50 percent above the maximum intended test speeds. Failure of the center idler mechanism was not critical.

SECTION 10
TOOLING

The most important part of the LFC leading edge flight test article to control dimensionally is the outer surface which must be of very accurate contour and free of waviness. Only those fabrication techniques that have a potential for yielding such a surface were considered in the design of the flight test article and in the design and fabrication of the tooling to control the more critical assemblies. The fabrication and bonding technique used to produce wind tunnel test panels had the best potential for meeting this objective.

The technique consists of building the panel from the outside in. Since the smooth and accurate surface is most important, a very accurately constructed molding and bonding tool is used as the basis for fabricating the fiberglass and carbon substructure. Silicone rubber mandrels with trapezoidal cross section provide the shape of the suction air carrying channels or flutes. Alternate flutes of the same shape but inverted in orientation separate the active flutes and also provide a narrow land surface for bonding the perforated titanium skin. A cross-sectional view of this arrangement is illustrated in Figure 47.

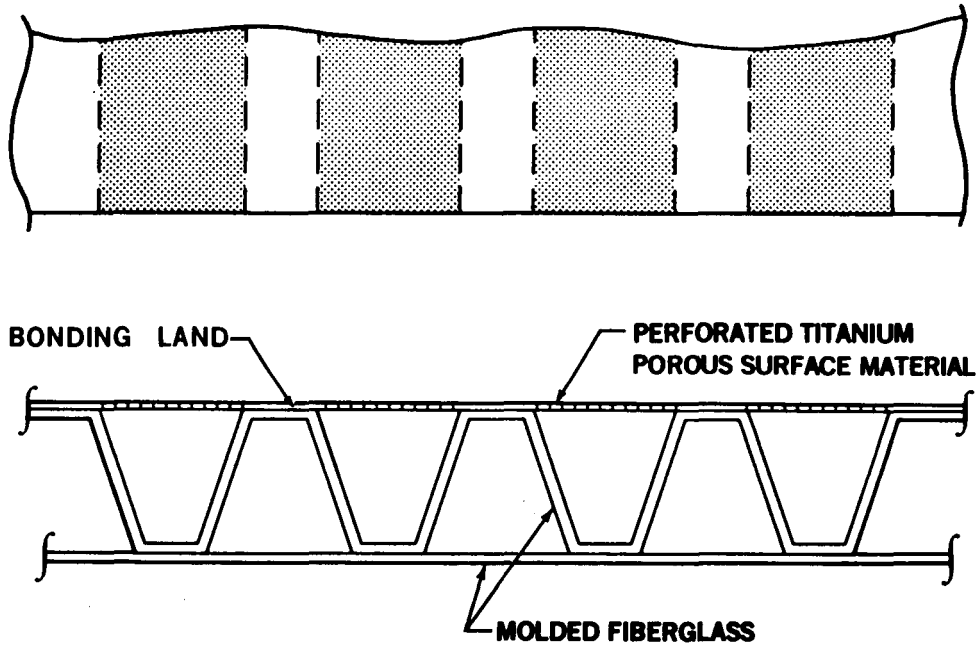

FIGURE 47. CROSS SECTION OF SUCTION PANEL

The fabrication of the LFC leading edge test article was very dependent upon accurate and precise tooling fabrication. The tooling was specified to control the accuracy of the outer airfoil contour within 0.010 inch and the waviness of the surface was not to exceed 0.002 in 1.0 inch. This is greater accuracy than is required on the finished part.

10.1 SUCTION PANEL

OF POOR QUALITY

For LFC, it is essential to have a very accurately shaped and stable outer surface. It is probably not sufficient to have the skin attached by conventional fasteners to even extremely accurate support structure such as ribs and stringers. External fasteners alone can create sufficient steps, gaps, protrusions and depressions to cause transition of laminar flow. To overcome the use of surface fasteners and to increase significantly the accuracy of the outer surface, tooling was specified to permit bonded assembly of the surface and stiffening substructure from the surface inward. The accuracy of the surface was thus dependent on providing a high-quality mold or bonding tool.

Molding/Bonding Tool

Although conventional fiberglass molds were successfully used to build wind tunnel models to initially prove the porous surface LFC concept, the stability of such molds proved to be poor with the critical surface, tending to change contour significantly with each cycle in the autoclave. To overcome this instability in the tool for forming the fiberglass and carbon substructure and bonding the porous titanium skin, a stabilized steel leading edge panel forming tool was designed by DAC and fabricated by STADCO Tool and Die Company. The basic tool was a stress-relieved weldment consisting of a contoured heavy steel plate supported by a flat steel plate "egg crate" strong back. This supporting structure was generously vented by lightening holes to allow uniform temperature distribution in the autoclave. The contoured plate was machined to the airfoil surface using numerical control equipment. The actual machine cuts were along straight element lines. The straight element lines were programmed by connecting the equivalent points on a lofted chordwise surface-cut at each end of the test section as defined by the Lockheed data.

The accuracy of the steel tool surface was in general much greater than specified. This resulted in a virtual wave-free surface. In areas where there was some deviation from the specified contour, the rate of change was very gradual so that no deviation in curvature was apparent. Slight machining marks that could be seen were bridged by the 0.025-inch-thick titanium surface during the final bonding operation and were not significant. Figure 48 is a photo of the steel leading edge panel forming tool.

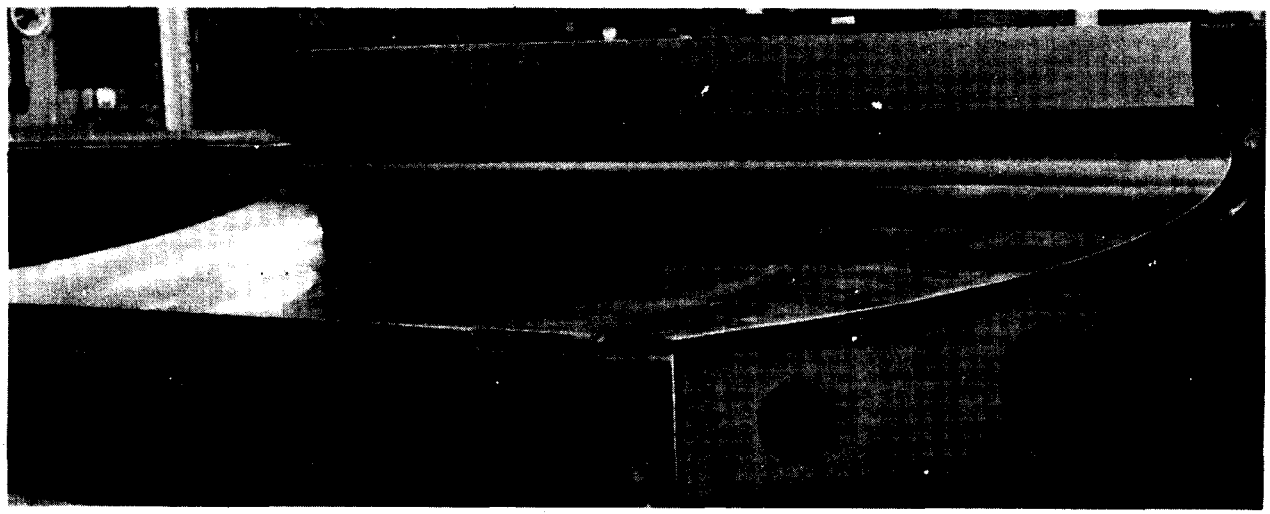

FIGURE 48. STEEL FORMING AND BONDING TOOL

ORIGINAL PAGE IS
OF POOR QUALITY

Flute Mandrel Tooling

The general procedures, processes, and tooling worked out during the preliminary design required further refinement to establish the preferred methods of assembling the fiberglass substructure and bonding the titanium to form the suction panel. Although silicone rubber mandrels were used for making the fiberglass substructure on previous programs, these were of constant cross section and were extruded. The use of tapered mandrels for the flight test article therefore required some special tooling development. Also there was concern for the deteriorating effect the candidate contamination avoidance fluids might have on the epoxies and adhesives that would be exposed to the fluid.

The design of the fiberglass substructure called for most of the flutes to be tapered. Several materials were considered for the mandrels including nylon, Teflon, and cast silicone rubber. Machining plastics like Teflon to accurate dimensions proved difficult. Also, even though good parts could be formed, the extraction of the plastic tooling could be a problem under some conditions due to minimal contraction of the cross section under tension. The main effort was therefore concentrated on developing a casting technique and machined molds for silicone rubber with characteristics as closely matched to those of the extruded type.

The tooling that evolved, utilizing the tapered mandrels, consists of a sheet of silicone rubber 0.025-inch thick to which the active flute forming mandrels are bonded. Figure 49 is a photo of this tooling ready to receive the layers of fiberglass. The mandrels are very carefully spaced on the silicone sheet to allow for the layers of fiberglass and the intermediate flute mandrels that must be inserted in the space between flute-forming mandrels, as depicted in Figure 50. This preassembled unit is then placed in the steel bonding tool for final bagging and curing in the autoclave.

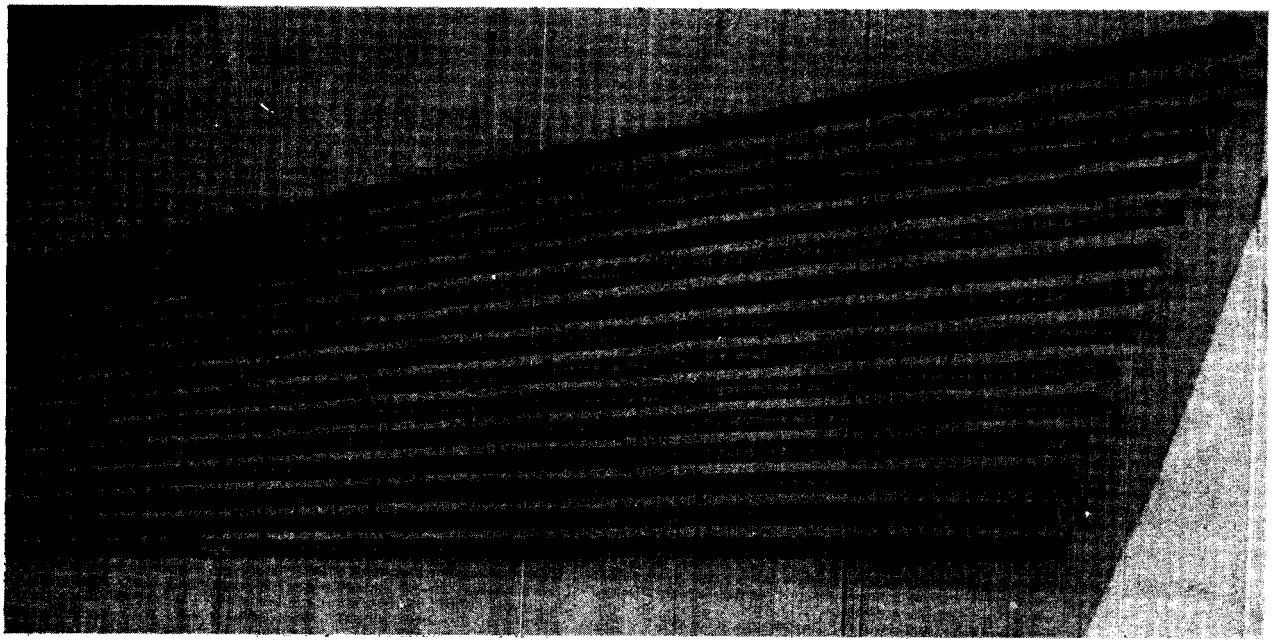

FIGURE 49. FLUTE FORMING MANDREL ASSEMBLY

ORIGINAL PAGE IS
OF POOR QUALITY

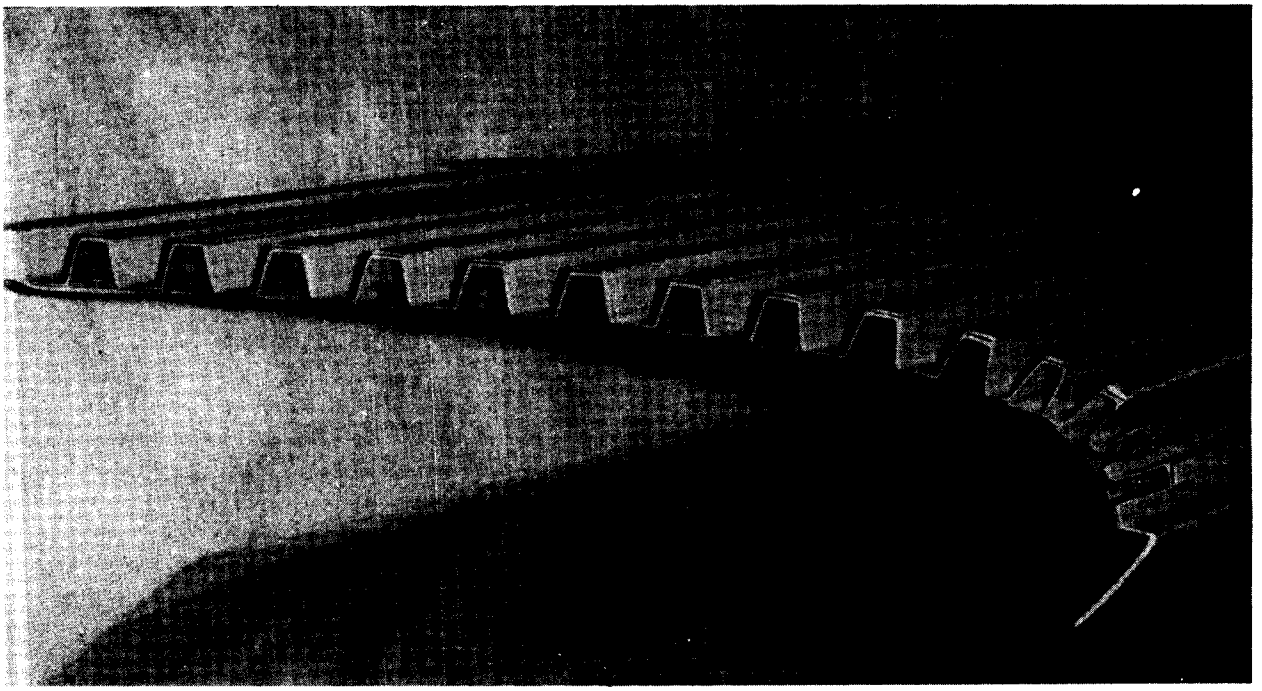

FIGURE 50. SPACER FLUTE-FORMING MANDRELS

A second set of mandrels for the active flutes is required when bonding the titanium skin. These mandrels must fit snugly in the active flute to help hold the AF31 sheet adhesive across the lands. They must just fill the flute so as to allow sufficient pressure to assure that the skin is against the contour of the steel bonding tool during the complete curing cycle in the autoclave. Figure 51 shows the adhesive on the lands being held in place by the active flute-forming mandrels.

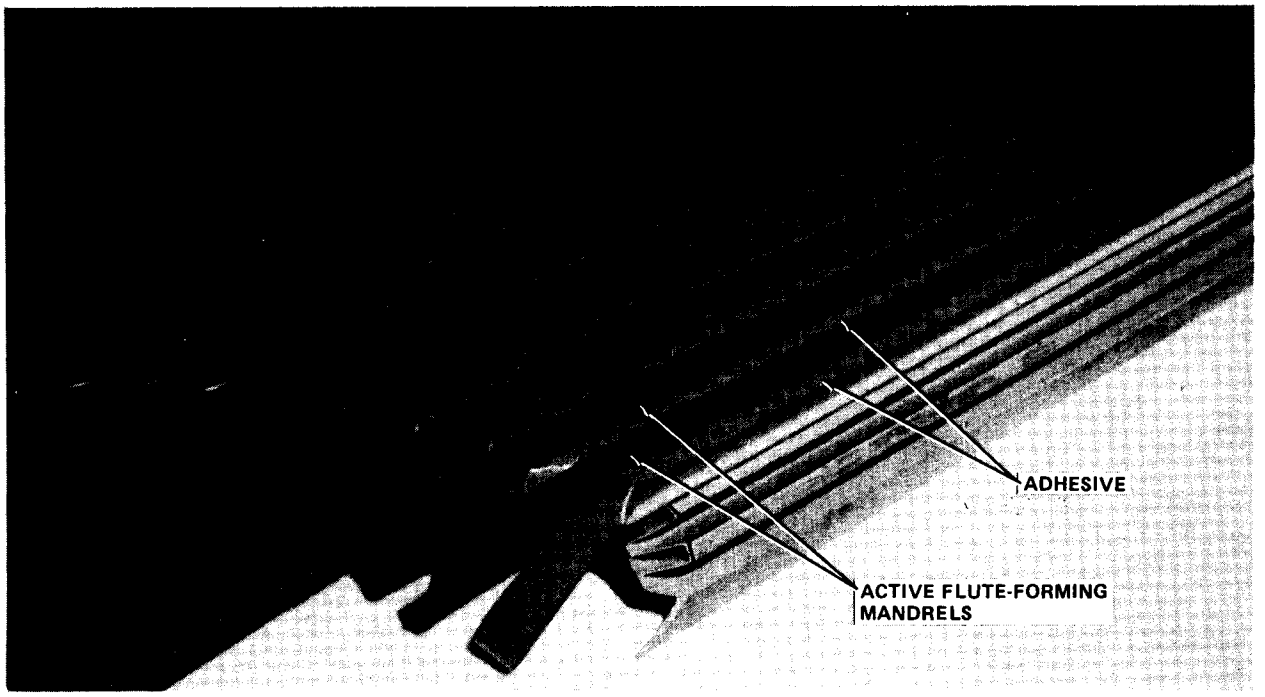

FIGURE 51. AF31 ADHESIVE ATTACHMENT TO LANDS

ORIGINAL PAGE IS
OF POOR QUALITY

Some anomaly in the curing process left the active flutes slightly less deep than the as-cast height of the mandrels used during formation of the substructure. A second set of mandrels had to be shaved and custom fitted to avoid their protruding above the lands and holding the skin away from the lands during bonding of the outer surface. Some additional development effort is needed in the application of silicone mandrel tooling to form and cure substructures.

10.2 LEADING EDGE SUPPORT STRUCTURE

The support structure is of conventional aircraft construction. Five ribs are machined from aluminimum plate. Photos of the drawing were used for tooling. The ribs attach to the JetStar spar through similarly machined attachment fittings. Two closure rib details at either end of the test section are sheet aluminum requiring only standard sheet metal tooling. The spanwise stringers and access doors are made of aluminum sheet in the same manner. The ribs are designed to not only support the leading edge panel but also the shield/slat pivot points and the actuating mechanism.

10.3 HIGH-LIFT SHIELD/SLAT AND ACTUATION SYSTEM

Two sets of identical actuators, bellcranks, and adjustment turnbuckle links are each held between a pair of ribs at leading edge stations (LES) 167.4 and 213.3. These two pairs of ribs and the center rib hold the three hinge points of the shield. The shield outer surface forms part of the airfoil's lower surface contour when retracted. This contour and the details on the back for hinge attachments were machined from a solid billet of 7075 aluminum on a three-axis numerical controlled mill. The shield in process on the NC machine is shown in Figure 52. The NC machine was programmed using the CAD-CAM equipment.

FIGURE 52. NC MACHINING OF SHIELD

ORIGINAL PAGE IS
OF POOR QUALITY

The hinges were machined from 7075 aluminum blocks. The outer hinges attach to the actuation links, with the central hinge providing stabilization. Matched tooling was designed to provide perfect alignment of the three hinge points. This tooling is shown in Figure 53 on the shield assembly jig. The matching tooling was designed to hold the hinge points as well as the actuator pivot points in the main assembly jig and holding fixure.

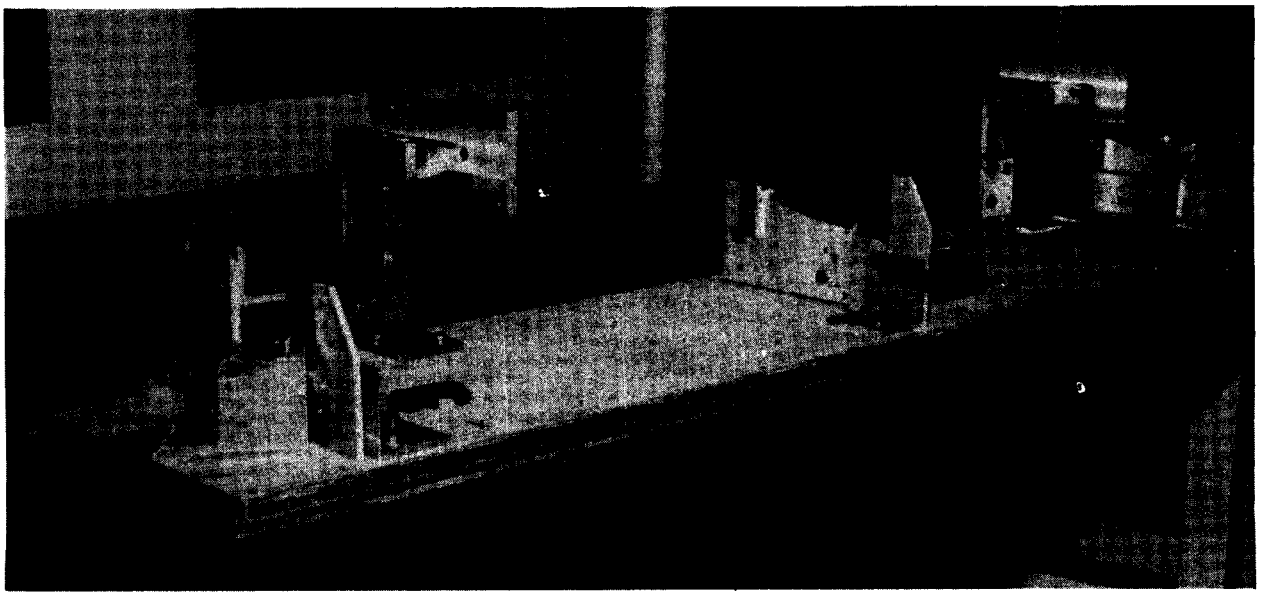

FIGURE 53. SHIELD ASSEMBLY JIG

10.4 ASSEMBLY JIG - HOLDING FIXTURE

The leading edge suction panel, once formed, is a rigid member of the assembly that must be held in exact register on the JetStar wing to form the upper surface of the airfoil. Additionally, the shield/slat must be rotatable from its retracted position, where its outer surface is held to form a portion of the bottom of the airfoil, to a position ahead of the leading edge to intercept oncoming airborne debris. These two critical items are held in alignment by the support structure.

The assembly jig shown in Figure 54 is designed to index and hold each member of the support structure in proper alignment during assembly. Critical index points built into the jig are the three hinge points of the shield, the two actuator pivot points and the outer contour of the suction panel. Several other less critical points are also fixed in the assembly jig such as the plane of the closure ribs and the end fittings of the shield stowage box.

Since the method of fabricating the fiberglass substructure allows the thickness to vary, allowance was made between the back of the suction panel and the top of the ribs. The tees are prealigned on the underside of the substructure when bonded in place using the tooling shown in Figure 55. The plane of each vertical leg of the tees becomes a key part of the assembly jig once the suction panel is positioned against the contour boards that locate the upper surface. The five main ribs are located on the hinge points and actuator pivots and then aligned to match the plane of the tees. Fixed in this manner, the ribs become the basis for the rest of the assembly.

ORIGINAL PAGE IS
OF POOR QUALITY

FIGURE 54. MAIN ASSEMBLY JIG

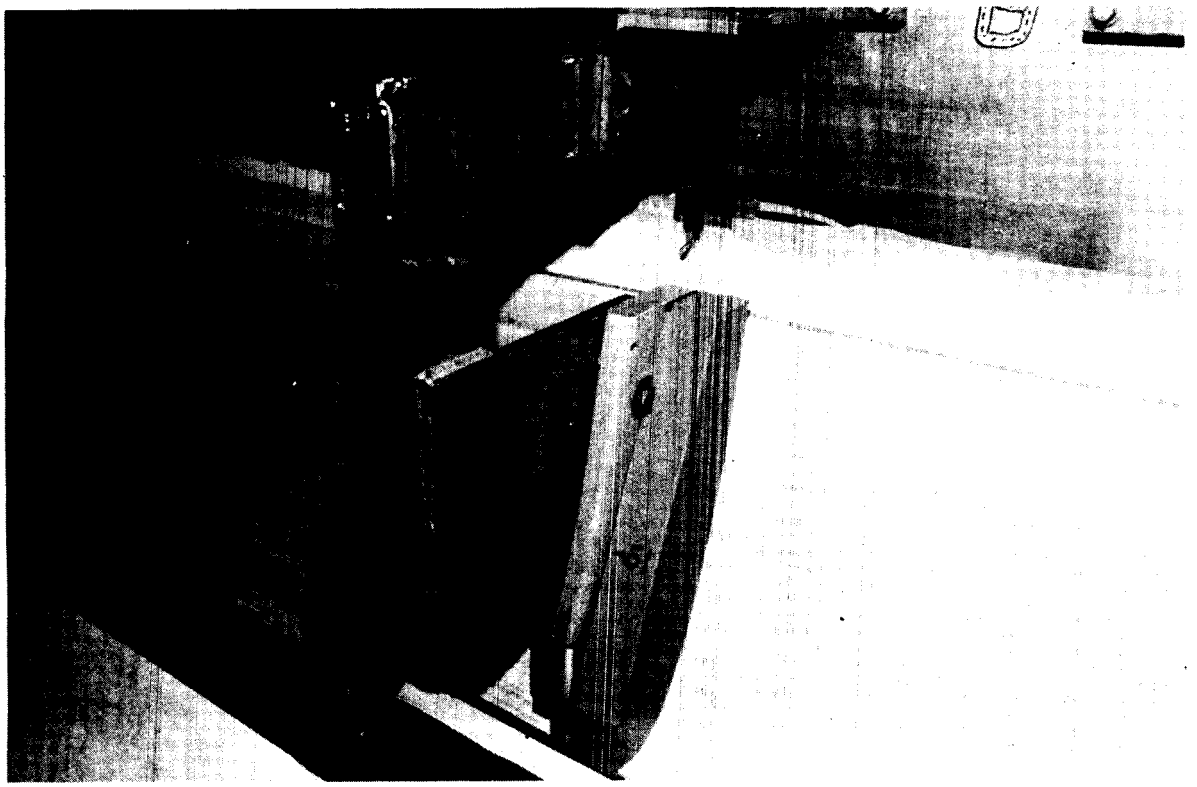

FIGURE 55. RIB ATTACH TEE TOOLING

Once assembled the support structure can stand alone in the assembly jig with the hinge line and actuator aligning details removed. The preassembled shield and the actuators can then be fitted in place. At this point, the assembly jig becomes the holding fixture to allow actuation of the shield and checkout of the contamination avoidance and ice protection systems.

A further use of the holding fixture feature is made when mounting the support structure on the JetStar wing. With the contour boards in place to accurately index the suction panel surface relative to the wing, the shield and actuator mechanisms are removed from the assembly. The five-point indexing frame is reinstalled to the hinge points and actuator pivots as during the initial assembly of the support structure. This allows the entire unit, with the suction panel in place, to be accurately controlled while being held only by the five-point indexing frame as shown in Figure 56. This unit can then be positioned relative to the spar and adjusted for best fit according to the wing airfoil templates. The wing attach fittings can then be located using the ribs for alignment. Once located on the spar, the rib attach fittings can be fastened permanently to the spar while the support structure and holding fixture five-point indexing frame are moved out of the way.

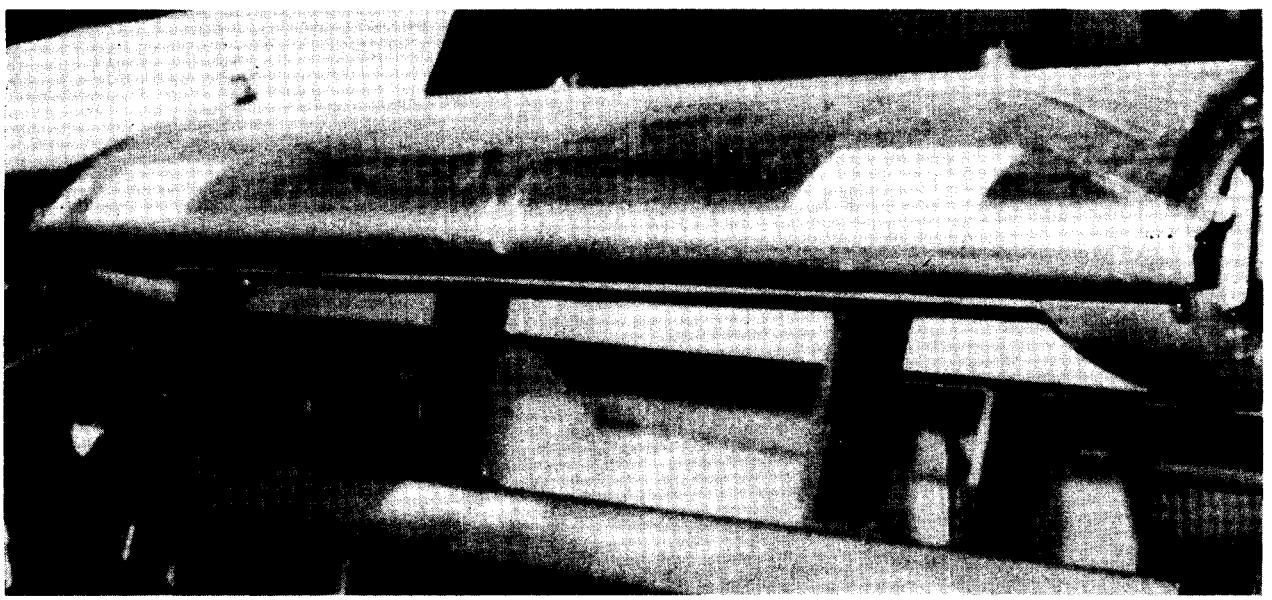

FIGURE 56. FIVE-POINT INDEXING FRAME

The last step in securing the support structure to the wing requires realigning the support structure in the five-point indexing frame of the holding fixture against the attach fittings and final drilling for the rib to attach fitting fasteners. With this attachment secured, the five-point indexing frame is removed and the shield and actuation system reinstalled.

ORIGINAL PAGE IS
OF POOR QUALITY

SECTION 11
FABRICATION AND ASSEMBLY

The leading edge test article is divided into two major subassemblies based primarily on the different type of fabrication techniques required to produce them. The leading edge suction panel fabrication employs specialized materials and tooling as well as complex procedures and close tolerance work. The support structure and systems required to hold the leading edge suction panel on the JetStar wing and operate it in flight are fabricated using standard aircraft construction, materials, methods, and tolerances.

11.1 SUCTION PANEL

The suction panel is composed of two major components, the fluted substructure of molded fiberglass and the perforated titanium skin. The primary tool used to shape and bond these components is described in Section 10.1. The leading edge bonding fixture controls the critical outer contour of the suction panel and contains all major reference lines and planes to define the finished part.

Substructure

The fluted substructure is composed primarily of fiberglass and stabilization strips of precured carbon/epoxy. The substructure is laid up using prepreg fiberglass cloth around the silicone rubber mandrels. One set of mandrels is prepositioned and bonded to a thin sheet of silicone rubber which simulates the outer skin of the leading edge panel. These mandrels are shaped and placed in the mold to form the active suction flutes. As the fiberglass cloth is positioned over these mandrels, other loose spacer flute mandrels are forced between the suction flute-forming mandrels to hold the fiberglass cloth in place and provide the required pressure to cure the fiberglass in the autoclave. Prior to closing out the mold and bagging for the autoclave, several layers of glass cloth are positioned to form the backing or inner surface of the panel. Also positioned at strategic locations within the layup are the precured carbon/epoxy stabilization strips.

The autoclave curing cycle consists of a 90-minute soak at 250°F and 50 psi. To provide a base for later bonding the rib attach tees, caul plates of aluminum sheet were placed at these locations on the underside of the fluted panel. The caul plates bridge over the wavy imprint of the mandrels and form a more uniform base on which to form and later bond the tees. See Figures 57 and 58.

The rib attach tees are formed on the underside of the cured panel substructure without removing it from the steel bonding fixture. Because the tees mount on the uncontrolled surface of the substructure, the tooling to form the tees "floats" in order to adjust to the surface. The tooling is attached firmly to the edges of the bonding fixture and locates the planes of the ribs precisely

ORIGINAL PAGE IS
OF POOR QUALITY

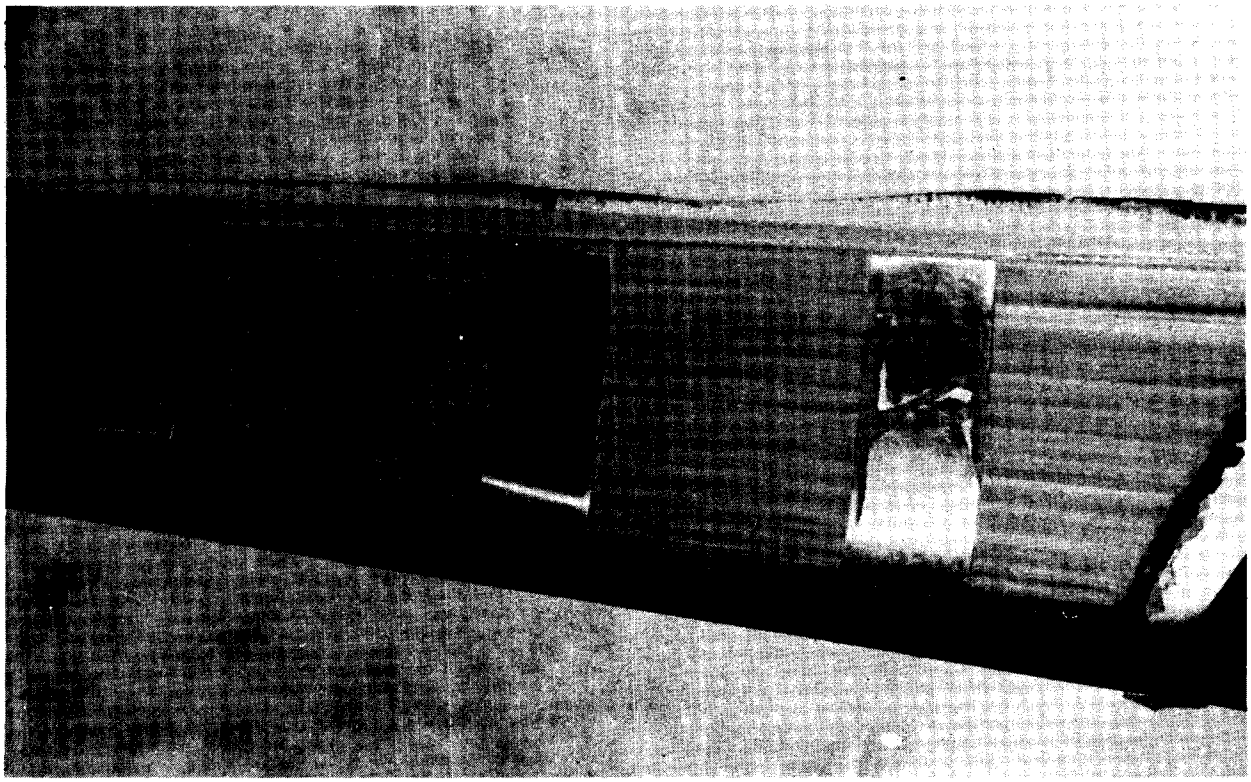

FIGURE 57. ATTACH TEE BASE FORMING CAUL PLATES

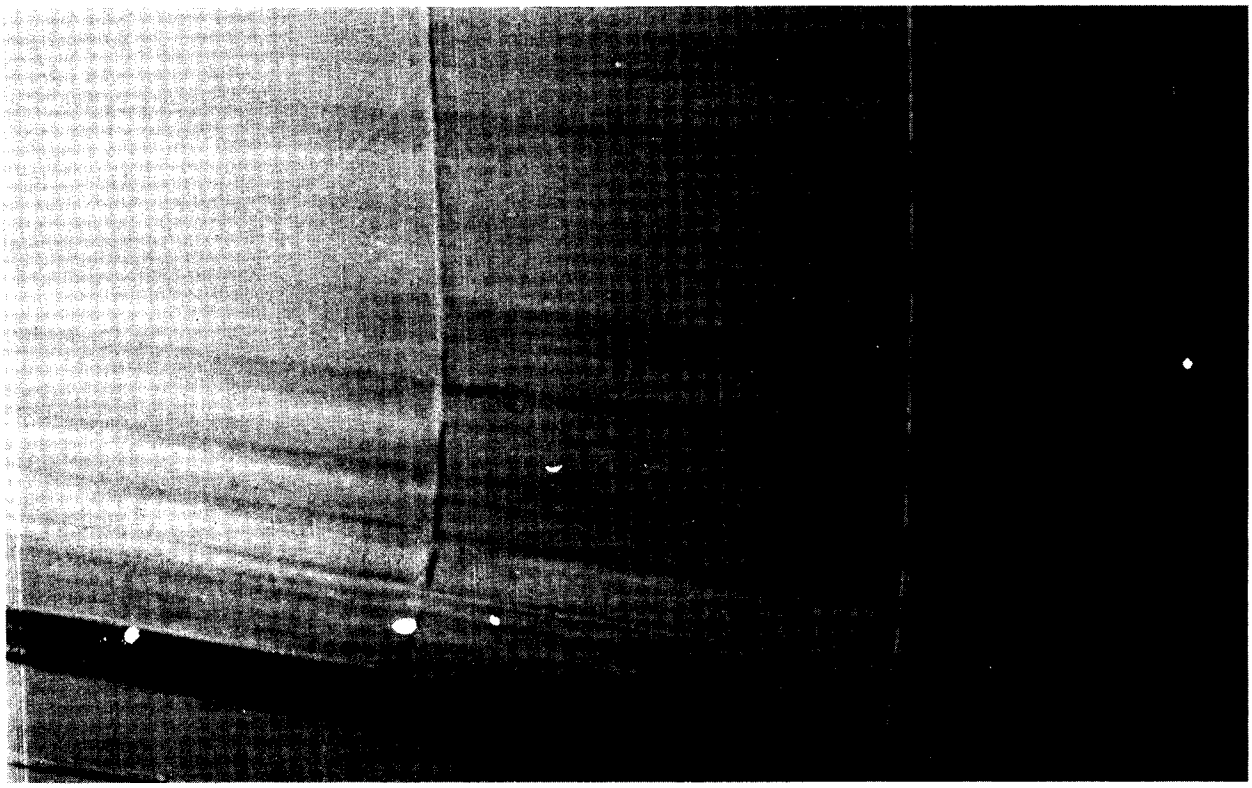

FIGURE 58. ATTACH TEE BASE FORMED BY CAUL PLATE

ORIGINAL PAGE IS
OF POOR QUALITY

while being allowed to move perpendicular to the surface and apply pressure to the tees during the cure cycle. The critical faces of the tees that align the ribs are formed against the hard tool faces while the non-critical backs of the tees are formed against soft silicone rubber tooling, as shown in Figure 55.

After the fiberglass tees are laid up and cured using the same autoclave cycle as for the main substructure, the tees are trimmed and bonded in a subsequent autoclave operation. This bonding is with the adhesive AF31 and utilizes a modified cure cycle of 4 hours at 250°F and 30 psi. The completed substructure assembly with tees bonded is shown in Figure 59 before it is removed from the bonding tool. The stiffening of the fluted structure with the tees bonded, prior to removal from the tool, is an added benefit and facilitates later bonding of the perforated titanium skin.

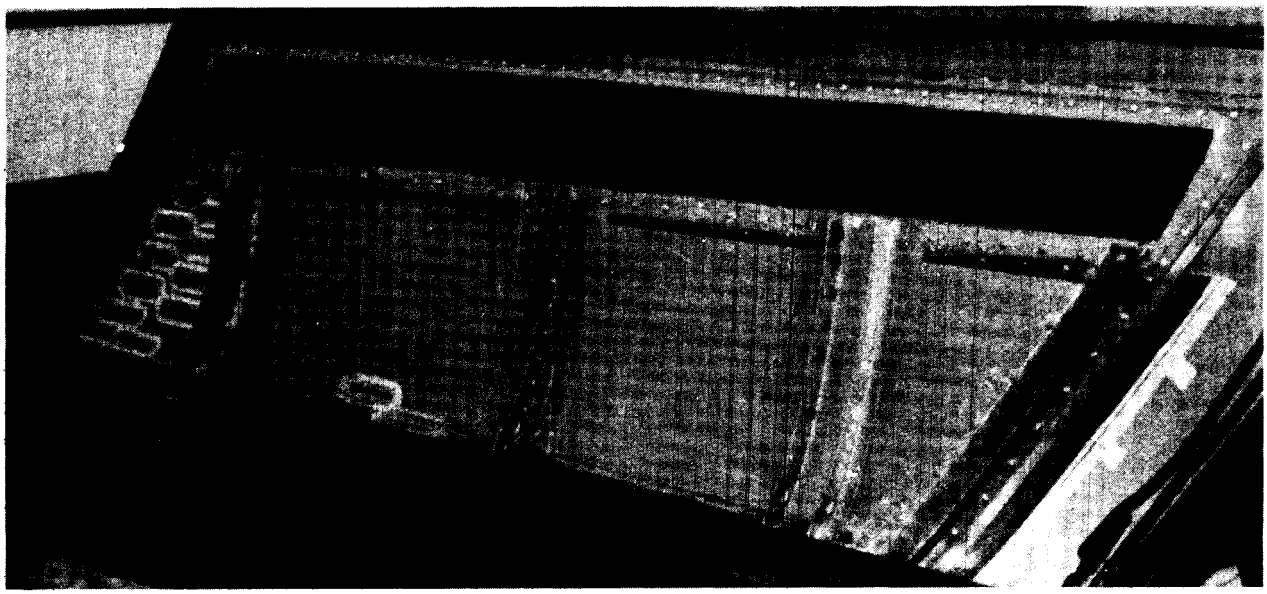

FIGURE 59. COMPLETED SUBSTRUCTURE ASSEMBLY

Suction Surface

The most suitable material for the outer porous surface of the suction panel is electron beam perforated titanium. This material, with hole sizes small enough for practical LFC use, only became available in the last few years. Improved electronic control by Pratt and Whitney of the Steigerwald electron beam drilling machine allows holes as small as 0.002 inch to be drilled in 0.025-inch-thick titanium. Successful use of this type of porous titanium to achieve LFC was demonstrated in the Douglas wind tunnel at Long Beach in 1981.

For both the demonstration wind tunnel model and the flight test article, several small sheets of the perforated titanium had to be welded together to form the approximately 80- by 30-inch sheets to cover the curved leading edge test articles. The largest sheets of titanium that can be fitted on the Steigerwald machine at Pratt and Whitney is 54 by 17 inches with the existing drum and vacuum chamber. Both the electron beam and tungston inert gas (TIG) welding techniques give excellent results in joining the perforated titanium. A weld line of about 0.080 to 0.100 is satisfactorily achieved with the TIG weld used for the flight test article skin. All weld joints were ground to within 0.001 inch of the surface prior to flattening the welded sheet. This was done to relieve all stresses and provide a perfectly flat sheet for rolling.

The perforated titanium skin was taper-rolled on a Farnham roll as close to the final contour as possible. The skin was then cleaned and primed on the inner surface in preparation for bonding to the fiberglass substructure. The titanium skin was rough trimmed, indexed, and secured in the steel bonding fixture at the aft joint line common to the sensor panel. The rest of the skin was thus free to adjust and conform to the shape of the bonding fixture during the cure cycle.

Bonded Assembly

The most critical operation in achieving a leak-free bond between adjacent flutes is the fitting of the silicone rubber mandrels in the active flute cavities, and the temporary attachment of the uncured AF31 adhesive on the bonding land between flutes. The flat sheet adhesives were precut to widths 0.4 inches wider than the lands. This excess width was distributed equally on either side, folded down along the side of the flute, and tacked at close intervals to the fiberglass with a heated soldering iron as shown in Figure 60. The prefitted silicone flute-forming mandrels were then inserted to fit uniformly in the flutes. The fit varied from flush to slightly below the adhesive surface on the bonding lands as shown in Figure 61. This precise fitting of the mandrels served several purposes. It first secured the folded-over AF31 adhesive strips on the lands and secondly provided proper support of the skin over the suction flutes during the heated and pressurized curing cycle. Also, during the autoclave cure cycle at 250^{o}F and 30 psi for four hours, the adhesive's tendency to be squeezed into any void was confined to the space between the mandrel and the flute wall rather than the space between the mandrel and the perforated titanium skin.

After bonding the titanium skin to the substructure, the silicone mandrels were extracted from the flute and alternate flute spaces by pulling and stretching the mandrels. This reduces the cross section and facilitates extraction. An inspection by borescope confirmed that there was a tight bond and that no adhesive squeezed out onto the underside of the perforated titanium, above the flute. The borescope light also was used to map the openness of the flutes and width of each suction strip including the taper in those flutes that are not constant.

ORIGINAL PAGE IS
OF POOR QUALITY

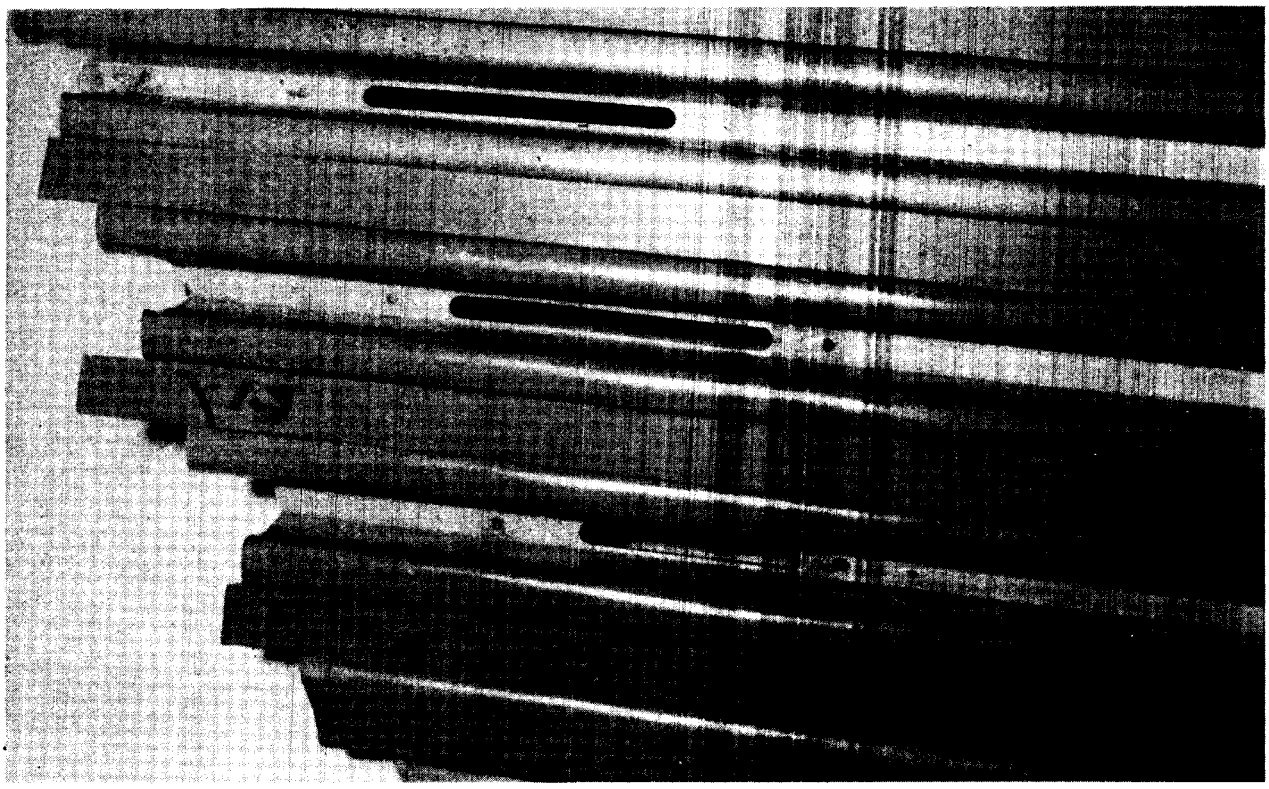

FIGURE 60. ADHESIVE ATTACHMENT AND FLUTE OPENINGS

FIGURE 61. FLUTE-FORMING MANDRELS IN PLACE

Extensive leak checks were made to ensure that each flute was isolated from adjacent flutes prior to sealing and closing out the ends of the fiberglass structure, and attaching the flute fittings shown in Figure 62.

FIGURE 62. FLUTE FITTING INSTALLATION

During the final leak check of each individual flute with the flute fitting installed, a serious leak was uncovered in flute number 3. The leak appeared to be from the non-active flute between flutes 2 and 3 into flute number 3. The leak could not be isolated. Therefore, it was decided to epoxy-coat the entire inner surface of the non-active flute. To accomplish this, a very fluid room-temperature curing epoxy was poured into the alternate flute at one end and caused to flow over all surfaces by tipping and rotating the panel. After setting overnight, the epoxy seal was determined to be effective. However, an unexpectedly large quantity of the very fluid epoxy penetrated the fiberglass wall between the non-active flute and flute 3. Some of this epoxy flowed onto the inner surface of the perforated titanium. Although most of this epoxy was removed, enough individual holes remained blocked to greatly reduce the porosity of the inboard 20 inches of flute 3.

11.2 SENSOR PANEL

The sensor panel was formed in a similar manner to the suction panel with a plain sheet of titanium bonded to a solid lay-up of fiberglass about 0.40-inch-thick. The joint between the suction panel and the sensor panel was fitted to very close tolerance and mated in the bonding tool using a liquid shim to allow perfect alignment of the two surfaces.

ORIGINAL PAGE IS
OF POOR QUALITY

C-2

11.3 HIGH-LIFT SHIELD

The retractable shield/slat is provided only to protect the perforated leading edge surface from airborne debris during takeoff and landing. It does, however, operate in a similar manner to a high-lift shield that would be used on a production LFC aircraft. On the JetStar test airplane, lift asymmetry was a potential problem and the shield was designed for minimal lift. The shield is assembled from three basic elements. A single solid aluminum "L" section contoured to the lower surface shape is the basic structural element. Attached to this, along the full span, is a half-round TKS deicing element that forms the leading edge in the extended position. In the stowed position, the shield is retracted into the underside cavity provided in the lower surface. Tubing that supplies the TKS fluid and the PGME for the spray system is installed so that it bends along a large radius during retraction and extension. The two bars of the spray system with their attached nozzles are fitted to the underside of the shield "L" section so as to be completely enclosed in the shield stowage box when the shield is retracted.

The shield is held to the leading edge support structure by three machined hinges. The two outer hinges are supported by double elements which also provide for attachment of the drive linkage. This linkage is assembled between the double ribs at either end of the assembly and is driven by two linear actuators coupled to the JetStar leading edge drive motor (see Figure 63). The JetStar leading edge slats are locked in position for these tests, allowing the use of the drive motor for powering the shield. The motor is relocated to a position just outboard of the test article in the outboard leading edge fairing.

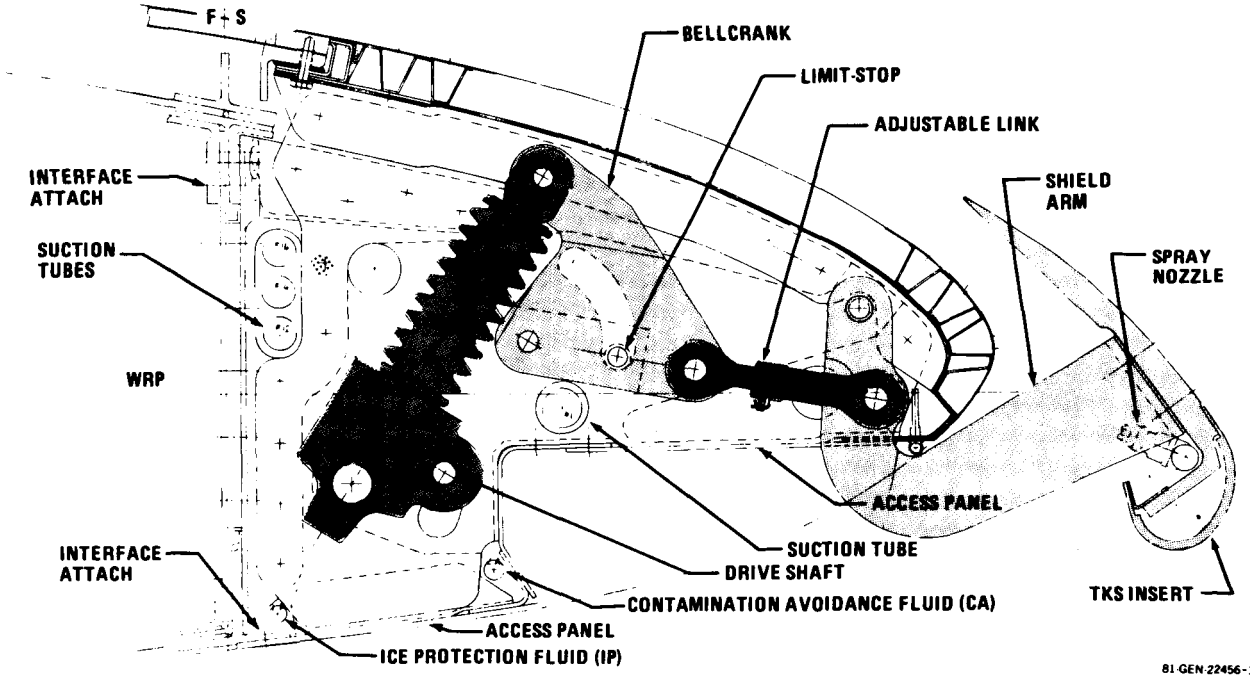

FIGURE 63. HIGH-LIFT SHIELD ASSEMBLY

11.4 ASSEMBLY

Since the suction panel was preassembled with the rib attach tees precisely installed on the underside (see Figure 59), this assembly becomes part of the assembly jig and provides for positioning the five main ribs of the support structure.

The assembly jig pictured in Figure 54 allows the LETA to be completely assembled by progressively removing details from the jig as the support components become fixed in their final positions. The critical points in the assembly that control the final alignment are the two actuator pivot points and the three shield hinge pins. By holding these five critical points in perfect alignment until the support structure components are tied together, the jig assures that the shield and its actuation linkage will fit properly and move freely when installed. This feature also allows the shield to be functioned and adjusted without removing the assembly from the jig.

For mounting on the JetStar, the portion of the jig that contains the five critical pivot points of the shield actuation linkage (see Figure 56) is installed in place of the shield linkage. This five-point support frame is then removed from the main jig with the LETA attached. The LETA is then positioned relative to the front spar while being held rigidly on the support frame. The rib attach angles are then temporarily attached to the ribs and permanently attached to the spar.

With the rib attach angles in final position, the ribs are fixed to the attach tees. At this point, the five-point support frame is removed and the shield and actuators reinstalled. With the support structure firmly attached to the spar, the sensor and suction panel can be removed at any time with assurance that they will be in proper alignment relative to the upper surface when reinstalled.

Attachment of the flute fittings to the suction lines and connection of the contamination and ice protection fluid lines in the inboard leading edge complete the assembly.

SECTION 12
LFC TEST ARTICLE INSTRUMENTATION

Laminar flow is very sensitive to surface conditions, and the instrumentation was carefully installed to be as nonintrusive as possible in the regions where laminar flow was anticipated. Surface pressure taps were arranged at these spanwise locations. Along the approximate centerline of the test article, one chordwise line of 15 subsurface pressure taps was installed (one tape behind each spanwise flute). One additional pressure tape is in the sensor panel with others in the fairing behind. Along the inboard and outboard edge other chordwise lines of 8 pressure taps each were installed behind every other flute. The general layout is shown in Figure 64.

Along the centerline, each of the 15 flutes is instrumented with a presssure tap to read flute pressure. These are designated by F#B in the tables of instrumentation locations. In each inboard and outboard array only 3 flutes have pressure taps (See Tables 7 through 9).

In addition to the pressure taps, a line of 6 hot film sensors were carefully flush mounted in the suction panel surface along a line not parallel to the chordwise flow. This was done so that no interference would occur with the laminar flow over subsequent downstream sensors in the event one should become exposed enough to transition the flow. The locations of the hot film sensor are listed in Table 10.

As a back up to the hot film sensors to detect the presence of laminar flow, 20 evenly spaced spanwise total pressure probes were mounted on the sensor panel approximately 0.060 inch above the trailing edge of the suction panel. At five of the 20 stations two additional probes were mounted at 0.020 inch and 0.150 inch above the surface to form a three tube rake at each of the five stations.

All pressures are measured on P.S.I. scani-values and recorded for future references.

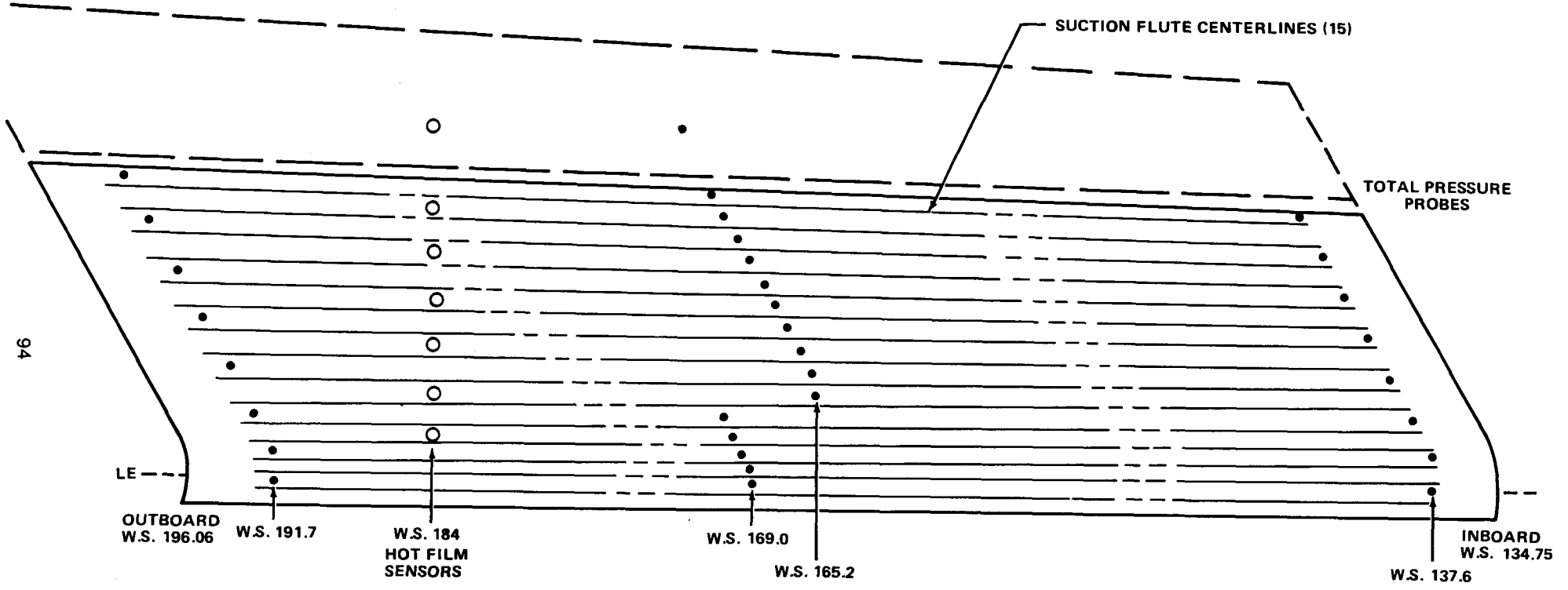

	HOT FILM SENSORS	STATIC PRESSURE TAPS OUTBOARD	CENTERLINE	INBOARD
SUCTION PANEL	6	8	15	8
SENSOR PANEL	1	0	1	0

FIGURE 64. DOUGLAS LFC LEADING EDGE SURFACE INSTRUMENTATION

TABLE 7

DOUGLAS LETA INSTRUMENTATION LOCATIONS

STATIC PORTS, OUTBOARD ARRAY - A

FLUTE/LOG	I.D.	Wing Station (in.)	Y (in.)	X (in.)	x/c (%)	
						Trailing Edge
	515A*	191.7	224.881	15.840	0.1502	
15						
14						
	S13A	191.7	223.471	13.230	0.1235	
13						
12						
	S11A*	191.7	222.021	10.820	0.0970	
11	F11A					
10						
	S9A	191.7	220.561	8.240	0.0710	
9						
8						
	S7A	191.7	219.271	5.710	0.0450	
7						
6						
	S5A*	191.7	218.021	3.170	0.0210	
5	F5A					
4						
	S3A	191.7	217.031	1.260	0.0053	
3	F3A					
2						
						Leading Edge
	S1A	191.7	216.461	-0.490	0.0006	
1						

* = #80 (.0135 Dia) drilled hole
Y = Trace Leading Edge Station cant
X = Dimensions normal from leading edge on lofted surface

TABLE 8

DOUGLAS LETA INSTRUMENTATION LOCATIONS

STATIC PORTS, CENTER ARRAY-B

FLUTE/LOG	I.D.	Wing Station (in.)	Y (in.)	X (in.)	x/c (%)	
	S16B*	165.2	195.559	19.680	0.1727	Sensor Panel Trailing Edge
	S15B*	165.2	193.105	15.00	0.1308	
15	F15B					
	S14B	165.2	192.375	13.800	0.1195	
14	F14B					
	S13B	165.2	191.825	12.660	0.1082	
13	F13B					
	S12B	165.2	191.085	11.470	0.0962	
12	F12B					
	S11B	165.2	190.385	10.260	0.0843	
11	F11B					
	S10B	165.2	189.770	9.080	0.0730	
10	F10B					
	S9B	165.2	189.075	7.960	0.0610	
9	F9B					
	S8B	165.2	188.405	6.740	0.0505	
8	F8B					
	S7B	165.2	187.865	5.610	0.0400	
7	F7B					
	S6B	165.2	187.245	4.420	0.0290	
6	F6B					
	S5B	169.0	191.015	3.250	0.0193	
5	F5B					
	S4B	169.0	190.545	2.180	0.0105	
4	F4B					
	S3B	169.0	190.020	1.270	0.0047	
3	F3B					
	S2B	169.0	189.635	0.490	0.0012	
2	F2B					
	S1B	169.0	189.455	-0.340	0.0008	Leading Edge
1	F1B					

* = #80 (.0135 Dia) drilled hole
Y = Trace Leading Edge Station Cant
X = Dimensions normal from leading edge on lofted surface

TABLE 9

DOUGLAS LETA INSTRUMENTATION LOCATIONS
STATIC PORTS, INBOARD ARRAY-C

FLUTE/LOG	I.D.	Wing Station (in.)	Y (in.)	X (in.)	x/c (%)	
						Trailing Edge
	S15C*	137.6	161.177	14.070	0.1135	
15						
14						
	S13C*	137.6	159.877	11.870	0.0930	
13						
12						
	S11C	137.6	158.702	9.735	0.0735	
11	F11C					
10						
	S9C	137.6	157.647	7.670	0.0545	
9						
8						
	S7C	137.6	156.408	5.445	0.0350	
7						
6						
	S5C	137.6	155.288	3.260	0.0172	
5	F5C					
4						
	S3C	137.6	154.407	1.310	0.0042	
3						
2	F2C	137.6				
						Leading Edge
	S1C	137.6	154.137	-0.480	0.0010	
1						

* = #80 (.0135 Dia) drilled hole
Y = Trace Leading Edge Station cant
X = Dimensions normal from leading edge on lofted surface

TABLE 10

DOUGLAS LETA INSTRUMENTATION LOCATIONS

HOT FILM SENSORS

FLUTE/LOG	I.D.	Wing Station (in.)	Y (in.)	X (in.)	x/c (%)	
	HF7	178.00	208.979	19.580	0.182	Sensor Panel Trailing Edge
15						
	HF6	179.05	209.369	14.210	0.1287	
14						
13						
	HF5	180.25	209.419	11.770	0.1040	
12						
11						
	HF4	181.55	209.449	9.280	0.0790	
10						
9						
	HF3	182.80	209.429	6.880	0.0550	
8						
7						
	HF2	184.00	209.449	4.410	0.0315	
6						
5						
	HF1	184.80	209.419	2.140	0.0117	
4						
3						
2						
						Leading Edge
1						

* = #80 (.0135 Dia) drilled hole
Y = Trace Leading Edge Station cant
X = Dimensions normal from leading edge on lofted surface

CONCLUDING REMARKS

The design and fabrication of the Douglas LFC Leading Edge Glove Flight Test Article involved new and innovative methods. Laminar flow control was provided by an electron beam perforated suction surface and a retractable high-lift shield incorporating a supplementary spray system was used to protect the LFC surface from contamination, particularly flying insects. This system also served for ice protection, with the shield itself protected by a TKS deicing system.

The electron beam perforated titanium surface was supported by a fiberglass substructure with integral suction flutes. Techniques were developed for welding, flatening and roll forming the titanium surface for the LFC panel. An accurate external surface was achieved by using an NC machined steel molding/bonding tool and silicone rubber mandrels to form the internal suction ducting in the fiberglass and carbon epoxy substructure during molding. The mandrels also served to retain the shape of the ducting during subsequent bonding of the perforated titanium surface. All of the molding and bonding were done in an autoclave. Carbon fiber layers were used in the substructure to compensate for differential thermal expansion and avoid surface waviness. Tolerances were taken up internally at the rib attachments to ensure overall contour control using production quality steel jigs and fixtures.

The resulting spanwise porous suction strips covered the entire upper surface, extending from below the attachment line in cruise back to the aft edge at the front spar. Suction levels were calculated to achieve laminar flow at the design condition of Mach 0.75 at 38,000 ft. with sufficient margin for experimentation.

The structure was designed to be fail safe with an ultimate factor of 2.0 and design features were incorporated to avoid overloading the basic JetStar wing structure.

REFERENCES

1. Raspet, A.: Mechanism of Automatic Trailing Edge Suction, Office of Naval Research Contract Nonr 223(00), 31 December 1951.

2. Pfenninger, W.: Laminar Flow Control Laminarization, Special Course on Concepts for Drag Reduction, AGARD-R-654, June 1977.

3. Lachmann, G.E., ed: Boundary Layer and Flow Control, Its Principles and Application, Volume 2, Pergamon Press, 1961.

4. Pearce, W.E.; et al: Evaluation of Laminar Flow Control System Concepts for Subsonic Commercial Transport Aircraft, Final Report, NASA CR-159251, June 1983.

5. Tranen, T.L.: Analysis and Design of Transonic Airfoils, McDonnell Aircraft Company Report No. MDC A3760, December 1975.

6. Henne, P.A. and Hicks, R.M.: Wing Analysis Using a Transonic Potential Flow Computation Method, NASA TM-78464, July 1978.

7. Giesing, J.P.: Lifting Surface Theory for Wing Fuselage Combinations, Douglas Aircraft Company, Report DAC-67212, Vol. 1, August 1968.

8. Bauer, F.; Garabedian, P.; Korn, D.; and Jameson, A.: Supercritical Wing Sections II., Lecture Notes in Economics and Mathematical Systems, Vol. 108, Springer-Verlag, 1975.

9. Nenni, J.P. and Gluyas, G.L.: Aerodynamic Design and Analysis of an LFC Surface, Astronautics and Aeronautics, July 1966.

10. Srokowski, A.J. and Orszag, S.A.: Mass Flow Requirements for LFC Wing Design, AIAA Paper 77-1222, 1977.

11. Callaghan, J.G. and Beatty, T.D.: A Theoretical Method for the Analysis and Design of Multi Element Airfoils - Part I. Douglas Aircraft Company, Report No. MDC J5358-01, January 1972.

12. Dagenhart, J. R.: Amplified Crossflow Disturbances in the Laminar Boundary Layer on Swept Wings with Suction, Masters Thesis. North Carolina State University, August 1979.

13. Carmichael, B.H.: Surface Waviness Criteria for Swept and Unswept Laminar Suction Wings, NORAIR Report NOR-59-438, August 1959.

14. Vennel, W.W.: Structural Requirements for JetStar LFC Leading Edge Glove Modification, Lockheed-Georgia Company, Report No. SRD 72-73-843, May 1981.

1. Report No. NASA CR-162137	2. Government Accession No.	3. Recipient's Catalog No.
4. Title and Subtitle LAMINAR FLOW CONTROL LEADING EDGE GLOVE FLIGHT TEST ARTICLE DEVELOPMENT		5. Report Date November 1984 6. Performing Organization Code
7. Author(s) W. E. Pearce, D. E. McNay and J. A. Thelander		8. Performing Organization Report No. 10. Work Unit No.
9. Performing Organization Name and Address McDonnell Douglas Corporation 3835 Lakewood Blvd Long Beach, California 90846		11. Contract or Grant No. NAS1-16220
12. Sponsoring Agency Name and Address National Aeroanutics and Space Administration Washington, D.C. 20546		13. Type of Report and Period Covered Contractor Report 14. Sponsoring Agency Code

15. Supplementary Notes
Langley Technical Monitor: Mike C. Fischer
Final Report

16. Abstract
A laminar flow control (LFC) flight test article was designed and fabricated to fit into the right leading edge of a JetStar aircraft. The article was designed to attach to the front spar and fill in approximately 70 inches of the leading edge that are normally occupied by the large slipper fuel tank. The outer contour of the test article was constrained to align with an external fairing aft of the front spar which provided a surface pressure distribution over the test region representative of an LFC airfoil.

LFC is achieved by applying suction through a finely perforated surface, which removes a small fraction of the boundary layer.

The LFC test article has a retractable high-lift shield to protect the laminar surface from contamination by airborne debris during takeoff and low-altitude operation. The shield is designed to intercept insects and other particles that could otherwise impact the leading edge. Because the shield will intercept freezing rain and ice, a TKS oozing glycol ice protection system is installed on the shield leading edge. In addition to the shield, a liquid freeqing point depressant (PGME) can be sprayed onto the leading edge from a series of spray nozzles mounted on the back of the shield. This spray can assist in preventing airborne debris from sticking to the leading edge as well as provide added capability to prevent or remove ice forming on the leading edge.

17. Key Words (Suggested by Author(s))	18. Distribution Statement		
Laminar Flow Control, Suction Surface, Contamination, Ice Protection, Shield, Leading Edge	[redacted]		
19. Security Classif. (of this report) Unclassified	20. Security Classif. (of this page) Unclassified	21. No. of Pages	22. Price

[redacted]